Damping Studies on Sandwich Structures with Viscoelastic Layers

Submitted in partial fulfilment of the requirements for the award of the degree of

DOCTOR OF PHILOSOPHY
in
Mechanical Engineering

by

K KISHORE KUMAR

Roll No. 700744

under the guidance of

Prof. P. BANGARU BABU
Department of Mechanical Engineering
NIT, Warangal.

&

Dr. Y. KRISHNA
Scientist `G',
Defence Research and Development Laboratory (DRDL)
Kanchanbagh, Hyderabad

DEPARTMENT OF MECHANICAL ENGINEERING
NATIONAL INSTITUTE OF TECHNOLOGY
WARANGAL – 506004

2015

Thesis Approval Sheet

Damping Studies on Sandwich Structures with Viscoelastic Layers

by

Mr. K Kishore Kumar

is approved for the degree of

Doctor of Philosophy

Prof. _____
Examiner

_____
Prof. P. Bangaru Babu
Supervisor

_____
Dr. Y. Krishna
Co-supervisor

_____
Prof. Ch. Surya Prakash Rao
Chairman, DSC
Department of Mechanical Engineering
National Institute of Technology
Warangal – 506004

Date:_____

DECLARATION

This is to certify that the work presented in the thesis entitled " **DAMPING STUDIES ON SANDWICH STRUCTURES USING VISCOELASTIC LAYERS**" is a bonafide work done by me under the supervision of Dr. P. Bangaru Babu, Professor Mechanical Department and was not submitted elsewhere for the award of any degree. I declare that this written submission represents my ideas in my own words and where others' ideas or words have not been included. I have adequately cited and referred the original sources. I also declare that I have adhered to all principles of academic honesty and integrity and have not misrepresented or fabricated or falsified any idea/data/fact/sources in my submission. I undertake that any violation of the above will be a cause for disciplinary action by the institute and can also evoke penal action from the sources which have thus not been properly cited or from whom proper permission has not been taken when needed.

Signature

K Kishore Kumar

Roll No. 700744

Date :

ABSTRACT

Viscoelastic materials are gaining importance for the control of vibrations in aerospace and automotive industry. Viscoelastic layers are sandwiched in the parent structure either in unconstrained or constrained layer configuration to attenuate the vibration levels and enhance the damping of a structure. The effectiveness of the viscoelastic layer in attenuating vibrations can be found from the dynamic behaviour of sandwich structure with unconstrained and constrained viscoelastic layers. The present work is focused on theoretical and experimental investigations of dynamic responses of sandwich beam and plate structures with viscoelastic layers.

Two viscoelastic materials developed by Naval Material Research Laboratory, NMRL (DRDO laboratory) for Defence applications are studied by sandwiching them with the parent structure. The frequency dependent Young's Modulus, shear modulus and loss factors of both the viscoelastic materials is obtained from Dynamic Mechanical Analyzer (DMA). The experimental data obtained from DMA are expressed in mathematical form using power fit for further use in dynamic models of sandwich structures.

Finite element based dynamic models are developed for sandwich beam and plate structures. The sandwich structure is discretized into finite elements and dynamic equations of motion are developed using Lagrangian method. The sandwich beam structure is modelled using Euler-Bernoulli beam theory for base and constraining layer and shear deformation is considered for constrained layer. For two dimensional structures, Mindlin-Reissner first order shear deformation theory is considered for all three layers. The frequency dependent material properties and loss factors of the viscoelastic materials are introduced into the dynamic models.
An iterative computational scheme is developed to solve the dynamic equations of motion of the sandwich structures and frequency response functions (FRF's) are computed. The FRFs and loss factors obtained from the finite element model with and without considering the variation of frequency dependent material properties of the viscoelastic layer are compared. These results are validated with experiments for sandwich beam and plate structures in unconstrained and constrained layer configurations. The Finite element model considering the frequency dependent material properties of viscoelastic layers are in close agreement with experiments compared to FE model considering constant material properties of viscoelastic layer.

The validated finite element model is further used in simulation studies of sandwich plate structure with different layer thicknesses and boundary conditions. The optimum layer thickness ratios of sandwich plate for high loss factors are identified. The high loss factors are obtained when the thickness ratio of constraining layer to total thickness of sandwich plate (t_c/t) lies between 0.41 to 0.46 and it is independent of mode and boundary condition. The loss factor increases for higher mode number for all the boundary conditions. The loss factor increases with increase in thickness of viscoelastic layer.

Keywords:- Unconstrained layer, Constrained layer, sandwich structure, viscoelastic layer, frequency dependent material properties, frequency response function (FRF), and loss factor.

CONTENTS

List of Figures

List of Tables

NOMENCLATURE

A_b	Area of base beam
A_c	Area of constraining layer
A_v	Area of the viscoelastic layer
$U_c(x,t)$	Constrained generalized displacement vector
M_{cc}	Constrained part of global mass matrix
K_{cc}^*	Constrained part of global stiffness matrix
κ	Curvature
κ_b	Curvature of sandwich beam
ρ_b	Density of base layer
ρ_c	Density of constraining layer
ρ_v	Density of viscoelastic layer
G_v^*	Frequency dependent complex shear modulus of the viscoelastic layer
$\ddot{U}(t)$	Generalized acceleration vector
$U(t)$	Generalized displacement vector
(K^I)	Imaginary part of complex stiffness matrix
u_i	In-plane displacement at mid plane in x direction of ith layer
v_i	In-plane displacement at mid plane in y direction ith layer
T	Kinetic energy
T_{eb}	Kinetic energy associated with longitudinal displacement of base beam
T_{ec}	Kinetic energy associated with longitudinal displacement of constraining layer
T_{bp}	Kinetic energy corresponding to in-plane vibration of base layer
T_{vp}	Kinetic energy corresponding to in-plane vibration of constrained layer
T_{cp}	Kinetic energy corresponding to in-plane vibration of constraining layer
T_{br}	Kinetic energy corresponding to rotary inertia of base layer
T_{vr}	Kinetic energy corresponding to rotary inertia of constrained layer
T_{cr}	Kinetic energy corresponding to rotary inertia of constraining layer
T_{eb}	Kinetic energy due to bending
T_{bb}	Kinetic energy due to bending of the base beam

T_{cb}	Kinetic energy due to bending of the constraining layer
T_{vb}	Kinetic energy due to bending of the viscoelastic layer
T_{ee}	Kinetic energy due to longitudinal displacement
$\mathcal{L}$	Lagrangian
L_c	Length of constraining layer
L	Length of the beam
l	Length of the Cartesian element
l_e	Length of the finite element
L_v	Length of viscoelastic layer
u_l	Longitudinal displacement of base beam
u_3	Longitudinal displacement of constraining layer
ξ_{mi}	Modal damping ratio of ith mode
η_{mi}	Modal loss factor of ith mode
$H_m(s)$	Modal transfer function
I	Moment of inertia
[H(S)]	Overall transfer function
P	Potential energy
w'	Rotation about x-axis
α_i	Rotation of transverse section of the ith layer about xz plane
β_i	Rotation of transverse section of the ith layer about yz plane
γ	Shear deformation of the viscoelastic layer
P_{bb}	Strain energy due to bending of the base beam
P_{cc}	Strain energy due to bending of the constrained layer beam
P_{be}	Strain energy due to longitudinal displacement of the base beam
P_{ce}	Strain energy due to longitudinal displacement of the constraining layer beam
P_{sv}	Strain energy due to shear deformation of viscoelastic layer
ε_b	Strain in the base beam
ε_c	Strain in the constraining layer beam
t_b	Thickness of the base plate
t_c	Thickness of the constraining layer
t_v	Thickness of the viscoelastic layer

t_b	Thicknesses of the base beam
t_c	Thicknesses of the constraining layer
t_v	Thicknesses of the viscoelastic layer
$\frac{t_v}{t}$	Ratio of thickness of viscoelastic layer to total thickness of sandwich plate
$\frac{t_c}{t}$	Ratio of thickness constraining layer to total thickness of sandwich plate
$t= t_b+t_v+t_c$	Total thickness of sandwich beam or plate
T_e	Total kinetic energy
P_e	Total strain energy
t	Total thickness of sandwich plate
w	Transverse displacement
$U_u(x,t)$	Unconstrained generalized displacement vector
M_{uu}	Unconstrained part of global mass matrix
K_{uu}^*	Unconstrained part of global stiffness matrix
b	Width of the Cartesian element
W	Work potential
E_b	Young's modulus of base beam
E_c	Young's modulus of constraining layer
E	Young's modulus of sandwich structure
$[K_{bb}]$	Bending stiffness of the base layer
$[K_{cb}]$	Bending stiffness of the constraining layer
$[K_e^*]$	Complex element stiffness matrix of sandwich plate
$[K_m^*]$	Complex modal stiffness matrix
$[M_{eb}]$	Element mass matrix due to transverse motion
$[M_{ee}]$	Element mass matrix for longitudinal displacement
$[M_e]$	Element mass matrix for the sandwich beam element
$[M_e]$	Element mass matrix for the sandwich plate
$[K_{eb}]$	Element stiffness matrix due to bending
$[K_{ee}]$	Element stiffness matrix due to longitudinal strain
$[K_{sv}^*]$	Element stiffness matrix due to shear deformation of the viscoelastic layer
$[K_e^*]$	Element stiffness matrix of sandwich beam

$[K^*]$	Frequency dependent global complex stiffness matrix
$[M]$	Global mass matrix
$[K_{bp}]$	Stiffness matrix due to in-plane displacement of the base layer
$[K_{cp}]$	Stiffness matrix due to in-plane displacement of the constraining layer
$[B]$	Input matrix
$[N_1]$	Interpolation for in-plane displacement of base layer in x-direction
$[N_2]$	Interpolation for in-plane displacement of base layer in y-direction
$[N_3]$	Interpolation for in-plane displacement of constraining layer in x-direction
$[N_4]$	Interpolation for in-plane displacement of constraining layer in y-direction
$[N_6]$	Interpolation for rotation of base layer in x-direction
$[N_7]$	Interpolation for rotation of base layer in y-direction
$[N_8]$	Interpolation for rotation of constraining layer in x-direction
$[N_9]$	Interpolation for rotation of constraining layer in y-direction
$[N_5]$	Interpolation for transverse displacement of all layers
$[J]$	Jacobian
$\left[M_{bp}\right]$	Mass matrices due to axial motion of base layer of sandwich plate
$\left[M_{cp}\right]$	Mass matrices due to axial motion of constraining layer of sandwich plate
$[M_{vp}]$	Mass matrices due to axial motion of viscoelastic layer of sandwich plate
$[M_{br}]$	Mass matrices due to rotary inertia of base layer of sandwich plate
$[M_{cr}]$	Mass matrices due to rotary inertia of constraining layer of sandwich plate
$[M_{vr}]$	Mass matrices due to rotary inertia of viscoelastic layer of sandwich plate
$[M_b]$	Mass matrix due to bending of sandwich plate
$[\Gamma_m]$	Modal force vector
$[M_m]$	Modal mass matrix
$[P]$	Modal matrix
$[D_{bb}]$	Rigidity matrix corresponding to bending strain of base layer
$[D_{cb}]$	Rigidity matrix corresponding to bending strain of constraining layer
$\left[D_{bp}\right]$	Rigidity matrix corresponding to longitudinal displacement of base layer
$\left[D_{cp}\right]$	Rigidity matrix corresponding to longitudinal displacement of constraining layer
$[D_{bs}]$	Rigidity matrix corresponding to shear strain of base layer
$[D_{cs}]$	Rigidity matrix corresponding to shear strain of constraining layer

$[D_{vs}^{*}]$	Rigidity matrix corresponds to shear strain of constrained layer
$[K_{bs}]$	Shear stiffness of the base layer
$[K_{cs}]$	Shear stiffness of the constraining layer
[A]	State matrix
$[P_{vs}^{*}]$	Strain energy due to shear deformation of viscoelastic layer
$[P_{bb}]$	Strain energy of base plate due to bending
$[P_{bp}]$	Strain energy of base plate due to in plane displacement
$[P_{bs}]$	Strain energy of base plate due to in shear rotation
$[P_{cb}]$	Strain energy of constraining plate due to bending
$[P_{cp}]$	Strain energy of constraining plate due to in plane displacement
$[P_{cs}]$	Strain energy of constraining plate due to in shear rotation
$[P_e]$	Total strain energy of the sandwich plate
$\{U_d\}$	Dynamic displacement vector
$\{U_i\}$	Element nodal displacement vector
$\{N_b\}$	Interpolation function for longitudinal displacement of base beam
$\{N_c\}$	Interpolation function for longitudinal displacement of constraining layer beam
$\{N_w\}$	Interpolation function for transverse displacement of sandwich beam
$\{N_{w'}\}$	Interpolation function for transverse rotation of sandwich beam
$\{u_i\}$	ith dof displacement vector
$\{\dot{u}_i\}$	ith dof velocity vector
$\{q_m(t)\}$	Modal response vector
$\{U_e\}$	Nodal displacement vector of sandwich beam
$\{U_s\}$	Pseudo-static displacement vector
$[k_{vs}^{*}]$	Shear stiffness of viscoelastic layer
$\{B_\gamma\}$	Shear strain interpolation of viscoelastic layer
$\{\gamma_s^c\}$	Shear strain matrix corresponds to constraining layer
$\{z(t)\}$	State space vector
$\{\mathcal{E}_{bp}\}$	Strain matrix corresponding to in-plane displacements of base layer
$\{\mathcal{E}_{cp}\}$	Strain matrix corresponding to longitudinal displacements of constraining layer
$\{\mathcal{E}_{bb}\}$	Strain matrix due to bending of base plate

$\{\varepsilon_{cb}\}$	Strain matrix due to bending of constraining plate
$\{\gamma_s^b\}$	Transverse shear strain matrix of base layer

CHAPTER 1

INTRODUCTION

1.1 MOTIVATION

All structures having elasticity and inertia undergo vibrations. Dynamic systems convert kinetic energy to strain energy and vice versa. The conservation of energy from one form to another causes vibration in the structure. When the excitation frequency coincides or gets close to any of the natural frequencies of the structure, resonance occurs and results in large amplitude vibrations. These resonant vibrations severely influence the dynamic characteristics of the structures and produce discomfort and noise. These vibrations can be minimized through the dissipation of vibrational energy present in the system. The dissipation mechanism of vibrational energy from the system is known as damping. The mere presence of damping brings down the resonant amplitude to finite values which are infinite otherwise. Due to the influence of resonant vibrations on the life of the structure, damping has become one of the major design considerations. Hence, the need to improve damping in a structure is undisputed. Enhancing damping of structure is very important in aerospace, mechanical and civil engineering.

Enhancement of damping in the structures can be achieved by passive or active means. In active damping, vibrations are controlled by external source of energy using sensors and actuators. Use of sensors and actuators increases the complexity of the system in active

damping. In passive damping, the vibrations are minimised by using the material's inherent ability in dissipating the energy. Hence, material selection plays a significant role in deciding the damping capability of a structure. In recent times, the sandwich structures are employed in place of conventional structures due to their ability in providing higher damping.

The current research is motivated by the organization goal of reducing the vibration levels of electronic packages when they are subjected to severe dynamic loads. The electronic packages are mounted on brackets that are attached inside the missile at designated locations. In general the electronic packages have very low material damping. So, there is a need to enhance the damping in the supporting structure of electronic packages to suppress the vibrations. The focus of the proposed research is on enhancing the damping by sandwiching viscoelastic layer in parent structure. Two viscoelastic materials developed by Naval Material Research Laboratory (NMRL, DRDO) are characterized to understand their damping properties when sandwiched between the base and constraining layers.

1.2 OBJECTIVES

The objective of the present research work is to minimize the vibrations of structures at resonance using viscoelastic materials. Two viscoelastic materials developed for defence application are chosen for this study.

(a) The first step to achieve this objective is to understand the behaviour of viscoelastic layer by sandwiching them between base and constraining layers. Since electronics packages do not experience high temperatures, the effect of temperature variation on the viscoelastic materials are not considered in the present study and the main focus is on the frequency dependent material properties. These frequency dependent material properties of viscoelastic layer viz; Young's modulus, shear modulus and loss factors (in tension and shear mode) are obtained experimentally using Dynamic Mechanical Analyzer (DMA) and expressed in a mathematical form using curve fit for further use in the FE model. The complex Young's modulus and shear modulus for both the viscoelastic materials are derived using the above properties. The frequency dependent Poisson's ratio is obtained from the complex Young's modulus and shear modulus data.

(b) The second step is to develop a FE Based dynamic model for sandwich beams and plate structures considering the frequency dependent material properties of viscoelastic layer. The stiffness matrix of the sandwich structure is complex quantity and depends on the frequency of excitation. The element matrices are assembled and dynamic equations of motion are developed. An iterative computational scheme is necessary to solve the dynamic equations of motion due to the frequency dependent complex stiffness matrix. The equations of motion are derived for base excitation. The experiments are performed on sandwich beam and plate structures with base excitation to minimise the contribution of armature dynamics of the shaker. The developed dynamic models are validated by comparing frequency response functions (FRF's) and loss factors calculated from the analytical results with experiments. Assuming constant material properties of the viscoelastic layer, FRFs and loss factors are also calculated and compared with the results obtained from the dynamic model considering frequency dependent material properties of the VE layer.

(c) The third step is to carry out simulation studies with the validated dynamic model to identify the optimum thickness ratios of sandwich layers for better vibration attenuation. The simulation studies are also carried out for three different boundary conditions.

Thus, the scope of this research is to:

- Characterize two viscoelastic materials for frequency dependent Young's Modulus, shear modulus and loss factors using Dynamic Mechanical Analyzer (DMA) and expressing the measured frequency dependent material properties in a mathematical form using power fit for further use in dynamic models of sandwich structures.
- Develop a finite element based dynamic models for sandwich beam and plate structures with viscoelastic materials considering the frequency dependent Young's modulus, shear modulus and loss factors of the viscoelastic material.
- Develop an iterative computational scheme to solve the dynamic equations of motion.
- Validate the dynamic model with experimental results on sandwich beam and plate structures.
- Carryout simulation studies on sandwich plate structures using dynamic model and computational scheme under different boundary condition for identifying optimum thickness ratios for higher damping.

1.3 ORGANISATION OF THESIS

The thesis is organized as follows.

Chapter 1 introduces the need for enhancing the damping of a structure. This chapter also brings out the motivation and objectives of the present work.

Chapter 2 brings out the research work presented by various investigators for modelling the viscoelastic materials, finite element models of sandwich beams and plate structures and the scope of the present research work.

Chapter 3 gives a brief review on the constitutive relations of viscoelastic materials, experiments for determining the frequency dependent material constants. It also includes the mathematical representation of the frequency dependent material constants. Two viscoelastic materials (EAP-2 and EAP-43) are characterised for their frequency dependent material properties.

Chapter 4 deals with the formulation of finite element based dynamic model of sandwich beam and plate structures. The dynamic model incorporates the frequency dependent Young's modulus, shear modulus and loss factors of the viscoelastic material. Dynamic equations of motion are developed using Lagrangian method.

Chapter 5 deals with an iterative computational scheme to solve the dynamic equations of motion with base excitation.

Chapter 6 deals with the details of instrumentation, preparation of test specimens, test setup and experimental procedure. Frequency response functions (FRFs) are obtained from the experimental data. Loss factors are calculated from the FRF's.

Chapter 7 deals with the validation of the dynamic models of sandwich beam and plate structures with experimental results. Eight case studies are considered to validate the dynamic models. Four of these cases are sandwich beam structures and four are sandwich plate structures.

Chapter 8 deals with the simulation studies of the sandwich plate structures using developed dynamic model. The objective of these simulation studies is to enhance the damping in

sandwich plate structures. Damping loss factors are obtained for different thickness proportions under various boundary conditions to identify optimal parameters.

Chapter 9 presents the summary and conclusions. It also includes the scope for further research in this field.

CHAPTER 2

LITERATURE SURVEY

2.1 INTRODUCTION

Minimisation of resonant vibrations is a major design consideration for structures subjected to cyclic loading. This makes damping an important parameter in the study of dynamic behaviour of structures. Damping is the phenomenon by which mechanical energy is dissipated in a dynamic system thereby reducing the vibration amplitudes. Hence, improvement of damping in the structures through various techniques has been attracting researchers for the past several years. The mechanism of damping is complex and sometimes difficult to comprehend. There are many ways of energy dissipation in a vibrating system and often more than one mechanism may be present simultaneously. The energy dissipation in a vibrating structure is mainly due to the material damping, structural damping and viscous damping. Among the available techniques, sandwiching viscoelastic layers in the parent structures is one technique to enhance damping. In this chapter, the published literature in the area of viscoelastic damping and the research work carried out by various investigators on finite element models of sandwich structures using viscoelastic layers is presented.

2.2 STATE OF THE ART

From the literature, it is understood that there are two types of damping treatment. They are unconstrained or free layer treatment and constrained layer treatment.

(A) UNCONSTRAINED LAYER DAMPING TREATMENT

In unconstrained layer damping treatment, the viscoelastic layer is glued to the surface of base structure as shown in Fig. 2.1. The mechanism of energy dissipation in unconstrained layer damping treatment is through cyclic extension or compression deformation of the damping layer during each cycle of flexural vibration of the base structure.

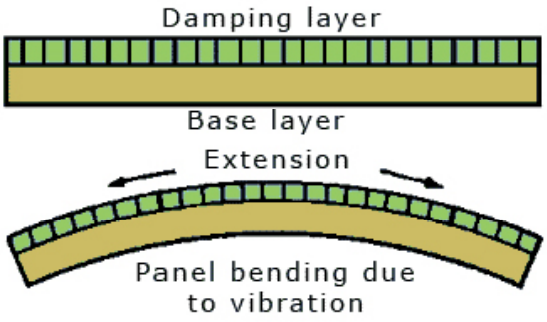

Figure 2.1 Unconstrained layer damping [48]

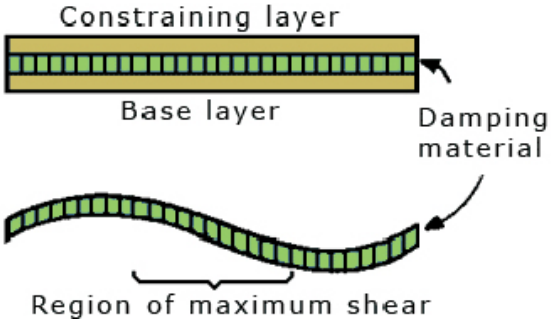

Figure 2.2 Constrained layer damping [48]

(B) CONSTRAINED LAYER DAMPING TREATMENT

In constrained layer damping treatment, a viscoelastic layer is constrained between base structure and a constraining layer as shown in Figure 2.2. The mechanism of energy dissipation in a constrained layer damping treatment is through shear deformation in the viscoelastic layer during each cycle of flexural vibration of the structure. Proper damping treatment requires the selection of appropriate damping material, location of the treatment and choice of configuration.

The published literature on sandwich structures is classified into three sub groups. It consists of modelling of viscoelastic materials, modelling of sandwich beam structures and modelling of sandwich plate structures with viscoelastic layers. The work carried out in each group is presented below.

2.2.1 VISCOELASTIC MATERIAL MODELS

The fundamental concepts and methods to characterize viscoelastic materials are presented by **Nashif et al (1985).** The detail of test setup and procedures for measurement of complex modulus of the viscoelastic materials is discussed by the author. When a viscoelastic sample is subjected to harmonic force, the steady state response around resonance is used to determine the damping. The complex modulus of the viscoelastic material depends on steady state harmonic excitation and temperature.

The temperature nomogram presented by **Jones (2001)** is considered as a standard temperature nomogram for representing complex modulus data. Using this nomogram, complex elastic modulus is obtained for a certain frequency and temperature. Nashif et al have shown such nomogram for various viscoelastic materials in this book.

Classical damping like Maxwell, Kelvin and Zener models available in the literature are reviewed by **Sun and Yu (1995)**. Fractional derivative model for describing viscoelastic material behaviour is presented by **Bagley and Torvik (1983)**. The author expressed the complex modulus of the viscoelastic material in Laplace domain as follows.

$$E^* = \frac{E_0 + E_1 s^\alpha}{1 + b s^\beta} \tag{2.1}$$

Five parameters $E_0, E_1, \alpha, \beta, b$ are used to curve fit the experimental data. This model is good only in the frequency domain. The drawback in their model is that it is difficult to transform frequency domain complex modulus into time domain using fractional derivative.

Some of the damping models that are developed by fitting a curve using the experimental data of viscoelastic materials are, Augmented Thermodynamic Field (ATF), An-elastic displacement field (ADF) and Golla Hughes & McTavish (GHM) models. These three models use an additional dissipation coordinate to account for the frequency dependent complex modulus. The ATF and ADF models are developed by **Lesieutre et al (1990, 1995)**. These are time domain models representing viscoelastic material behaviour, which also preserves the characteristics of frequency dependent modulus of the viscoelastic material. According to **Vasques et al (2010**), the limitations in using ATF and ADF are that they are first order damping models and only state space forms can be used to combine with structural analytical models.

Golla et al (1985) developed GHM model. It is a second order Laplace equation to represent variation of complex elastic modulus with frequency. Mini oscillators are used to represent the behaviour of viscoelastic material. The parameters used in the mini oscillators to curve fit the experimental data are, the storage modulus and the loss factor that vary with frequency and temperature. Once these parameters are obtained from the curve fit, the GHM model can be used in the conventional dynamic structural analysis of sandwich structures. According to **Vasques et al (2010),** the limitation of GHM model is increase in the size of the element stiffness matrix due to the additional dissipation coordinate. In their review paper on viscoelastic damping technologies, **Vasques et al (2010)** discussed about the constitutive model including the historical developments of viscoelasticity. According to the authors, it is difficult to develop a mathematical model considering the effects of frequency, temperature, amplitude and type of excitation simultaneously. Many researchers have overlooked the effects of amplitude and type of excitation. For practical considerations, isothermal conditions are assumed and they focused on developing frequency dependent constitutive models. The modelling of storage modulus proposed by **Fernando Cortes et al (2006)** is constant with frequency and loss factor is the representative peak damping of the material.

Martinez et al (2010) considered two mathematical models for viscoelastic materials using homogenized and multi layered approaches. The frequency dependent complex shear modulus is represented as a function of polynomial involving many coefficients. These are complicated models where many coefficients have to be determined by fitting a curve to the experimental data and are also difficult to be transformed into time domain.

From the above literature on viscoelastic material models, it is found that most of the authors used the commercially available data sheets of viscoelastic materials. The viscoelastic models mentioned in the literature are complex and many parameters are required to fit a curve for representing the viscoelastic behaviour. The proposed work provides a simple relation between storage modulus, loss factors and frequency with few parameters.

2.2.2 SANDWICH BEAM STRUCTURES

A sandwich beam comprises of base layer, constrained layer and constraining layer. The constrained layer is usually a viscoelastic layer. The modelling of sandwich structures is a

challenging task due to frequency dependent properties of viscoelastic materials. A summary of the analytical models of sandwich beams developed by various investigators is discussed below.

Kerwin et al (1959) proposed the analysis of the sandwich beam with viscoelastic layer using a complex modulus approach. The simply support boundary condition is considered during modelling of sandwich structure. A theory has been developed to calculate the loss factor of sandwich beam. Also relationship between the shear strains of the damping layer to the transverse motion of the structure has been presented in this paper. This theory is accurate only for thin constrained layer sandwich beams and for small loss factors of the viscoelastic layer.

DiTaranto et al (1965) modified **Kerwin et al (1959)** model by considering the extensional deformation of viscoelastic layer. A sixth order linear differential equation of motion for freely vibrating sandwich beams is developed in terms of longitudinal displacements. The assumptions introduced by this model are that both the elastic layers undergo same lateral displacement and only transverse inertia is considered neglecting the longitudinal inertia. Shear deformation is considered only for the viscoelastic layer and shear strain is assumed to be constant through the thickness of viscoelastic layer. From this model, natural frequencies and composite loss factors are obtained for a three layer sandwich beam. The authors have concluded that for a given thickness of viscoelastic layer, the variation of composite loss factors with frequency does not change appreciably by changing the thickness of the elastic layer. The authors have also concluded that the relationship between the modal loss factors of the sandwich beam and the corresponding modal frequency is independent of boundary conditions.

Mead and Markus (1969, 1970) modified **DiTaranto's** model and developed a sixth order differential equation considering the transverse motion of a harmonically excited sandwich beam. Natural frequencies and loss factors are estimated for sandwich beam using these equations.

Di Taranto (1965) and **Mead et al (1969, 1970)** used Kerwin's assumptions, which account for the complex modulus for the viscoelastic layer. They concluded that the dissipation of energy is through shear deformation of the viscoelastic layer. The authors have

examined the developed model for various possible boundary conditions encountered in practice.

Nakra (1976, 1981 and 1984) and Mead (1982) reviewed the work carried out by previous investigators and discussed the similarities and differences between various theories.

Douglas and Yang (1978) studied the passive constrained layer damping (PCLD) treatment for beam structures. Experiments were conducted to obtain the dynamic responses and compared them with theory. They considered two types of damping mechanisms in a sandwich beam structure. The first mechanism is due to shear deformation and is called shear damping. The other type of mechanism is due to relative transverse motion of base and constraining layer and is called as compression damping in the viscoelastic layer. They concluded that shear damping is a broad band mechanism useful in most engineering applications, whereas the compression damping must be considered only within a certain spectral band. The damping of transverse dynamics of the thin sandwich beam is outside the spectral influence of compression damping. Therefore, the shear damping mechanism was mainly considered in thin sandwich structures. The authors also presented the comparison of experiment results with the model developed by Mead and Markus model (1969). From the results, it is understood that Mead and Markus model deviates from the experimental results at higher modes.

Johnson et al (1982) proposed finite element model to predict the characteristics of constrained layer damped structures. The authors considered solid element (Hexa8) for the viscoelastic layer and quadrilateral thick shell element with offsets for the base and constraining layer structure. Nastran software is used for the analysis of constrained layer damped structure. They derived an expression for the modal loss factor from purely elastic analysis by suppressing the imaginary part of complex stiffness. The Modal Strain Energy (MSE) method is used to predict the loss factors. The MSE method overestimates the loss factors at high modes.

Soni et al (1982) presented isoparametric thin shell elements for the base and constraining layer and solid element (Hexa8) for the viscoelastic layer. However **Mace (1994)** has criticized both Johnson et al and Soni et al work. The author has mentioned that the above two approaches are complex and costly to use.

Mace (1994) has modelled the constrained layer sandwich beam structure using finite element technique. A layer wise displacement field is considered to study the dynamic behaviour of sandwich beams. The author developed FE model for very thin viscoelastic layer and five degrees of freedom per node is considered. However, it is found to be less accurate compared with FE models developed by **Jonson et al (1982)** and **Soni (1982).**

Bai et al (1995) proposed a finite element model for harmonically excited viscoelastic sandwich beam. A three layer sandwich beam is considered in which base and constraining layer are elastic and isotropic. Non linear longitudinal and transverse displacement fields are considered for the viscoelastic layer. The author has considered adhesive effect in the FE model. The stiffness at the interface between viscoelastic layer and base beam and constraining layer possesses finite value. Due to this, discontinuity in the longitudinal displacements is observed which is proportional to the shear stress.

Baber et al (1998) extended the FE model presented by **Bai and Sun.** The adhesive is considered as stiff layer and neglected during formulation of FE model. Twelve degrees of freedom per node is considered during FE formulation. Both **Bai et al and Baber et al** models found to be complex and computationally expensive. The author's have neglected frequency dependent loss factors in their FE model.

Tso-Liang et al (2001) investigated the damping characteristics of the sandwich beam with viscoelastic layer. The constrained layer damping structures are modelled using Ross-Kerwin-Ungar (RKU) equations. The effect of various parameters like frequency, temperature, length and thickness of damped structure on the vibration characteristics are presented in this paper. The author has not presented experimental work to validate the theoretical model. **DiTanto** and **Mead et al** improved the **Kerwin (1959),** where as the author used **Kerwin (1959)** model without considering these improvements.

Wang et al (2002) proposed a sandwich beam with viscoelastic layer using spectral finite element method (SFEM). The displacement fields considered in the model are exponential (higher order polynomials) in nature compared to lower order polynomials in conventional finite element model (CFEM). GHM method is used to model the viscoelastic layer which considers the complex storage modulus. To account for the frequency dependent complex modulus, an internal dissipation coordinate is added which increases the size of the stiffness matrix and also increase computational time.

Barbosa and Farage (2008) presented a GHM based finite element model for sandwich viscoelastic beam. Experiments are carried out to evaluate the GHM parameters. The model is validated with experiments by comparing frequency domain response curves. To account for the frequency dependent complex modulus, an internal dissipation coordinate is added which increases the size of the stiffness matrix and also increase computational time.

Zapfe et al (1999), Trindade (2001), Sainsbury and Zhang (1999) and **Galucio (2004)** developed FE models of sandwich beams using viscoelastic layers. The authors have not considered frequency dependency of loss factors in their model.

Fernando Cortes and Maria Jesus Elejabarrieta (**2008**) analyzed the dynamic behaviour of free layer damping beams with a thick viscoelastic layer. The viscoelastic material is characterized by a fractional derivative model, which takes into consideration the variation of complex modulus with frequency. The complex modulus is represented in Laplace domain and it is difficult to transform this into time domain using fractional derivative.

Kamel A et al (2009) proposed a sandwich finite element for laminated steels. It is based on discrete displacement approach and allows for both symmetrical and unsymmetrical configurations. The three layer sandwich beam is modelled considering Timoshenko hypothesis for viscoelastic layer and Euler-Bernoulli hypothesis for base and constraining layer. The model accounts for the rotational influence of the transverse shear in the viscoelastic layer. The results obtained using this model is validated with analytical, finite element model for various boundary conditions. Frequency dependent loss factors are not considered in the FE model and they validated the model with previous published literature.

Martinez et al (2011) have carried out dynamic characterization of high damping viscoelastic material from vibration test data. In this paper, an inverse method is developed to characterize high damping and strong frequency dependent viscoelastic material. This method minimizes the difference between the theoretical and experimental transfer functions obtained by the forced vibration test with resonance at certain discrete frequencies selected by the user. In this method, the parameters of the material constitutive model are identified and the properties are determined in the whole bandwidth. In this paper, the constrained layer damping (CLD) structure is completely characterized. The elastic properties of the metallic layers and the viscoelastic material properties are identified from the dynamic response.

Grewalet al (2013) presented sandwich beam structure using finite element method. Linear and non linear displacement fields are considered for viscoelastic layer. Results obtained by both the methods are compared with experimental data available in the literature. The results obtained by linear and non linear finite element models for the natural frequency and loss factors at the first mode of clamped-free sandwich beam model do not show considerable difference. However, the results differ at higher modes for clamped-clamped boundary condition. Non-liner finite element model show lower natural frequencies and higher loss factors compared to the results obtained from linear finite element model. The author validated the model with published literature. From the results it is observed that, the loss factors obtained from his models are over estimated compared to experimental results.

Won et al (2013) proposed a sandwich beam element using virtual work principle. The virtual strain energy and potential energies of the sandwich beam element are expressed in terms of the lateral displacements and the transverse shear strain of the viscoelastic layer. The forced vibration equations of constrained layer sandwich required three pairs of boundary of conditions. So, the rotation of the mid surface derived from the lateral displacements is added for the sandwich beam element to have three degrees of freedom per node. The shape functions are analytically derived using the compatibility relation between the lateral displacement and the transverse shear strain. The developed beam element is validated with Nastran-3 D element. This developed sandwich beam is valid only for symmetric structure and further refinement is required for the forced vibration analysis of asymmetric sandwich beam structures. The author has validated the developed beam element with experiments.

From the above literature, it is understood that most of the authors did not consider the variation of loss factors with frequency in their model and not validated with experimental results. Most of the author validated their model with those of previous investigators. Many authors have validated their models using the data of viscoelastic material **scotchdamp, 3M (1993)** that is readily available in the open literature. It is also found that very few authors have validated their model with experimental results. Most of the authors consider force excitation for computing the frequency responses on the sandwich beam structure.

2.2.3 SANDWICH PLATE STRUCTURES

The analytical models based on FE formulation of sandwich plates developed by various investigators are presented below.

Ross et al (1959) investigated simply supported plates and assumed a perfect interface and compatibility of transverse displacement in each layer. The simply support boundary condition is considered during FE modelling of sandwich plate. A theory has been developed to calculate the loss factor of sandwich plate. Also relationship between the shear strains of the damping layer to the transverse motion of the structure has been presented in this paper. This theory is accurate only for thin constrained layer sandwich plates and for small loss factors of the viscoelastic layer. The authors have not considered the variation of loss factor with frequency and used same loss factor in tension and shear.

DiTaranto and McGraw (1969) studied three layer asymmetric sandwich plate structures. Only transverse inertia effect of the sandwich plate is considered during the analysis. Simple support at the four edges is considered as boundary condition. The author has presented relationship between modal frequencies and loss factors similar to one presented for the sandwich beam results (1965).

Sadasiva Rao et al (1974) studied unsymmetrical sandwich plate with viscoelastic layer. Previous work in this area is reviewed and it is found that only transverse inertia of the sandwich plate is considered during analysis of sandwich plate neglecting longitudinal inertia. In addition to transverse inertia, longitudinal transverse inertia and rotary inertia is also considered during analysis of sandwich plate. The base plate and constraining layer chosen for this work are isotropic and elastic and the constrained layer is considered as viscoelastic layer. The influence on the longitudinal inertia on the response of sandwich plate is presented. The longitudinal stress of the sandwich plate is considerably affected by the inclusion of these inertias.

Ioannides et al (1979) presented a Finite element analysis of damped three layer plate under harmonic excitation. The base and constraining layer are isotropic and viscoelastic layer is used as constrained layer. Damping has been introduced by replacing the real modulus of viscoelastic material by a complex modulus. Triangular elements are considered during FE formulation and the dynamic stiffness for the sandwich plate is computed. The FE results are validated with experiments.

Lu et al (1979) presented analysis of damped plate structure for free-free boundary condition using NASTRAN. Experiments are also carried out in free-free boundary conditions to validate the FE model. They assumed constant Poisson's ratio of 0.48 for viscoelastic layer. The Young's modulus is derived from the shear modulus using constitutive relationship. The author has considered same loss factors in tension and shear mode.

Asnani et al (1984) investigated dynamic analysis of multi-layered rectangular plates with constrained viscoelastic layer. A Multi-layered plate is considered with arbitrary number of stiff and soft layer. Extension, bending and shear deformation is considered for stiff layers and only transverse shear deformation is considered for viscoelastic layers. The authors have presented results for three, five and seven layer sandwich structure. The results show that, the loss factors increases with increase in number of layers. The longitudinal, transverse and rotary inertias along with the transverse inertia are considered in the analytical model. Both symmetric and asymmetric sandwich structures are presented in this paper. Symmetric sandwich structures provide slightly higher loss factors compared to asymmetric sandwich structure.

Ganeshan et al (1986) carried out analysis of unconstrained layer plate. The unconstrained layer plate results are compared with base plate. Different layer thicknesses are considered and the variation of loss factor with thickness is presented. The author concluded that loss factors increases with increase in layer thickness.

Ha K.H (1990) has presented an overview of finite element analysis of sandwich plates till 1990. Finite element models presented by various investigators are analyzed by the author and classified them into two categories based on the type of finite element used. The first type of finite element is based on the assumed displacement approach and the second type is based on the assumed stress hybrid approach. Within each element, the characteristics vary in terms of the formulation, complexity, accuracy and applicability.

Lee et al (1996) investigated finite element analysis of composite sandwich plate. The base plate and constraining layer are composite (orthotropic) and viscoelastic layer is used as constrained layer. The sandwich plate is modelled using Reissner -Mindlin plate theory. The displacement fields of the viscoelastic layer are linearly interpolated in terms of the displacement of the base and constraining layer. The authors presented the effect of transverse normal deformation of the viscoelastic core on the sandwich plate when it is subjected to static load and free vibrations. From the analytical studies, it is concluded that transverse normal deformation of the viscoelastic core should not be neglected and natural frequencies

decreases when the viscoelastic layer is considered to be flexible. The limitation of this model is that the viscoelastic layer is considered as homogenous and its properties do not vary with frequency.

Cupial et al (1995) analysed the natural frequencies and loss factors for a rectangular three layered plate. The base and constraining layers are composite plates and viscoelastic layer is chosen as the constrained layer. First order shear deformation theory is considered during modelling of sandwich plate. Results of numerical analysis are presented for simple supported boundary condition. The results are compared with and without considering shear deformation of the base and constraining layers. Young's modulus, shear modulus and loss factors are considered as constant during numerical simulations.

Wang et al (2003) studied sandwich plate structure using viscoelastic layer as a constrained layer. The base and constraining layer are elastic and isotropic material where as viscoelastic layer is used as a constrained layer. GHM method is used to account for the frequency dependent complex shear modulus of the viscoelastic layer. For the base plate CFCF boundary condition and for the constraining and constrained layers FFFF boundary conditions are considered in the model. The numerical results are validated with experiments. The errors in the loss factors are found to be high.

Hammami et al (2005) presented sandwich plates using viscoelastic layer. The author has considered quadrilateral plate element with seven degrees of freedom per node during modelling of the sandwich plate. In this work, main focus is on characterization of modal damping sandwich plate coefficients and their assessment. The numerical results shows that eigen modes are not orthogonal to the damping matrix but are only weakly coupled. The modal damping matrix coefficient vary according to the ratio of the core thickness to the total thickness of sandwich plate and follow a second order polynomial function of this ratio. The author has not validated the model with the experimental results.

Torvik and Runyon (2007) investigated the loss factor of rectangular sandwich plates with CLD treatment for various boundary conditions. A method is developed and validated predicting loss factors for different boundary conditions for asymmetric sandwich plate. The method is referred as equivalent lengths. This method is used in predicting the loss factors of sandwich plate using the loss factors and natural frequencies obtained from RKU analysis of sandwich beams. Application of this method requires storage modulus, thickness and density of the base plate, constraining and constrained layer as well as natural frequency of the plate and boundary condition to which the constrained layer treatment is to be applied. This method

is validated with finite element method for various boundary conditions. The Young's modulus, shear modulus and loss factors are considered as constant and do not vary with the frequency.

Saeed et al (2012) presented transverse response of sandwich plate with viscoelastic core under random excitation. Quadratic displacement field is adopted for core to capture higher modes under random excitation. The Love-Kirchhoff plate theory is considered for base and constraining layers. GHM is used to model the viscoelastic layer taking care of complex storage modulus. To account for the frequency dependent complex modulus, an internal dissipation coordinate is added which increases the size of the stiffness matrix.

Zhicheng et al (2014) investigated vibration and damping characteristics of sandwich plates with viscoelastic layer. The sandwich plate element is modelled as a four node rectangular element with seven degrees of freedom at each node. First order shear deformation theory is used for all the layers. The finite element equations of motion are derived using the Hamilton principle in variational form. Numerical examples are given to validate the developed model. The influence of layer thickness, loss factors of the viscoelastic layer on the natural frequency are presented. The author has not accounted for the frequency dependent material properties of viscoelastic layer and not validated the model with experiments.

From the above literature, it is understood that most of the authors did not consider the variation of loss factors with frequency in their model and not validated with experimental results. Most of the authors considered forced excitation for computing the frequency responses on the sandwich plate structure. The exciter dynamics also contributes to the estimation of the loss factors of sandwich plate structure. This research gap can be filled with the proposed base excitation method which can accurately predict the loss factors of the sandwich structures.

2.3 SCOPE OF THE PRESENT RESEARCH

The literature review on modelling of sandwich beam and plate structures with viscoelastic layers is well reported. However, improving the effectiveness and accuracy of solutions for those sandwich structures is still an important goal. In the present work, two viscoelastic materials developed for defence applications have been characterized and used in the dynamic models of sandwich beam and plate structures. Further, a better dynamic model

for sandwich beam and plate structures along with a computational scheme to solve the dynamic equations of motion is presented. This dynamic model considers the frequency dependent materials properties of the viscoelastic material that is ignored by the previous investigators. The results with and without considering the viscoelastic material properties are validated with experimental results.

2.3.1 VISCOELASTIC MATERIALS AND MODELLING

In the present work, two viscoelastic materials have been characterized using Dynamic Mechanical Analyzer (DMA). The frequency dependent material properties like: Young's modulus, shear modulus and loss factors are obtained by testing the viscoelastic samples in tension and shear mode. The obtained experimental data from DMA is expressed in mathematical form using power fit. These mathematical expressions are used during the development of dynamic models of sandwich beam and plate structures.

2.3.2 SANDWICH BEAM STRUCTURES

In the present work, a sandwich finite element is developed considering the frequency dependent material properties of the viscoelastic material. The model is based on the discrete displacement approach and curvature effect is taken into account. It is a beam element with four degrees of freedom per node. The primary field variables are longitudinal displacements of base and constraining layer and transverse displacement and rotation of sandwich beam. The element uses linear and cubic polynomial to interpolate longitudinal and transverse displacements. The rotational influence of the shear in the viscoelastic layer on the base and constraining layer ensures displacement consistency over the interface between the viscoelastic layer, base layer and constraining layer. Experiments have been carried out to validate the developed sandwich beam element to estimate frequency response functions, natural frequencies, amplifications and loss factors.

2.3.3 SANDWICH PLATE STRUCTURES

In the present work, a sandwich plate element is developed considering the frequency dependent storage modulus of viscoelastic material. The primary displacement field variables in the sandwich plate element are in-plane displacement of base and constraining layer, rotation of base and constraining layer and transverse displacement of sandwich plate. It is a quadrilateral plate element with nine degrees of freedom. The model is based on the discrete displacement approach and also account for the curvature effect. The transverse shear deformation of viscoelastic layer is obtained from the in-plane displacements and rotations of the base and constraining layer. The rotational influence of the transversal shear in the viscoelastic layer on the base plate and constraining layer ensures displacement consistency over the interface between the viscoelastic layer, base plate and constraining layer. Experiments have to be carried out to validate the developed sandwich plate element to estimate frequency response function, natural frequencies, amplification factors and loss factors.

2.3.4 SIMULATION STUDIES

In the present work, simulation studies are carried out to identify optimal layer thicknesses for a given sandwich plate thickness to achieve high loss factors. Damping loss factors are obtained for different thickness proportions under various boundary conditions to identify these optimal parameters.

2.4 SUMMARY

The published literature on viscoelastic material models and FE model of sandwich beam and plate structures by various investigators are presented in this chapter. From the literature it is understood that the frequency dependent material properties like Young's modulus, shear modulus, loss factors and Poisson's ratio of the viscoelastic materials are not considered during modelling of sandwich structures. Based on this literature, the research problem is identified and scope of the work is presented.

CHAPTER 3

VISCOELASTIC MATERIALS AND THEIR CHARACTERIZATION

3.1 INTRODUCTION

The objective of this chapter is to describe the behaviour of viscoelastic materials and their characterization through DMA tests. The viscoelastic material plays a significant role in enhancing the damping of a sandwich structures. Hence, it is necessary to understand their behaviour in detail. Two viscoelastic materials developed for Defence application are chosen for this study.

Viscoelasticity is defined as material response that exhibits characteristics of both viscous fluid and an elastic solid. An elastic material regains its original shape when stretched and released, whereas viscous fluid retains its deformed shape. Viscoelastic material (VEM) combines these two properties. It returns to its original shape after being stressed, but does it slowly enough to oppose the next load cycle. The degree to which a material behaves either viscously or elastically under cyclic loading depends on temperature and frequency. The material properties namely Young's modulus, shear modulus and loss factors of viscoelastic material are generally represented in complex modulus form. The complex modulus brings in lot of convenience in understanding the behaviour of viscoelastic materials. The properties of

viscoelastic material depend significantly on environmental and loading conditions such as temperature, frequency, pre-load and humidity etc.,

3.2 BEHAVIOUR OF VISCOELASTIC MATERIALS

Viscoelastic material exhibits both elastic and viscous behaviour. The time responses of stress and strain behaviour under cyclic loading for an ideal elastic and viscous material are shown in Figures 3.1and 3.2. For an ideal elastic material, dynamic stress $\sigma(t)$ is linearly proportional to dynamic strain $\epsilon(t)$, where the proportionality constant is Young's modulus 'E' related by the standard expression as follows.

$$\sigma(t) = E\epsilon(t) \tag{3.1}$$

From the stress strain behaviour as shown in Figure 3.1, it can be observed that the stress and strain for elastic materials are completely in phase. In this process, energy is completely conserved i.e. during loading the work done by external force is stored in the form of strain energy and this entire energy is released during unloading cycle. The stress-strain behaviour of ideal viscous material is shown in Figure 3.2. Under cyclic loading, the strain lags the stress by a quarter time period indicating that the stress is proportional to rate of strain. The proportionality constant is the coefficient of viscosity (μ_v). This is a non conservative process and the work done by the applied force is dissipated due to phase lag between stress and strain. The constitutive relation for this ideal viscous material is given as follows.

$$\sigma(t) = \mu_v\dot{\epsilon}(t) \tag{3.2}$$

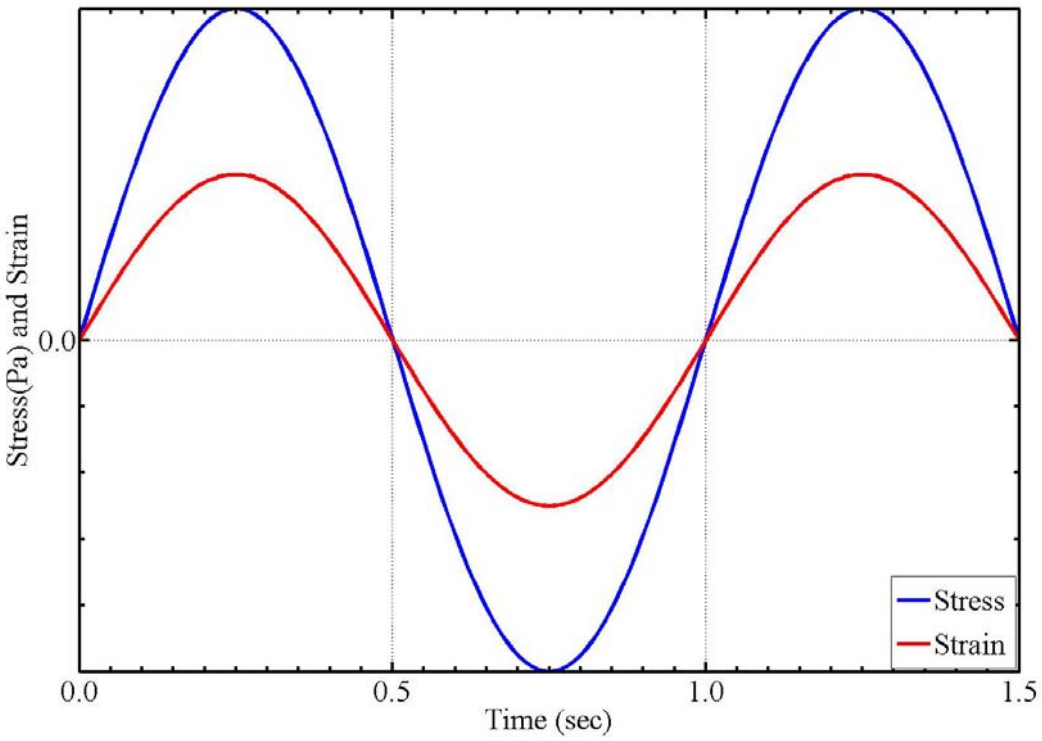

Figure 3.1 Response under cyclic loading for purely elastic material [22]

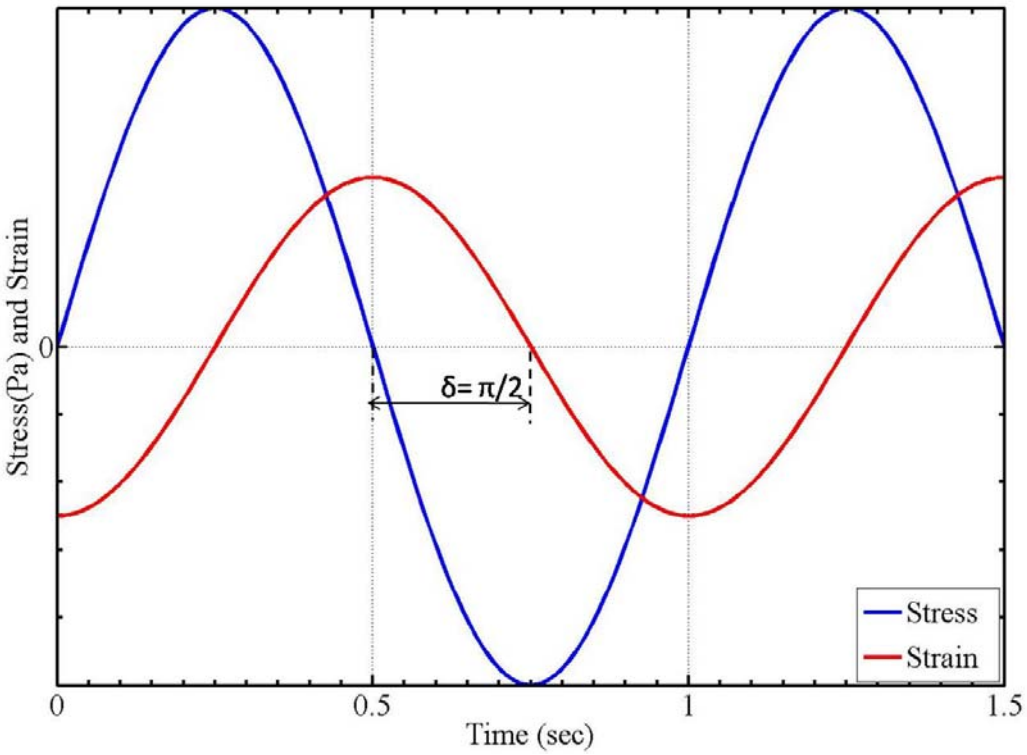

Figure 3.2 Response under cyclic loading for purely viscous material [22]

The viscoelastic material exhibits both elastic and viscous properties. The variation of stress and strain under cyclic loading for viscoelastic material is shown in Figure 3.3, where it

can be observed that strain lags the stress by less than a quarter period unlike ideal viscous fluid. When this time responses are seen in frequency domain, usually the phase is represented as an angular quantity(δ)expressed in radians. For viscoelastic materials, this phase angle (δ) is between 0 and $\pi/2$. Justifying their name, viscoelastic materials exhibit partly elastic and partly viscous behaviour. During a loading cycle, the energy associated with elasticity is conserved while the energy associated with viscosity is dissipated. The viscoelastic materials are characterized by the ratio of the energy dissipated to the total energy in a cycle. This energy dissipation is vital in vibration control as it deals with dissipation of energy which is causing vibration. This dissipation is referred as damping in the vibration terminology. The phase angle (δ) is a measure of the material damping. The larger the angle the greater is the damping.

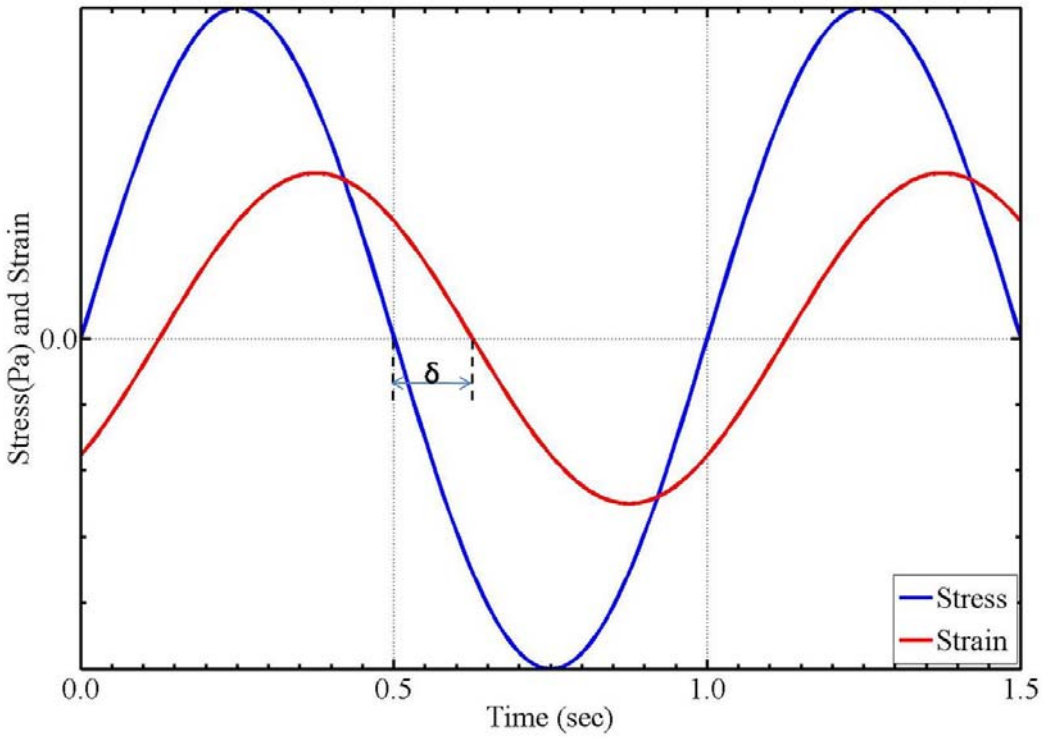

Figure 3.3 Response under cyclic loading for viscoelastic material [22]

For viscoelastic material, the stress is proportional to strain and strain rate. The constitutive relation for the time dependent stress and strain can be expressed as follows.

$$\sigma(t) = E\varepsilon(t) + \mu_v\dot{\epsilon}(t) \tag{3.3}$$

The dynamic stress and strain induced in viscoelastic material under harmonic force can be expressed as,

$$\sigma(t) = \sigma_0 \sin(\omega t) \tag{3.4}$$

$$\mathcal{E}(t) = \mathcal{E}_0 \sin(\omega t - \delta) \tag{3.5}$$

Where, σ_0 is the stress amplitude, $\mathcal{E}_0$ is the strain amplitude, ω is the frequency of excitation force and δ is the phase angle between stress and strain. By manipulating equation 3.4, it can be written as,

$$\sigma(t) = \sigma_0 \sin[(\omega t - \delta) + \delta] \tag{3.6}$$

By expanding the above equation, it can be expressed as follows.

$$\sigma(t) = \sigma_0[\sin(\omega t - \delta)cos\delta + \cos(\omega t - \delta)\, sin\delta] \tag{3.7}$$

Equation 3.5 can be re-written as follows.

$$\mathrm{Sin}(\omega t - \delta) = \frac{\mathcal{E}(t)}{\mathcal{E}_0} \tag{3.8}$$

By differentiating the above equation with respect to time and suitable manipulation, it can be expressed as,

$$\cos(\omega t - \delta) = \frac{1}{\omega\, \mathcal{E}_0} \frac{d\mathcal{E}(t)}{dt} \tag{3.9}$$

By substituting equation 3.8 and 3.9 in equation 3.7, it can expressed as follows,

$$\sigma(t) = \frac{\sigma_0}{\mathcal{E}_0} \mathcal{E}(t) cos\delta + \frac{\sigma_0}{\omega \mathcal{E}_0} \frac{d\mathcal{E}(t)}{dt} sin\delta \tag{3.10}$$

The term corresponds to $\frac{\sigma_0}{\mathcal{E}_0} cos\delta$ and $\frac{\sigma_0}{\omega \mathcal{E}_0} sin\delta$ in the above equation are replaced with E' and E'', it can be expressed as follows,

$$E' = \frac{\sigma_0}{\mathcal{E}_0} cos\delta \;\; ; \quad E'' = \frac{\sigma_0}{\omega \mathcal{E}_0} sin\delta \; ; \tag{3.11}$$

By substituting E' and E'' of the equation in equation (3.10), it can be expressed as follows,

$$\sigma(t) = E' \mathcal{E}(t) + E'' \frac{d\mathcal{E}(t)}{dt} \tag{3.12}$$

Where, E' is known as storage modulus and E'' is known as loss modulus and it depends on frequency of loading and unloading cycle.

By introducing $\eta = \tan\delta$ and manipulating equation (3.11), it can be expressed as

$$\frac{E''}{E'} = \frac{tan\delta}{\omega} = \frac{\eta}{\omega} \tag{3.13}$$

By substituting the above equation in equation (3.12), it can be expressed as follows,

$$\sigma(t) = E' \mathcal{E}(t) + \frac{E' \eta}{\omega} \frac{d\mathcal{E}(t)}{dt} \tag{3.14}$$

The stress-strain relationship can also be expressed in terms of complex exponential function. The dynamic stress and strain can be expressed as follows

$$\mathcal{E}(t) = \mathcal{E}_0 \exp(j\omega t) \quad \text{and} \quad \frac{d\mathcal{E}(t)}{dt} = j\omega\mathcal{E}(t) \tag{3.15}$$

where, $j = \sqrt{-1}$

By introducing equation 3.15 in equation 3.12, it can be expressed as follows

$$\sigma(t) = E'\mathcal{E}(t) + \frac{E'\eta}{\omega} j\omega\mathcal{E}(t) = E'(1 + j\eta)\mathcal{E}(t) \tag{3.16}$$

$$\frac{\sigma(t)}{\mathcal{E}(t)} = E^* = E(1 + j\eta) \tag{3.17}$$

where E^* is the complex Young's modulus of viscoelastic material.

Similarly, the dynamic stress and strain induced in viscoelastic material under harmonic shear force can be expressed as

$$\tau(t) = G'\varphi(t) + \frac{G'\eta}{\omega}\frac{d\varphi(t)}{dt} \tag{3.18}$$

$$\varphi(t) = \varphi_0 \exp(j\omega t) \quad \text{and} \quad \frac{d\varphi(t)}{dt} = j\omega\varphi(t) \tag{3.19}$$

$$\tau(t) = G'(1 + j\eta)\varphi(t) \tag{3.20}$$

$$\frac{\tau(t)}{\varphi(t)} = G^* = G(1 + j\eta) \tag{3.21}$$

where, G^* is the complex shear modulus of viscoelastic modulus

Equations (3.17) and (3.21) give the complex modulus relationship for Young's modulus and shear modulus respectively. From these equations it is clearly evident that Young's and shear modulus also called as storage modulus are dependent on frequency.

3.3 EFFECT OF FREQUENCY

The frequency is one of the important factors affecting the dynamic properties of viscoelastic materials. Figure 3.4 shows the effect of frequency on storage modulus and loss factor [22]. Experiments have shown that vibration frequency or the rate of loading has significant effect on the loss factor and storage modulus of viscoelastic materials. In the rubbery region, the storage modulus and loss factor increase slowly with frequency. In the transition region, the storage modulus increases rapidly with frequency, whereas the loss

factor increases for some portion of frequency and then decreases rapidly with frequency. In glassy region, the storage modulus increases slowly whereas the loss factors decreases rapidly with frequency.

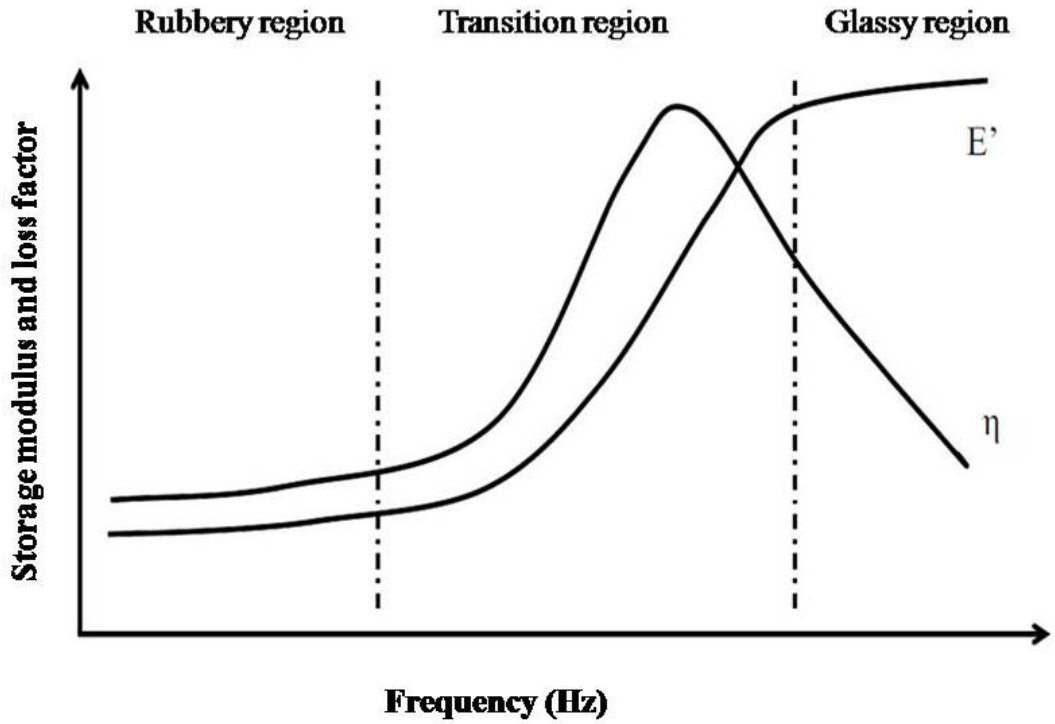

Figure 3.4 Effect of frequency on storage modulus and loss factor [22]

3.4 EFFECT OF TEMPERATURE

The temperature is also an important environmental factor affecting the dynamic properties of viscoelastic materials. The typical variation of storage modulus and loss factor [22] with temperature for a viscoelastic material is shown in Figure 3.5. It has four distinct regions. The first region is glassy state where the material has very large storage modulus (dynamic stiffness) but very low loss factor. The storage modulus in this region changes slowly with temperature, while the loss factor changes significantly with increasing temperature. In the transition region where the material changes from a glassy state to a rubbery state, the material modulus decreases rapidly with increasing temperature. Due to increase in temperature, the viscoelastic material softens and this is the reason for increase in

loss factor in this region. The loss factor usually peaks around the glass transition region. In rubbery stage, both modulus and loss factor decreases slowly with temperature. The flow region is typical for a few damping material such as vitreous enamels and thermoplastics, where the material continue to soften as temperature increases while the loss factor reach very high value.

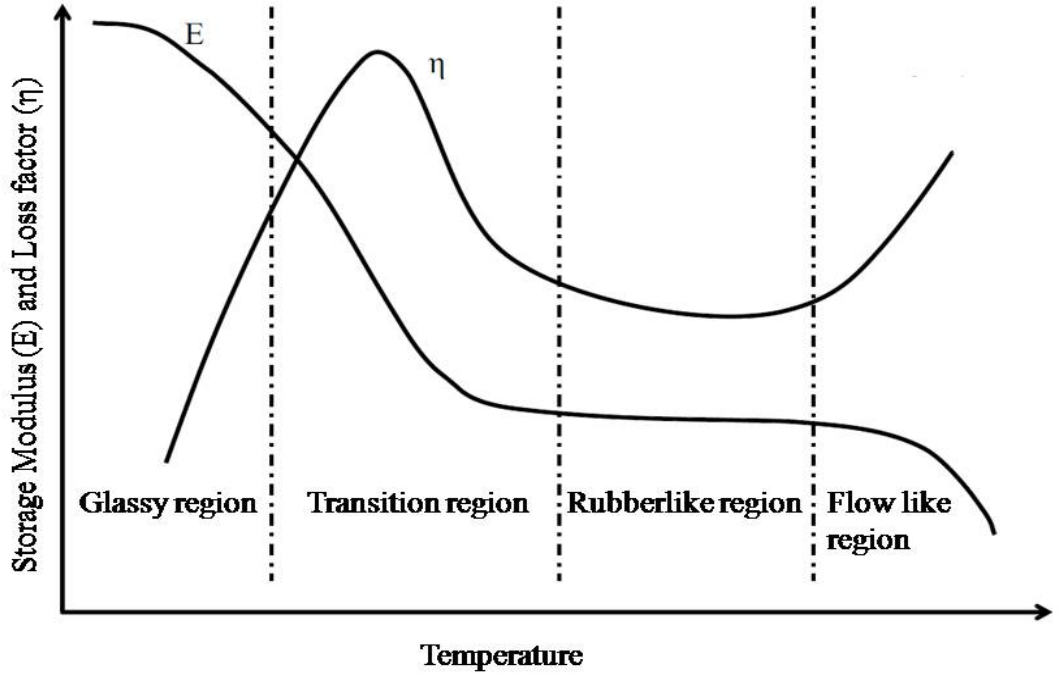

Figure 3.5 Effect of temperature on storage modulus and loss factor [22]

3.5 CHARACTERIZATION OF VISCOELASTIC MATERIALS

Two viscoelastic materials namely EAP-2 and EAP-43 developed for Defence applications are chosen in the present work and characterized using Dynamic Mechanical Analyzer (DMA). The properties of these viscoelastic materials namely Young's modulus, shear modulus and loss factors are frequency and temperature dependent. These properties are obtained at discrete frequencies from 10^{-2} Hz to 10^{6} Hz at room temperature. The frequency dependent data is expressed in a mathematical form using power fit to incorporate into the dynamic model. The polymers used in EAP-2 and EAP-43 are Nitrile Butadiene Rubber (NBR) and Polyvinyl Chloride (PVC) blend. The two materials differ in terms of type of filler used. EAP-2 has titanium dioxide as a pigment and semi reinforced filler, while EAP-43 has

carbon black as reinforced filler. The sample details of viscoelastic material are discussed in next section

3.5.1 SAMPLE DETAILS

The viscoelastic samples are prepared as per ASTM D4065 for tension and shear mode. The size of the sample for tensile mode is 50 mm X 10 mm X 2 mm and the size of the sample for shear mode is 15 mm X 15 mm X 2 mm. The photograph of samples holders for tensile and shear mode are shown in Figure 3.6.

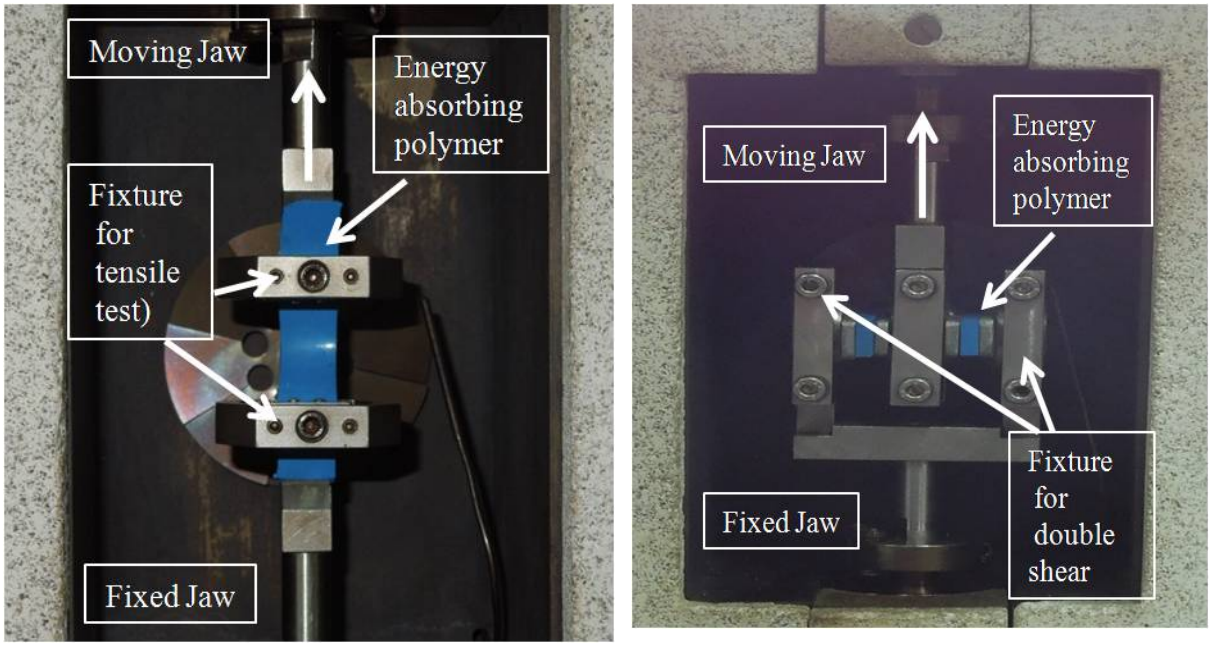

(a) Tension (b). Double Shear

Figure 3.6 Photograph of Energy Absorbing Polymer (EAP-2) with fixtures in DMA

3.5.2 DYNAMIC MECHANICAL ANALYZER (DMA)

Dynamic Mechanical Analyzer examines variation in viscoelastic material properties under thermal and dynamic loading. The DMA tests are carried out as per standard ASTM D4440-15. The instrument applies a sinusoidal stress and measures the resulting strain. The applied force is well within the linear viscoelastic range. The material properties of

viscoelastic materials are evaluated for a frequency range from 10^{-2} Hz to 10^{6} Hz at room temperature. Viscoelastic samples are placed in the holders either in tension mode or shear mode. The photograph of DMA is shown in Figure. 3.7.

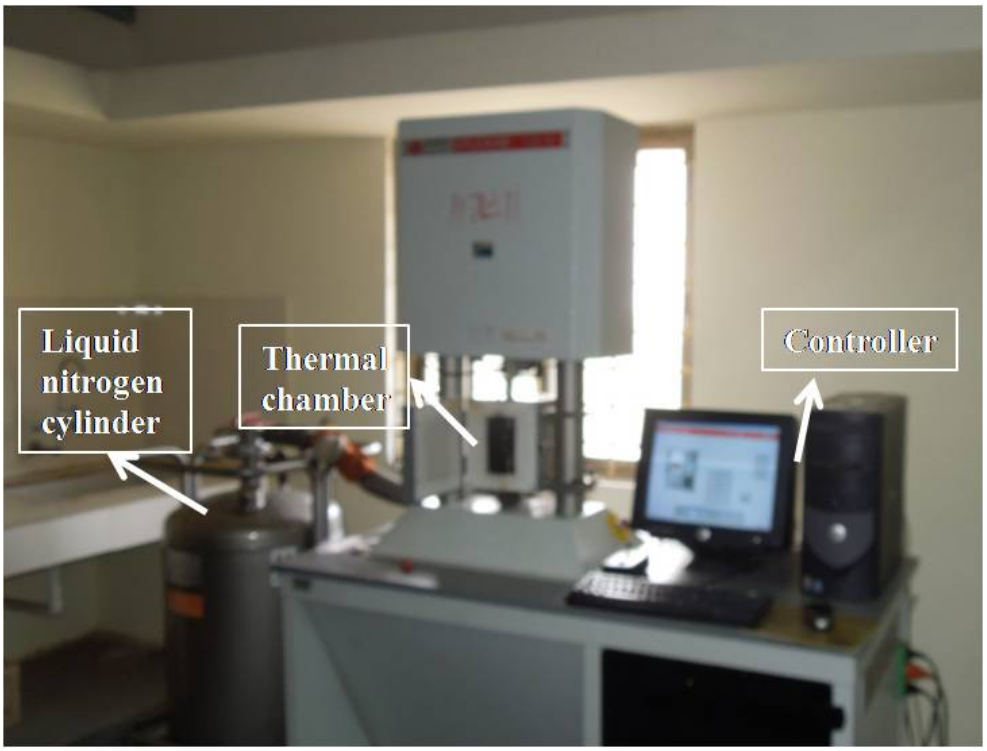

Figure 3.7 Dynamic Mechanical Analyzer (EPLEXOR 150 N)

DMA test allows the estimation of the Young's modulus (E'), loss modulus (E'') and loss factor (tan δ) by positioning the viscoelastic sample in tension mode. Similarly, for estimation of the shear modulus (G'), loss modulus (G'') and loss factor (tan δ) the viscoelastic sample is positioned in shear mode. These moduli are defined as the ratio of dynamic stress to dynamic strain developed in the viscoelastic material. Therefore, by measuring stress, strain and phase angle during the experiment, complex moduli of viscoelastic materials are calculated.

3.5.3 RESULTS OF DMA TEST FOR EAP-2 AND EAP-43

The two viscoelastic materials, EAP-2 and EAP-43 are characterized for their frequency dependent material properties. These materials are tested in tension and shear mode for discrete frequencies ranging from 10^{-2} Hz to 10^{6} Hz at room temperature. The experimentally obtained material data for EAP-2 along with curve fit are shown in Figures

3.8-3.11. The comparison of material properties of EAP-2 and EAP-43 with curve fit up to 1000 Hz are shown in Figures 3.12 to 3.15.

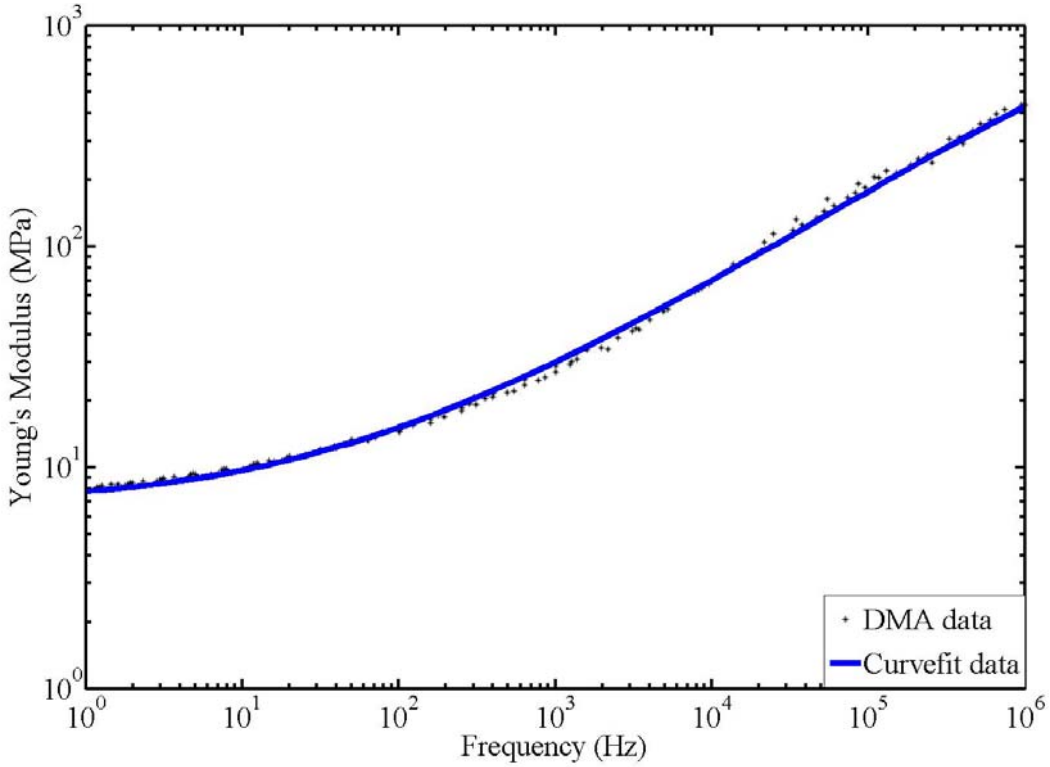

Figure 3.8 Variation of Young's modulus with frequency (EAP-2)

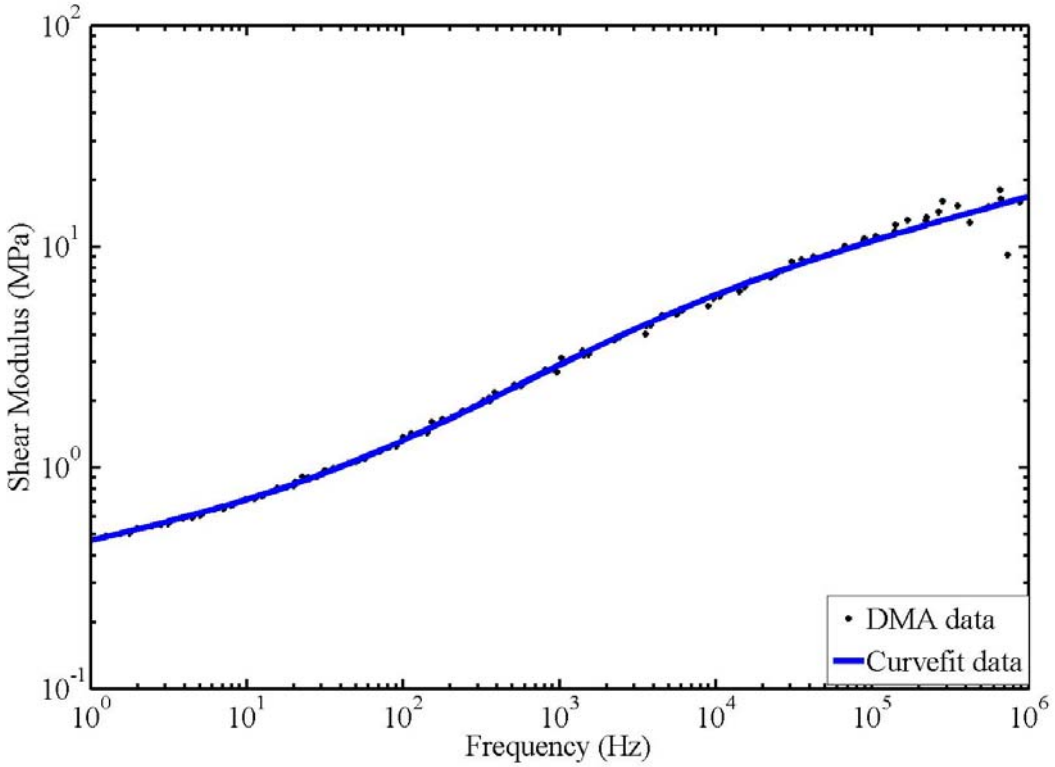

Figure 3.9 Variation of shear modulus with frequency (EAP-2)

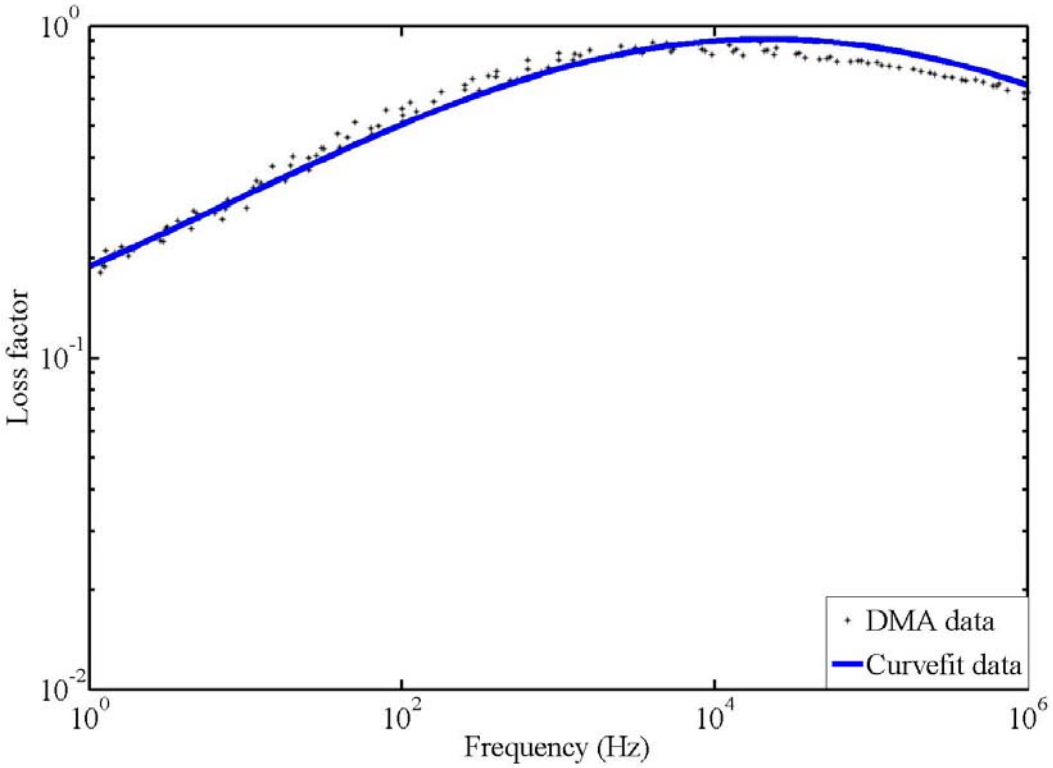

Figure 3.10 Variation of Loss factor with frequency in tensile mode (EAP-2)

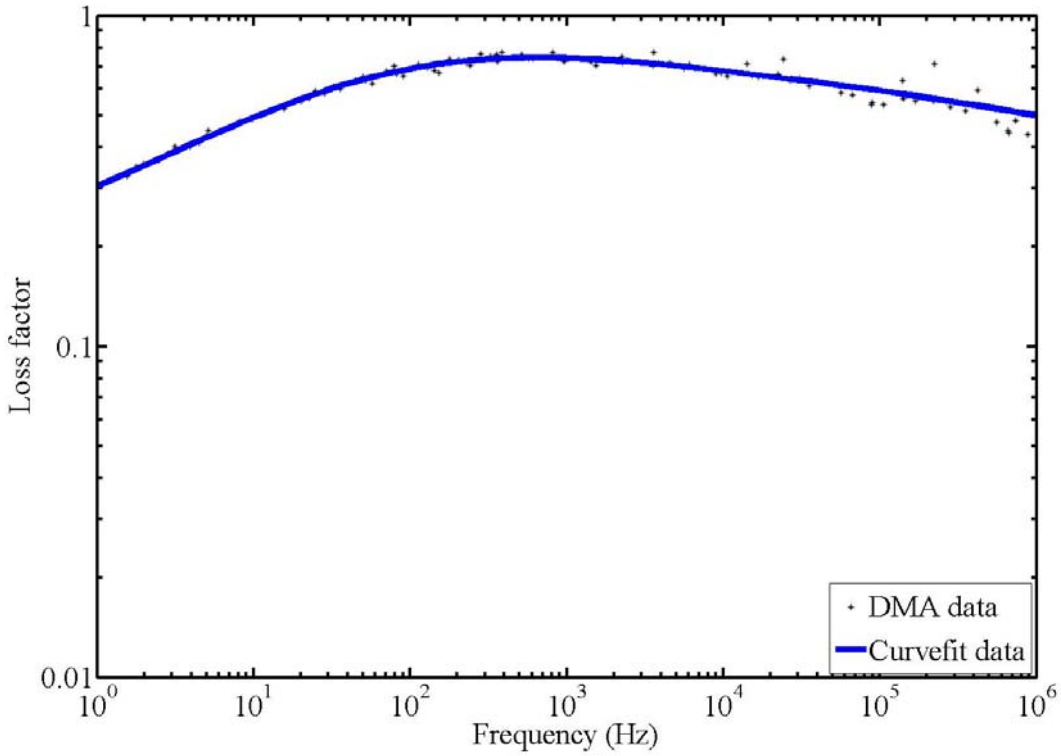

Figure 3.11 Variation of Loss factor with frequency in shear mode (EAP-2)

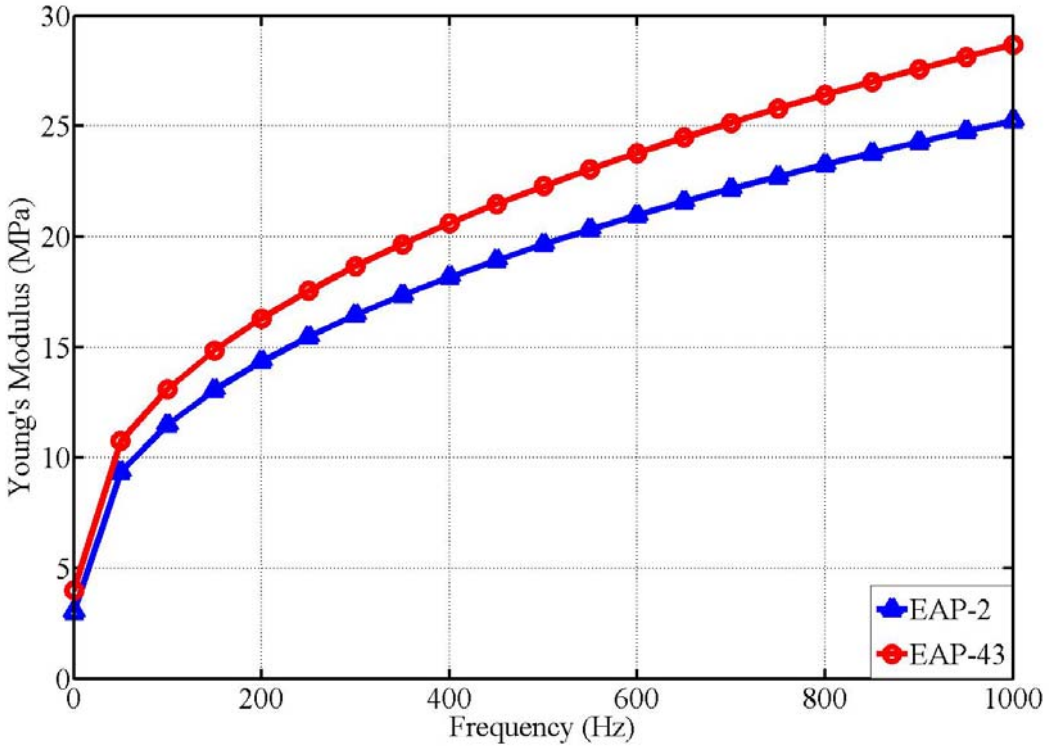

Figure 3.12 Variation of Young's modulus with frequency for EAP-2 and EAP-43

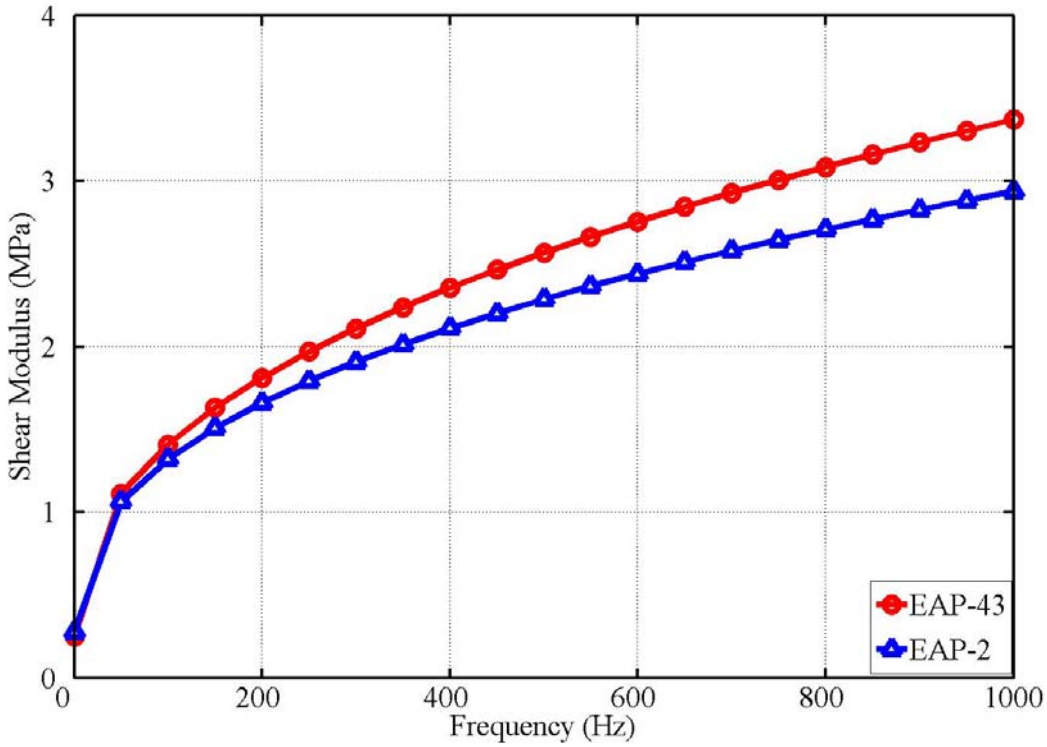

Figure 3.13 Variation of shear modulus with frequency for EAP-2 and EAP-43

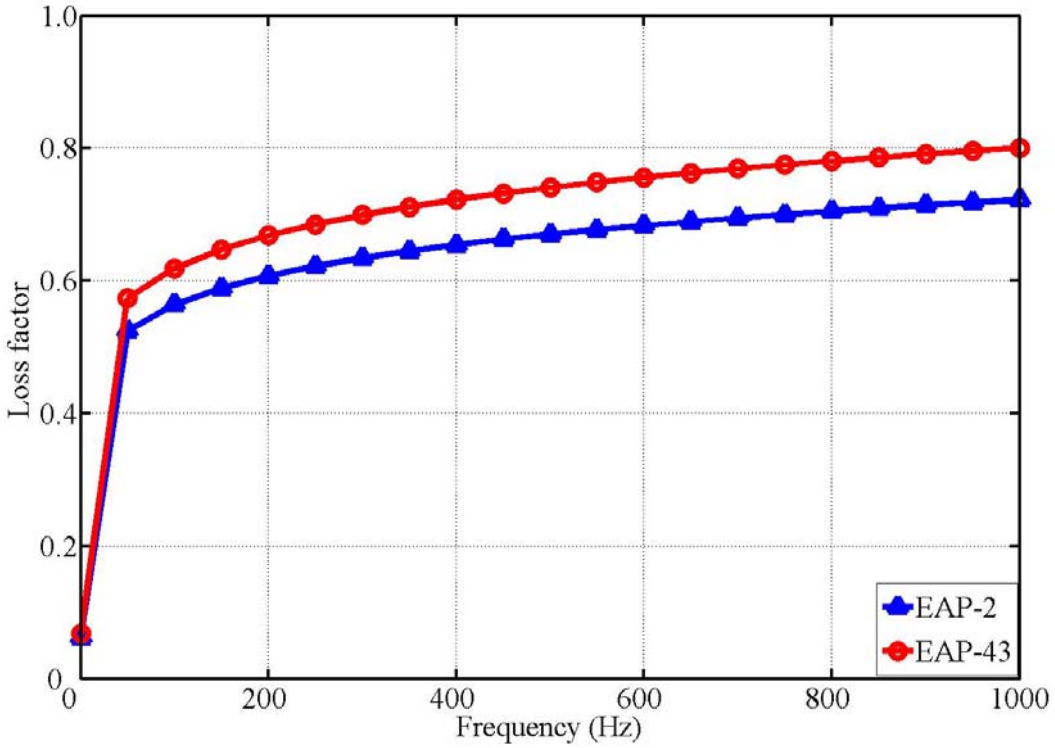

Figure 3.14 Variation of loss factors with frequency for EAP-2 and EAP-43 (Tension mode)

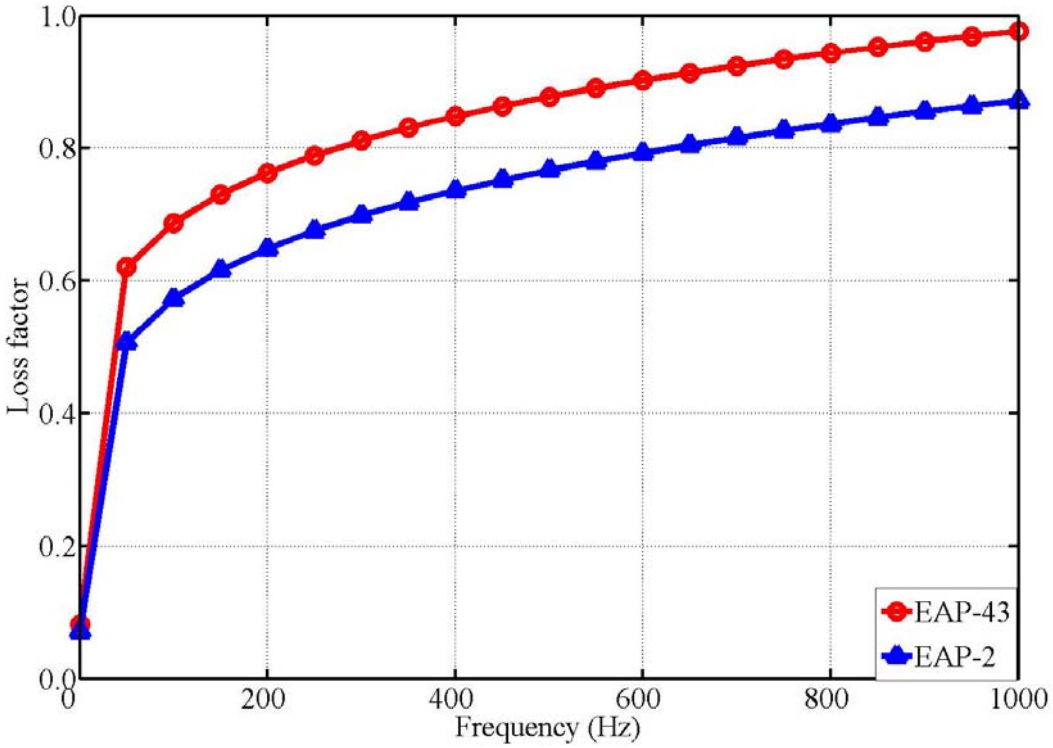

Figure 3.15 Variation of loss factors with frequency for EAP-2 and EAP-43 (Shear mode)

The material properties as a function of frequency are mathematically using a power fit available in MATLAB and are given in the following equations:

$$E_v(f) = a_{11} f^{b_{11}} + c_{11} \tag{3.22}$$

$$G_v(f) = a_{12} f^{b_{12}} + c_{12} \tag{3.23}$$

$$\eta_v^t(f) = a_{13} f^{b_{13}} + c_{13} \text{(Tensile mode)} \tag{3.24}$$

$$\eta_v^s(f) = a_{14} f^{b_{14}} + c_{14} \text{ (Shear mode)} \tag{3.25}$$

where E_v and G_v are the real part of Young's modulus and shear modulus of the viscoelastic material. $\eta_v^t(f)$ and $\eta_v^s(f)$ are the loss factors in tension and shear mode of viscoelastic material.

The complex Young's modulus and shear modulus are expressed in complex form using equations (3.22 to 3.25) as follows.

$$E_v^* = E_v(f)\{1 + j\eta_v^t(f)\} \tag{3.26}$$

$$G_v^* = G_v(f)\{1 + j\eta_v^s(f)\} \tag{3.27}$$

where, E_v^* and G_v^* are the complex Young's modulus and shear modulus of viscoelastic material.

The constants in the equations 3.22 to 3.25 for EAP-2 and EAP-43 are given in Table 3.1.

Table 3.1 Constants of EAP-43 and EAP-2 obtained from Curve fit of DMA data

	Viscoelastic materials				
Tension mode			**Shear mode**		
Constants	**EAP-43**	**EAP-2**	**Constants**	**EAP-43**	**EAP-2**
a_{11}	$1.6\text{x}10^6$	$1.24\text{x } 10^6$	a_{12}	$0.16\text{x } 10^6$	$0.18\text{x } 10^6$
b_{11}	0.4330	0.4179	b_{12}	0.430	0.4069
c_{11}	$4\text{x}10^5$	$3.00\text{x } 10^5$	c_{12}	$0.25\text{x}10^5$	$0.278\text{x } 10^5$
a_{13}	0.29	0.3112	a_{14}	0.2781	0.1977
b_{13}	0.1189	0.124	b_{14}	0.1692	0.2026
c_{13}	0.0629	0.0678	c_{14}	0.08141	0.007035

3.6 SUMMARY

In this chapter, two viscoelastic materials, EAP-2 and EAP-43 are characterized using Dynamic Mechanical Analyzer (DMA) for their frequency dependent material properties: Young's modulus, Shear Modulus, Poisson's ratio and loss factors. The sample details, test setup and procedure for characterising viscoelastic material are explained. The frequency dependent material properties obtained from experiments at a reference temperature of 25^0 Centigrade for both the viscoelastic materials are presented in this chapter. The experimental data obtained from DMA is expressed in mathematical form using power fit as a continuous function of frequency in the range 10^{-2} Hz to 10^6 Hz. Through these equations, frequency dependent material properties of the viscoelastic layers are introduced in the dynamic models of sandwich structures.

CHAPTER 4

MODELLING OF SANDWICH STRUCTURES WITH VISCOELASTIC LAYERS

4.1 INTRODUCTION

In the previous chapter, viscoelastic materials and their characterization have been discussed. This chapter deals with dynamic modelling of sandwich beam containing beams and plates with viscoelastic damping layer. In this dynamic model, frequency dependent Young's modulus, shear modulus and loss factors of viscoelastic materials are considered. A curve fit is developed with the experimental data to express elastic moduli and loss factor as a function of frequency. In the sandwich beams and plate structures, the base and constrained layers are elastic and the material properties are independent of frequency, whereas the constrained layer is viscoelastic layers and the material properties are frequency dependent. Generally, the Young's modulus and shear modulus of viscoelastic materials are represented as complex quantities in which the real and imaginary parts denote the elastic modulus and loss modulus respectively. Hence, the the stiffness matrix is also complex. This chapter deals with finite element based dynamic modelling of sandwich beam and plate structures with viscoelastic layers.

4.2 DYNAMIC MODELLING OF SANDWICH STRUCTURES

The sandwich structure is discretized into finite elements and dynamic equations of motion of the structure are developed using Lagrangian method. The Lagrangian $\mathcal{L}$ is defined as

$$\mathcal{L} = T - P \tag{4.1}$$

Where T is the kinetic energy and P is the potential energy of the element.

The equations of motion can be derived using the following Lagrangian

$$\frac{\partial}{\partial t}\left(\frac{\partial \mathcal{L}}{\partial \dot{u}_i}\right) - \frac{\partial \mathcal{L}}{\partial u_i} = \frac{\partial W}{\partial u_i} \tag{4.2}$$

$$\text{for i} = 1, 2, 3 \cdots\cdots, \text{n}$$

where, n is the number of degrees of freedom (DOF), u_i is the i^{th} generalized displacement,$\dot{u}_i$ is the i^{th} generalized velocity and 'W' is the work potential.

The above equation can be expressed in vectors form as follows.

$$\frac{\partial}{\partial t}\left(\frac{\partial \mathcal{L}}{\partial \{\dot{u}\}}\right) - \frac{\partial \mathcal{L}}{\partial \{u\}} = \frac{\partial W}{\partial \{u\}} \tag{4.3}$$

where $\{\dot{u}\}$ is the generalized velocity vector and $\{u\}$ is the generalized displacement vector and 'W' is the work potential. In the present case, the kinetic energy is a function of velocity and potential energy is a function of displacement. The equations are solved for base excitation. So, work potential is not present in the above equation. Hence, the above equation can be written as

$$\frac{\partial}{\partial t}\left(\frac{\partial T}{\partial \{\dot{u}\}}\right) - \frac{\partial P}{\partial \{u\}} = 0 \tag{4.4}$$

These equations are used to derive the dynamic equations of motion for sandwich beam and plate structures. The elemental equations of motions are obtained by introducing the expression for potential energy and kinetic energy in the above equation. The work potential term is not included in the present chapter and it is dealt separately through base excitation in next chapter. The elemental equations are assembled by imposing the connectivity and compatibility across the element boundaries. The sandwich beam and plate structures with viscoelastic layers are generally used either in unconstrained layer or constrained layer configuration. The detailed process of formulation of these equations of motion for sandwich beams and plates are presented in the following sections.

4.2.1 SANDWICH BEAM STRUCTURES

The sandwich beam considered in this study consists of three layers namely base beam, constrained layer and constraining layer. The base and constraining layers are elastic materials whereas constrained layer is a viscoelastic material. The viscoelastic layer is sandwiched between base and constraining layer using an epoxy adhesive. Perfect bonding is ensured between all the glued surfaces of the sandwich beam. Linear theories of elasticity and viscoelasticity are used. A finite element based dynamic model is developed for constrained layer sandwich beam structure considering the shear effect of the viscoelastic layer.

The formulation is based on the following assumptions [24]

i. The longitudinal displacement of base and constrained layer are independent primary field variables.
ii. Neutral axis is computed for the sandwich beam and transverse displacement is considered about neutral layer and is assumed to be same for all three layers. The transverse displacement is another primary variable.
iii. Perfect bonding is assumed among the glued surfaces.
iv. The longitudinal displacement of the viscoelastic layer can be expressed as a function of base and constraining layer displacements assuming continuity across the glued surfaces.
v. Linear theories of elasticity and viscoelasticity are used.
vi. The inertia effects in both longitudinal and transverse direction are considered for the base beam and constraining layer. The inertia effect is considered only in transverse direction for viscoelastic layer. The rotary inertia effects are neglected for all three layers.

The configuration of sandwich beam with viscoelastic layer is shown in Figure 4.1. The un-deformed configuration of sandwich beam is shown in Figure 4.1(a). The lengths of base beam, constrained and constraining layers are given by L, L_v and L_c respectively. The viscoelastic and constrained layers are free at both ends. The thicknesses of the base beam, viscoelastic layer and constraining layer are t_b, t_v and t_c respectively. The deformed configuration of sandwich beam is shown in Figure 4.1(b). The section AA′ BB′ of the deformed configuration is shown in Figure 4.1(c) indicating the displacement and rotations of individual layers. The nodal displacements of constrained layer sandwich beam are shown in

Figure 4.2. The longitudinal displacement of base beam (u_1) and constraining layer (u_3), the transverse displacement (w) and rotation $\left(w' = \frac{\partial w}{\partial x}\right)$ are considered as primary variables. The transverse displacement (w) and rotation $\left(w' = \frac{\partial w}{\partial x}\right)$ is assumed to be same for all the three layers. Linear and cubic polynomials are employed to interpolate longitudinal and transverse displacement fields respectively.

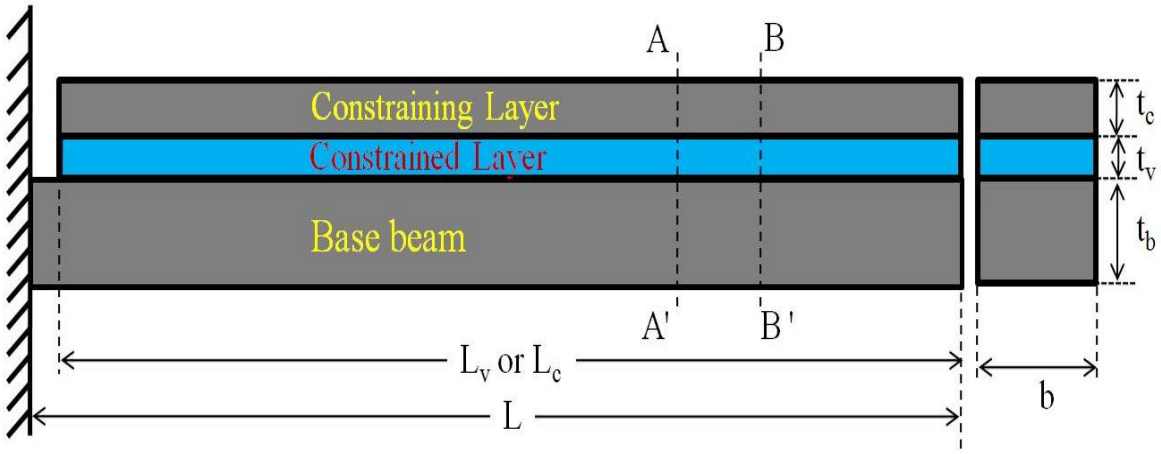

Figure 4.1 (a) Cantilever sandwich beam with viscoelastic layer

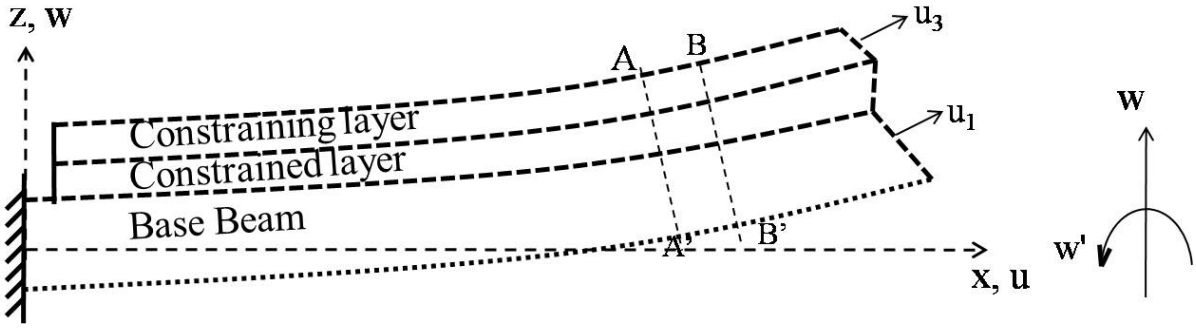

Figure 4.1 (b) Deformed configuration of sandwich beam

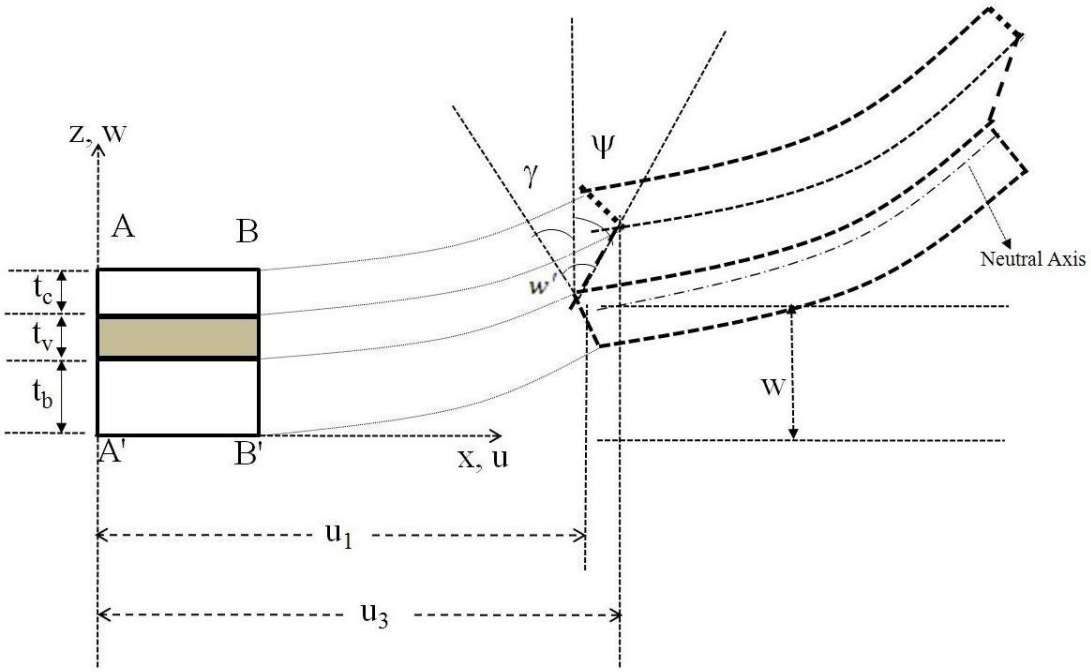

Figure 4.1 (c) Deformed configuration of section AA'BB'

The shear strain of the viscoelastic layer can be expressed as,

$$\gamma = \frac{(u_3 - u_1)}{t_v} + \frac{t_b + 2t_v + t_c}{2t_v} w' \tag{4.5}$$

(A) INTERPOLATION OF DISPLACEMENT FIELDS

The sandwich beam element considered is a two noded element with four degrees of freedom per node as described in Figure 4.2. The nodal degrees of freedom are the longitudinal displacement of base beam (u_1), longitudinal displacement of the constraining layer (u_3), the transverse displacement (w) and rotation (w′). Assuming Euler-Bernoulli beam theory, the transverse rotation (w′) is the gradient of the transverse displacement (w).

The chosen primary field variables within the element are interpolated in terms of the corresponding nodal displacements and they are mapped to the sandwich beam element nodal displacements. Assuming no coupling between longitudinal and transverse displacement, the field variables are interpolated in terms of corresponding discrete nodal displacements.

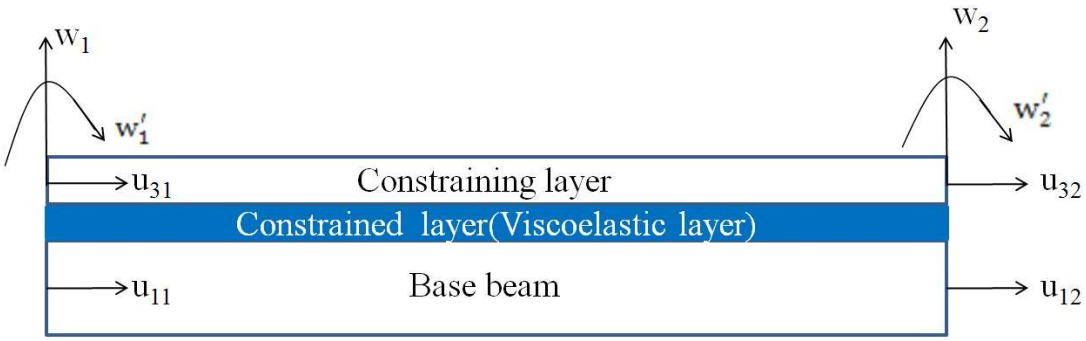

Figure 4.2 Nodal displacements of sandwich beam element

The longitudinal displacement of base beam 'u_1' is purely a function of the nodal longitudinal displacements 'u_{11}' and 'u_{12}'. Similarly, the longitudinal displacement of constraining layer 'u_3' is purely a function of the nodal longitudinal displacements 'u_{31}' and 'u_{32}'. The transverse displacement 'w' is assumed to be same for all the three layers and they are interpolated in terms of nodal transverse displacements and rotations w_1, w_1', w_2 and w_2'. The derived displacements and rotations of the viscoelastic layer are functions of the primary variables of base and constraining layer. Hence, interpolation functions of all the primary variables are mapped to the entire nodal displacement vector of the sandwich beam element.

For convenience, the nodal displacements of the sandwich beam are expressed in a column vector as given below.

$$\{U_e\} = [\, u_{11}, u_{12}, u_{31}, u_{32}, w_1, w_1', w_2, w_2']^T \tag{4.6}$$

Where $\{U_e\}$ is referred as the nodal displacement vector of sandwich beam element

The interpolation functions for the element displacements can be expressed in the polynomial form as follows.

$$\begin{aligned} u_1 &= a_1 + a_2 x \\ u_3 &= a_3 + a_4 x \\ w &= a_5 + a_6 x + a_7 x^2 + a_8 x^3 \\ w' &= a_6 + 2a_7 x + 3a_8 x^2 \end{aligned} \tag{4.7}$$

By replacing the polynomial coefficients {a_1, a_2, a_3,…….,a_8} with the nodal displacement variables, the following interpolations can be obtained.

The longitudinal displacement 'u_1' of base beam can be expressed as,

$$u_1 = \left\{\left(1 - \frac{x}{l_e}\right) \quad \frac{x}{l_e}\right\}\begin{Bmatrix} u_{11} \\ u_{12} \end{Bmatrix} \tag{4.8}$$

The chosen primary field variable 'u_1'within the element is interpolated in terms of the corresponding nodal displacements and they are mapped to the sandwich beam element nodal displacements as follows.

$$u_1 = \{\mathrm{N_b}\}\{U_e\}^T \tag{4.9}$$

where $\{\mathrm{N_b}\}$ is the interpolation function for longitudinal displacement of base beam and it can be expressed as follows.

$$\{\mathrm{N_b}\} = \left\{\left(1 - \frac{\mathrm{x}}{\mathrm{l_e}}\right) \quad \frac{\mathrm{x}}{\mathrm{l_e}} \quad 0 \quad 0 \quad 0 \quad 0 \quad 0 \quad 0\right\} \tag{4.10}$$

The strain due to longitudinal displacement of base beam can be expressed as,

$$\mathcal{E}_b = \{B_b\}\{U_e\}^T \tag{4.11}$$

where $\{B_b\}$ is the row vector relating strain due to longitudinal displacement of base beam and nodal displacements of sandwich beam element

By differentiating longitudinal displacement of equation (4.9) with respect to time, the velocity vector ($\dot{u}_1$) of the base beam can be expressed as,

$$\dot{u}_1 = \{\mathrm{N_b}\}\{\dot{U}_e\}^T \tag{4.12}$$

where,$\dot{u}_1$ is the velocity of the base beam in longitudinal direction and $\{\dot{U}_e\}$ is the nodal velocity vector of sandwich beam.

The longitudinal displacement 'u_3' of the constraining layer can be expressed as,

$$u_3 = \left\{\left(1 - \frac{\mathrm{x}}{\mathrm{l_e}}\right) \quad \frac{\mathrm{x}}{\mathrm{l_e}}\right\}\begin{Bmatrix} u_{31} \\ u_{32} \end{Bmatrix} \tag{4.13}$$

The chosen primary field variable 'u_3'within the element is interpolated in terms of the corresponding nodal displacements and they are mapped to the sandwich beam element nodal displacements as follows.

$$u_3 = \{\mathrm{N_c}\}\{U_e\}^T \tag{4.14}$$

where $\{\mathrm{N_c}\}$ is the interpolation function for longitudinal displacement of constraining layer and it can be expressed as

$$\{\mathrm{N_c}\} = \left\{0 \quad 0 \quad \left(1 - \frac{\mathrm{x}}{\mathrm{l_e}}\right) \quad \frac{\mathrm{x}}{\mathrm{l_e}} \quad 0 \quad 0 \quad 0 \quad 0\right\}\{U_e\}^{\mathrm{T}} \tag{4.15}$$

The strain due to longitudinal displacement of the constraining layer can be expressed as,

$$\mathcal{E}_c = \{B_c\}\{U_e\}^T \tag{4.16}$$

where $\{B_c\}$ is the row vector relating strain due to longitudinal displacement of the constraining layer and nodal displacements of sandwich beam.

By differentiating longitudinal displacement in equation (4.14) with respect to time, the velocity vector ($\dot{u}_3$) of the constraining layer can be expressed as,

$$\dot{u}_3 = \{\mathrm{N_c}\}\{\dot{U}_e\}^T \tag{4.17}$$

The transverse displacement 'w' of sandwich beam can be expressed as,

$$w = \left\{\frac{(2x^3 - 3x^2 l_e + l_e^3)}{l_e^3} \quad \frac{(x^3 l_e - 2x^2 l_e^2 + x l_e^3)}{l_e^3} \quad \frac{(-2x^3 + 3x^2 l_e)}{l_e^3} \quad \frac{(l_e x^3 - x^2 l_e^2)}{l_e^3}\right\} \begin{Bmatrix} w_1 \\ w_1' \\ w_2 \\ w_2' \end{Bmatrix} \tag{4.18}$$

The chosen primary field variable 'w' within the element is interpolated in terms of the corresponding nodal displacements and rotations and they are mapped to the sandwich beam element nodal displacements as follows.

$$\mathrm{W} = \{\mathrm{N_w}\}\{U_e\}^T \tag{4.19}$$

Where $\{\mathrm{N_w}\}$ is the interpolation function for transverse displacement of sandwich beam and it can be expressed as:

$$\{\mathrm{N_w}\} = \left\{0 \quad 0 \quad 0 \quad 0 \quad \frac{(2x^3 - 3x^2 l_e + l_e^3)}{l_e^3} \quad \frac{(x^3 l_e - 2x^2 l_e^2 + x l_e^3)}{l_e^3} \quad \frac{(-2x^3 + 3x^2 l_e)}{l_e^3} \quad \frac{(l_e x^3 - x^2 l_e^2)}{l_e^3}\right\} \tag{4.20}$$

By differentiating the transverse displacement of equation (4.19) twice with respect to 'x', the beam curvature 'κ' can be obtained as follows

$$\kappa = \frac{\partial^2 w}{\partial x^2} = \{B_w\}\{U_e\}^T \tag{4.21}$$

where $\{B_w\}$ is the row vector relating beam curvature and nodal displacements of sandwich beam element.

The transverse rotation (w′) of the sandwich beam can be derived by differentiating equation (4.18) with respect to time and can be expressed as,

$$\mathrm{w'} = \left\{\frac{6x(x - l_e)}{l_e^3} \quad \frac{(3x^2 - 4x l_e + l_e^2)}{l_e^2} \quad \frac{6x(l_e - x)}{l_e^3} \quad \frac{x(3x - 2l_e)}{l_e^2}\right\} \begin{Bmatrix} w_1 \\ w_1' \\ w_2 \\ w_2' \end{Bmatrix} \tag{4.22}$$

The above equation can also be expressed as,

$$\mathrm{w'} = \{N_{w'}\}\{U_e\}^T \tag{4.23}$$

Where $\{N_{w'}\}$ is the interpolation function for transverse rotation of sandwich beam and it can be expressed as,

$$\{N_{w'}\} = \left\{0 \quad 0 \quad 0 \quad 0 \quad \frac{6x(x-l_e)}{l_e^3} \quad \frac{(3x^2-4xl_e+l_e^2)}{l_e^2} \quad \frac{6x(l_e-x)}{l_e^3} \quad \frac{x(3x-2l_e)}{l_e^2}\right\} \tag{4.24}$$

From equations (4.5), the shear strain in the constrained layer (γ) can be expressed in terms of nodal displacements as follows:

$$\gamma = \{B_\gamma\}\{U_e\}^T \tag{4.25}$$

Where $\{B_\gamma\}$ is the row vector relating shear strain of viscoelastic layer and nodal displacement of sandwich plate and it can be expressed as given below:

$$\{B_\gamma\} = \frac{1}{t_v}(\{N_c\} - \{N_b\}) + \left(\frac{(t_b + 2t_v + t_c)}{2t_v}\right)\{N_{w'}\} \tag{4.26}$$

(B) STRAIN ENERGY OF SANDWICH BEAM

The strains due to longitudinal displacements and transverse displacement of sandwich beam are assumed to be uncoupled and they are expressed separately. The strain energy of sandwich beam has contributions from the longitudinal displacement of base and constraining layer, transverse displacement of the three layers and transverse shear deformation of viscoelastic layer. These contributions of individual strain energies of the sandwich beam are derived as below.

The contribution of strain energy due to longitudinal displacement of the base beam (Pb_e) can be expressed as follows:

$$P_{be} = \frac{1}{2}A_b \int_0^{l_e} \{\mathcal{E}_b\}^T E_b \ \{\mathcal{E}_b\} dx \tag{4.27}$$

By introducing equation (4.11) for $\{\mathcal{E}_b\}$ in the above equation, it can be expressed as,

$$P_{be} = \frac{1}{2}E_b A_b \int_0^{l_e} \{U_e\}^T\{B_b\}^T \ \{B_b\}\{U_e\} dx \tag{4.28}$$

The strain energy due to longitudinal displacement of the constraining layer (Pc_e) can be expressed as follows.

$$P_{ce} = \frac{1}{2}A_c \int_0^{l_e} \{\mathcal{E}_c\}^T E_c\{\mathcal{E}_c\} dx \tag{4.29}$$

By introducing equation (4.16) for $\{\mathcal{E}_c\}$ in the above equation, it can be expressed as,

$$P_{ce} = \frac{1}{2}E_c A_c \int_0^{l_e} \{U_e\}^T\{B_c\}^T \ \{B_c\}\{U_e\} dx \tag{4.30}$$

The strain energy due to longitudinal displacement of base beam and constraining layer can be combined and it can be expressed as follows.

$$P_{ee} = P_{be} + P_{ce} \tag{4.31}$$

By substituting equations (4.28) and (4.30) for $(\mathrm{P_{be}})$ and $(\mathrm{P_{ce}})$ in the above equation, it can be expressed as follows.

$$P_{ee} = \frac{1}{2}\{\mathrm{U_e}\}^{\mathrm{T}}\left[\mathrm{E_bA_b}\int_0^{\mathrm{l_e}}\{\mathrm{B_b}\}^{\mathrm{T}}\{\mathrm{B_b}\}\mathrm{dx} + \mathrm{E_cA_c}\int_0^{\mathrm{l_e}}\{\mathrm{B_c}\}^{\mathrm{T}}\{\mathrm{B_c}\}\mathrm{dx}\right]\{\mathrm{U_e}\} \tag{4.32}$$

The above equation can also be expressed as follows.

$$P_{ee} = \frac{1}{2}\{\mathrm{U_e}\}^{\mathrm{T}}[\mathrm{K_{ee}}]\{\mathrm{U_e}\} \tag{4.33}$$

Where, $[K_{ee}]$ is the element stiffness matrix due to the longitudinal deformation of base beam and constraining layer and can be expressed as follows.

$$[K_{ee}] = \left[\mathrm{E_bA_b}\int_0^{\mathrm{l_e}}\{\mathrm{B_b}\}^{\mathrm{T}}\{\mathrm{B_b}\}\mathrm{dx} + \mathrm{E_cA_c}\int_0^{\mathrm{l_e}}\{\mathrm{B_c}\}^{\mathrm{T}}\{\mathrm{B_c}\}\mathrm{dx}\right] \tag{4.34}$$

The strain energy due to transverse displacement of the sandwich beam can be expressed as,

$$P_{eb} = \frac{1}{2}(EI)_{eq}\int_0^{l_e}(\kappa)^T(\kappa)\,dx \tag{4.35}$$

where, $(EI)_{eq}$ is the equivalent rigidity of sandwich beam [46].

Where, (κ) is the curvature of sandwich beam. By introducing equation (4.21) for κ in the above equation, it can be expressed as follows.

$$P_{eb} = \frac{1}{2}(EI)_{eq}\{U_e\}^T\left[\int_0^{l_e}\{B_w\}^T\{B_w\}\right]\{U_e\}dx \tag{4.36}$$

The above equation can also be expressed as follows.

$$P_{eb} = \frac{1}{2}\{U_e\}^T[K_{eb}]\{U_e\} \tag{4.37}$$

where, $[K_{eb}]$ is the element stiffness matrix of the sandwich beam due to transverse displacement of the sandwich beam and it can be expressed as follows.

$$[K_{eb}] = (EI)_{eq}\left[\int_0^{l_e}\{B_w\}^T\{B_w\}\right] \tag{4.38}$$

The viscoelastic layer is sandwiched between base beam and constraining layer which undergoes shear deformation. The shear strain energy for this shear deformation can be expressed as

$$P_{sv} = \frac{1}{2}G_v^*A_v\int_0^{l_e}\gamma^T\,\gamma\,dx \tag{4.39}$$

where, G_v^* is the complex shear modulus of viscoelastic material. The shear modulus is frequency dependent and equation (3.27 of chapter 3) is introduced in the above equation. So, the above equation is also frequency dependent. An iterative computational scheme is developed for solving these equations which will be explained in next chapter.

By substituting equation (4.25) for the shear strain of viscoelastic layer, it can be expressed as

$$P_{sv} = \frac{1}{2}\{U_e\}^T \left[G_v^* A_v \int_0^{l_e} \{B_\gamma\}^T \{B_\gamma\} dx \right] \{U_e\} \tag{4.40}$$

The above equation can also written as,

$$P_{sv} = \frac{1}{2}\{U_e\}^T [K_{sv}^*] \{U_e\} \tag{4.41}$$

where $[K_{sv}^*]$ is the element complex stiffness matrix due to shear deformation of the viscoelastic layer and can be expressed as,

$$[K_{sv}^*] = G_v^* A_v \int_0^{l_e} \{B_\gamma\}^T \{B_\gamma\} dx \tag{4.42}$$

The total strain energy (P_e) of the sandwich beam element can be expressed as

$$P_e = P_{ee} + P_{eb} + P_{sv} \tag{4.43}$$

By substituting equations (4.33), (4.37) and (4.41) for P_{ee} , P_{eb} and P_{sv} in the above equation, it can be expressed as follows.

$$P_e = \frac{1}{2}\{U_e\}^T [K_e^*] \{U_e\} \tag{4.44}$$

where $[K_e^*]$ is the stiffness matrix of sandwich beam element and can be expressed as follows.

$$[K_e^*] = [K_{ee}] + [K_{eb}] + [K_{sv}^*] \tag{4.45}$$

Due to the complex nature of the shear modulus, the element stiffness matrix $[K_e^*]$ is also complex in nature. The above element stiffness matrix of the sandwich beam can be partitioned for convenience as follows;

$$[K_e^*] = \begin{bmatrix} [K_{11}^*] & [K_{12}^*] \\ [K_{12}^*] & [K_{22}^*] \end{bmatrix} \tag{4.46}$$

$$[K_{11}^*] = \begin{bmatrix} \frac{E_b A_b}{l_e} + \frac{G_v^* A_v l_e}{3t_v^2} & -\frac{E_b A_b}{l_e} + \frac{G_v^* A_v l_e}{6t_v^2} & -\frac{G_v^* A_v l_e}{3t_v^2} & -\frac{G_v^* A_v l_e}{6t_v^2} \\ -\frac{E_b A_b}{l_e} + \frac{G_v^* A_v l_e}{6t_v^2} & \frac{E_b A_b}{l_e} + \frac{G_v^* A_v l_e}{3t_v^2} & -\frac{G_v^* A_v l_e}{6t_v^2} & -\frac{G_v^* A_v l_e}{3t_v^2} \\ -\frac{G_v^* A_v l_e}{3t_v^2} & -\frac{G_v^* A_v l_e}{6t_v^2} & \frac{E_c A_c}{l_e} + \frac{G_v^* A_v l_e}{3t_v^2} & -\frac{E_c A_c}{l_e} + \frac{G_v^* A_v l_e}{6t_v^2} \\ -\frac{G_v^* A_v l_e}{6t_v^2} & -\frac{G_v^* A_v l_e}{3t_v^2} & -\frac{E_c A_c}{l_e} + \frac{G_v^* A_v l_e}{6t_v^2} & \frac{E_c A_c}{l_e} + \frac{G_v^* A_v l_e}{3t_v^2} \end{bmatrix} \tag{4.47}$$

$$[K_{12}^*] = \begin{bmatrix} \frac{G_v^* A_v d}{2t_v^2} & \frac{G_v^* A_v d}{12t_v^2} & \frac{G_v^* A_v d}{2t_v^2} & -\frac{G_v^* A_v d}{12t_v^2} \\ -\frac{G_v^* A_v d}{2t_v^2} & -\frac{G_v^* A_v d}{12t_v^2} & \frac{G_v^* A_v d}{2t_v^2} & \frac{G_v^* A_v d}{12t_v^2} \\ \frac{G_v^* A_v d}{2t_v^2} & -\frac{G_v^* A_v d}{12t_v^2} & -\frac{G_v^* A_v d}{2t_v^2} & \frac{G_v^* A_v d}{12t_v^2} \\ \frac{G_v^* A_v d}{2t_v^2} & \frac{G_v^* A_v d}{12t_v^2} & -\frac{G_v^* A_v d}{2t_v^2} & -\frac{G_v^* A_v d}{12t_v^2} \end{bmatrix} \tag{4.48}$$

$$[K_{22}^*] = \begin{bmatrix} \frac{12(EI)_{eq}}{l_e^3} + \frac{6G_v^* A_v d^2}{5l_e t_v^2} & \frac{6(EI)_{eq}}{l_e^2} + \frac{G_v^* A_v d^2}{10l_e t_v^2} & -\frac{12(EI)_{eq}}{l_e^3} - \frac{6G_v^* A_v d^2}{5l_e t_v^2} & \frac{6(EI)_{eq}}{l_e^2} + \frac{G_v^* A_v d^2}{10l_e t_v^2} \\ \frac{6(EI)_{eq}}{l_e^2} + \frac{G_v^* A_v d^2}{10l_e t_v^2} & \frac{4(EI)_{eq}}{l_e} + \frac{2G_v^* A_v d^2}{15l_e t_v^2} & -\frac{6(EI)_{eq}}{l_e^2} - \frac{G_v^* A_v d^2}{10l_e t_v^2} & \frac{2(EI)_{eq}}{l_e} - \frac{G_v^* A_v d^2}{30l_e t_v^2} \\ -\frac{12(EI)_{eq}}{l_e^3} - \frac{6G_v^* A_v d^2}{5l_e t_v^2} & -\frac{6(EI)_{eq}}{l_e^2} - \frac{G_v^* A_v d^2}{10l_e t_v^2} & \frac{12(EI)_{eq}}{l_e^3} + \frac{6G_v^* A_v d^2}{5l_e t_v^2} & \frac{6(EI)_{eq}}{l_e^2} - \frac{G_v^* A_v d^2}{10l_e t_v^2} \\ \frac{6(EI)_{eq}}{l_e^2} + \frac{G_v^* A_v d^2}{10l_e t_v^2} & \frac{2(EI)_{eq}}{l_e} - \frac{G_v^* A_v d^2}{30l_e t_v^2} & -\frac{6(EI)_{eq}}{l_e^2} - \frac{G_v^* A_v d^2}{10l_e t_v^2} & \frac{4(EI)_{eq}}{l_e} + \frac{2G_v^* A_v d^2}{15l_e t_v^2} \end{bmatrix}$$

(4.49)

(C) KINETIC ENERGY OF SANDWICH BEAM

The assumptions made in the formulation of potential energy are considered in the formulation of kinetic energy also. The longitudinal and transverse motions of the sandwich beam structure are uncoupled and they are expressed separately. The individual contribution of kinetic energy associated with longitudinal motion of base beam (T_{eb}) and constraining layer (T_{ec}) can be expressed as follows:

$$T_{eb} = \frac{1}{2}\rho_b A_b \int_0^{l_e} (\dot{u}_1)^T (\dot{u}_1) dx \tag{4.50}$$

By introducing equation (4.12) for velocity of base beam in the above equation, it can be expressed as,

$$T_{eb} = \frac{1}{2}\rho_b A_b \int_0^{l_e} \left(\dot{U}_e\right)^T \{N_b\}^T \{N_b\} \left(\dot{U}_e\right) dx \tag{4.51}$$

The kinetic energy associated with longitudinal motion of constraining layer (T_{ec}) can be written as,

$$T_{ec} = \frac{1}{2}\rho_c A_c \int_0^{l_e} (\dot{u}_3)^T (\dot{u}_3) dx \tag{4.52}$$

By introducing equation (4.15) for velocity of constraining layer in the above equation, it can be expressed as,

$$T_{ec} = \frac{1}{2}\rho_c A_c \int_0^{l_e} \{N_c\}^T \left(\dot{U}_e\right)^T \{N_c\}\left(\dot{U}_e\right) dx \tag{4.53}$$

where, ρ_b, ρ_v and $\rho_c$are the densities of base layer, viscoelastic layer and constraining layer respectively.

The kinetic energy due to longitudinal motion of base beam and constraining layer can be combined and can be expressed as,

$$T_{ee} = \frac{1}{2}\{\dot{U}_e\}^T \left[\rho_b A_b \int_0^{l_e} \{N_b\}^T\{N_b\} + \rho_c A_c \int_0^{l_e} \{N_c\}^T\{N_c\}\right]\{\dot{U}_e\} dx \tag{4.54}$$

The above equation can also be expressed as

$$T_{ee} = \frac{1}{2}\{\dot{U}_e\}^T [M_{ee}]\{\dot{U}_e\} \tag{4.55}$$

where, $[M_{ee}]$ is the element mass matrix due to longitudinal motion of base beam and constraining layer and it can be expressed as

$$[M_{ee}] = \rho_b A_b \int_0^{l_e} \{N_b\}^T\{N_b\}\, dx + \rho_c A_c \int_0^{l_e} \{N_c\}^T\{N_c\}\, dx \tag{4.56}$$

The kinetic energy due to transverse motion of the base beam, viscoelastic and constraining layer can be expressed as

$$T_{eb} = \frac{1}{2}\ \rho A_{eq} \int_0^{l_e} \left(\frac{\partial w}{\partial t}\right)^2 dx \tag{4.57}$$

where, $\rho A_{eq} = \rho_b A_b + \rho_v A_v + \rho_c A_c$

The kinetic energy due to transverse motion of sandwich beam in terms of nodal velocities can be expressed as

$$T_{eb} = \frac{1}{2}\{\dot{U}_e\}^T \left[\ [\rho A]_{eq} \int_0^{l_e} \{N_w\}^T\{N_w\}\right]\{\dot{U}_e\} dx \tag{4.58}$$

The above equation can also be expressed as

$$T_{eb} = \frac{1}{2}\{\dot{U}_e\}^T [M_{eb}]\{\dot{U}_e\} \tag{4.59}$$

Where, $[M_{eb}]$ is the element mass matrix due to transverse motion of base beam and constraining layer and it can be expressed as follows

$$[M_{eb}] = \int_0^{l_e} \{N_w\}^T\{N_w\}\mathrm{dx} \tag{4.60}$$

The total kinetic energy of sandwich beam can be written as

$$T_e = T_{ee} + T_{eb} \tag{4.61}$$

using equation (4.49) and (4.52), the above equation can be expressed as

$$T_e = \frac{1}{2}\{\dot{U}_e\}^T [M_e]\{\dot{U}_e\} \tag{4.62}$$

where $[M_e]$ is the element mass matrix of sandwich beam and it can be expressed as

$$[M_e] = [M_{ee}] + [M_{eb}] \tag{4.63}$$

The above element mass matrix can be partitioned in terms of $[m_{11}]\ and\ [m_{22}]$

$$[M_e] = \begin{bmatrix} [M_{11}] & [0_{4x4}] \\ [0_{4x4}] & [M_{22}] \end{bmatrix} \tag{4.64}$$

Where,

$$[M_{11}] = \frac{l_e}{6}\begin{bmatrix} 2\rho_b A_b & \rho_b A_b & 0 & 0 \\ \rho_b A_b & 2\rho_b A_b & 0 & 0 \\ 0 & 0 & 2\rho_c A_c & \rho_c A_c \\ 0 & 0 & \rho_c A_c & 2\rho_c A_c \end{bmatrix} \tag{4.65}$$

$$[M_{22}] = \frac{[\rho A]_{eq} l_e}{420}\begin{bmatrix} 156 & 22l_e & 54 & -13l_e \\ 22l_e & 4l_e^2 & 13l_e & -3l_e \\ 54 & 13l_e & 156 & -22l_e \\ -13l_e & 3l_e & -22l_e & 4l_e^2 \end{bmatrix} \tag{4.66}$$

By introducing the total potential energy of equation (4.43) and total kinetic energy of equation (4.61) in Lagrangian equation (4.4), the element dynamic equation of motion can be obtained as

$$[M_e]\{\ddot{U}_e\} + [K_e^*]\{U_e\} = 0 \tag{4.67}$$

By assembling the elemental equations by ensuring continuity across the element boundaries, the equations of motion for the sandwich beam can be obtain in the following form

$$[M]\{\ddot{U}\} + [K^*]\{U\} = 0 \tag{4.68}$$

The same formulation is used for unconstrained layer sandwich structures by degrading the material constants of the constraining layer to near zero value.

(D) FE MODEL

The sandwich beam is modelled considering Euler – Bernoulli assumptions for base and constraining layer and transverse shear for constrained layer to evaluate the dynamic properties. The sandwich beam is discretized using two noded beam elements, with four degrees of freedom (DOF) at each node. The FE mesh of sandwich beam is shown in Fig.4.3.

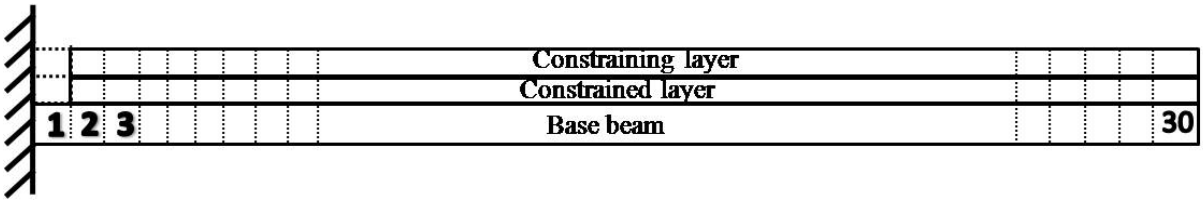

Figure 4.3 Finite element mesh of sandwich beam

The constrained and constraining layer length is 290 mm compared to base beam length of 300 mm. The sandwich beam is discretized into 30 elements with each element of 10 mm length. During FE model constraining and constrained layer are modelled up to fixed end. The material properties of constrained and constraining layer for the first element are degraded to low value to represent the absence of this layer in the sandwich element. The dotted line in the above Figure 4.3 indicates these details. i.e. only the base layer is clamped to simulate cantilever boundary condition. The element mass matrix and complex stiffness matrix are assembled using standard assembly procedure to ensure continuity and compatibility across the boundaries. The assembled dynamic equation of motion of sandwich beam is expressed by equation (4.68). All DOF's corresponding to clamped edge is constrained to simulate clamped-free (cantilever) boundary condition. The detailed procedure of solving dynamic equations of motion is described in chapter 5. The same FE code is used to model the unconstrained layer by setting the material properties of the constraining layer to zero.

4.2.2 SANDWICH PLATE STRUCTURES

This section deals with the dynamic modelling of sandwich plates. The three layer plate structure consists of a viscoelastic layer sandwiched between the base plate and constraining layer with an adhesive. The base and constraining layer are made of elastic and isotropic material. Perfect bonding is ensured between all the glued surfaces of sandwich plate. The actual challenge lies in introducing the complex elastic moduli and loss factors of the viscoelastic layer in the dynamic model.

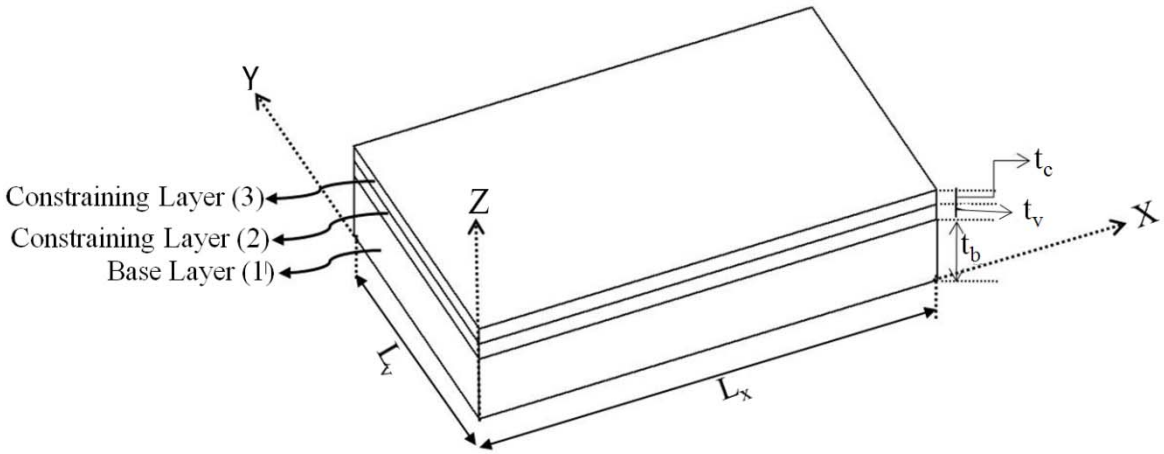

Figure 4.4 Sandwich plate

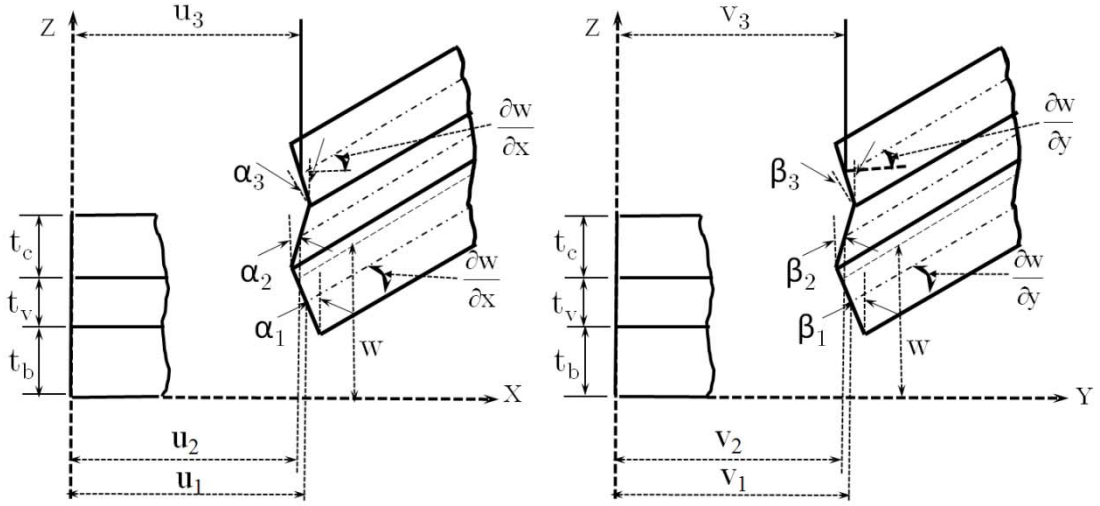

(a) (b)

Figure 4.5 Deformed configuration of transverse section of sandwich plate [7]
pp. X-Z Plane (b) Y-Z Plane

The sandwich plate under consideration is shown in Figure 4.4. The deformed configuration of a section of sandwich plate along with the displacements and rotations in both the transverse planes are shown in Figures 4.5 (a) and (b) respectively. During formulation, it is assumed that no coupling exist between the longitudinal and transverse displacement of each layer. The shear deformation is considered for all the three layers. From Figure 4.5, the transverse displacement (w) is assumed to be same for the sandwich plate. The longitudinal displacements of the base layer are ($u_1$and v_1) and transverse rotations are (α_1 and β_1). In a similar way, the field variables of the constraining layer are u_3, v_3, $\alpha_3$and β_3.

Transverse displacement (w) of the sandwich plate, longitudinal displacements and transverse rotations of base and constraining layer plate are chosen as the primary field variables. The longitudinal displacement and transverse rotation of the viscoelastic layer (u_2, v_2, α_2 and β_2) are related to the primary variables to ensure the continuity of displacement field at the interfaces between the base plate, constrained (viscoelastic) layer and constraining layer.

The continuity requirement for displacement field at the interfaces between the base layer, constrained layer and constraining layer leads to the following constraint equations.

$$u_1 + \frac{t_b}{2}\alpha_1 = u_2 - \frac{t_v}{2}\alpha_2; \tag{4.69}$$

$$u_2 + \frac{t_v}{2}\alpha_2 = u_3 - \frac{t_c}{2}\alpha_3; \tag{4.70}$$

$$v_1 + \frac{t_b}{2}\beta_1 = v_2 - \frac{t_v}{2}\beta_2 \tag{4.71}$$

$$v_2 + \frac{t_v}{2}\beta_2 = v_3 - \frac{t_c}{2}\beta_3 \tag{4.72}$$

From these equations the longitudinal displacements and rotations of the viscoelastic core are expressed in terms of the longitudinal displacements and rotations of the base and constraining layer as given below:

$$\mathrm{u}_2 = \frac{1}{2}(\mathrm{u}_1 + \mathrm{u}_3) + \frac{1}{4}(\mathrm{t}_\mathrm{b}\alpha_1 - \mathrm{t}_\mathrm{c}\alpha_3) \tag{4.73}$$

$$\mathrm{v}_2 = \tfrac{1}{2}(\mathrm{v}_1 + \mathrm{v}_3) + \tfrac{1}{4}(\mathrm{t}_\mathrm{b}\beta_1 - \mathrm{t}_\mathrm{c}\beta_3), \tag{4.74}$$

$$\alpha_2 = \frac{1}{\mathrm{t}_\mathrm{v}}(u_3 - u_1) - \frac{1}{2\mathrm{t}_\mathrm{v}}(\mathrm{t}_\mathrm{b}\alpha_1 + \mathrm{t}_\mathrm{c}\alpha_3) \tag{4.75}$$

$$\beta_2 = \frac{1}{\mathrm{t}_\mathrm{v}}(v_3 - v_1) - \frac{1}{2\mathrm{t}_\mathrm{v}}(\mathrm{t}_\mathrm{b}\beta_1 + \mathrm{t}_\mathrm{c}\beta_3) \tag{4.76}$$

The strains corresponding to the longitudinal loading are expressed as follows

$$\epsilon_x^b = \frac{\partial u_1}{\partial x}; \qquad \epsilon_y^b = \frac{\partial v_1}{\partial y}; \qquad \gamma_{xy}^b = \frac{\partial u_1}{\partial y} + \frac{\partial v_1}{\partial x} \tag{4.77}$$

$$\epsilon_x^c = \frac{\partial u_3}{\partial x}, \qquad \epsilon_y^c = \frac{\partial v_3}{\partial y}, \qquad \gamma_{xy}^c = \frac{\partial u_3}{\partial y} + \frac{\partial v_3}{\partial x} \tag{4.78}$$

The shear strains corresponds to bending of sandwich plate and rotations of base and

constraining layer are expressed as,

$$\gamma_{xz}^{b} = \frac{\partial w}{\partial x} - \alpha_1, \qquad \gamma_{yz}^{b} = \frac{\partial w}{\partial y} - \beta_1, \tag{4.79}$$

$$\gamma_{xz}^{c} = \frac{\partial w}{\partial x} - \alpha_3, \qquad \gamma_{yz}^{c} = \frac{\partial w}{\partial y} - \beta_3 \tag{4.80}$$

The curvatures corresponds to bending of base plate and constraining layer can be expressed as,

$$\kappa_x^b = \frac{\partial \alpha_1}{\partial x}, \qquad \kappa_y^b = \frac{\partial \beta_1}{\partial y}, \qquad \kappa_{xy}^b = \frac{\partial \alpha_1}{\partial y} + \frac{\partial \beta_1}{\partial x} \tag{4.81}$$

$$\kappa_x^c = \frac{\partial \alpha_3}{\partial x}, \qquad \kappa_y^b = \frac{\partial \beta_3}{\partial y}, \qquad \kappa_{xy}^b = \frac{\partial \alpha_3}{\partial y} + \frac{\partial \beta_3}{\partial x} \tag{4.82}$$

(A) FINITE ELEMENT DISCRETIZATION

The displacement field of the sandwich plate is discretized by assigning nine degrees of freedom (DOF) at each node. These are longitudinal displacements and transverse rotations of base and constraining layer and transverse displacement of the sandwich plate.
In a vector form the nodal displacement vector $\{U_i\}$ can be represented as follows:

$$\{U_j\} = [\, u_1, v_1, u_3, v_3, w, \alpha_1, \beta_1, \alpha_3, \beta_3]^T \tag{4.83}$$

By combining the displacements of all the four nodes, the element displacement vector of the sandwich plate element can be obtained and it can be expressed as

$$\{U_e\} = \begin{Bmatrix} \{U_1\} \\ \{U_2\} \\ \{U_3\} \\ \{U_4\} \end{Bmatrix} \tag{4.84}$$

The size of each nodal displacement vector of sandwich plate $\{U_1\}$ is 1 x 9 and the size of element nodal displacement is 1 x 36.

The interpolation of the longitudinal displacements of base and constraining layer, u_i and v_i, transverse displacement w, transverse rotations α_i and β_i over an element of the sandwich plate, are approximated with second order polynomials in the natural coordinates space (ξ, η)

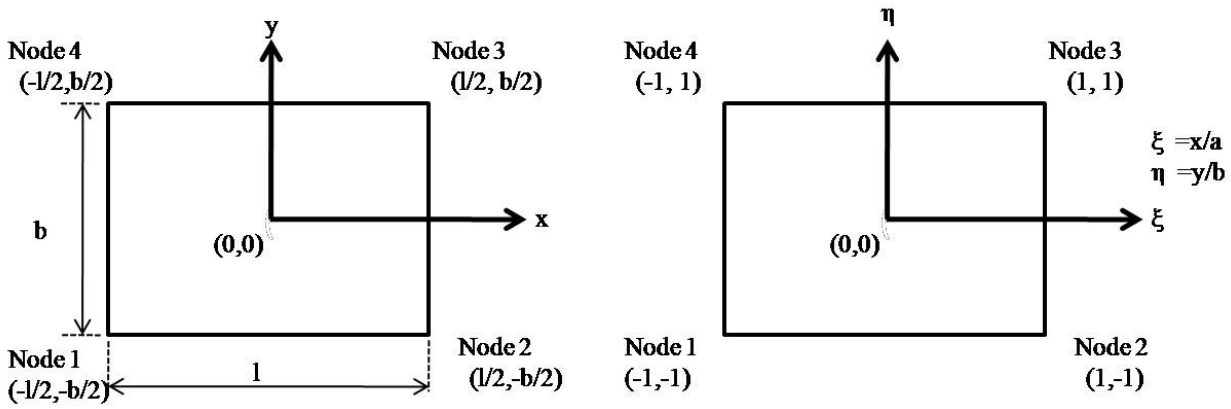

(a) (b)

Figure 4.6 Quadrilateral sandwich plate element in (a) Cartesian (b) Natural co-ordinates

Figure 4.6 depicts the quadrilateral sandwich element in Cartesian co-ordinate space and natural co-ordinates space. In the present case a rectangular element is being used. Isoparametric formulation is employed by choosing same interpolation polynomials for the geometry as well as field variables. The natural and Cartesian coordinates are related by the following interpolation functions

$$\begin{Bmatrix} u \\ v \end{Bmatrix} = \begin{bmatrix} n_1 & n_2 & n_3 & n_4 & 0 & 0 & 0 & 0 \\ 0 & 0 & 0 & 0 & n_1 & n_2 & n_3 & n_4 \end{bmatrix} \begin{Bmatrix} x_1 \\ x_2 \\ x_3 \\ x_4 \\ y_1 \\ y_2 \\ y_3 \\ y_4 \end{Bmatrix} \tag{4.85}$$

Where (x_i,y_i) are the Cartesian co-ordinates of node i

$$n_i = \frac{1}{4}(1 + \xi\xi_i)(1 + \eta\eta_i) \tag{4.86}$$

where i= 1, 2, 3 and 4

Where ξ_i and η_i are the natural coordinate values at the node I as given in Fig. 4.5(b) and are also given below for the respective nodes of the element

$$(\xi_1,\eta_1) = (-1,-1)\ ,\ (\xi_2,\eta_2) = (1,-1)\ ,\ (\xi_3,\eta_3) = (\ 1,\ 1)\ ,\ (\xi_4,\eta_4) = (-1,1) \tag{4.87}$$

The gradients of any field variable 'ϕ' within the element in Cartesian co-ordinate space and natural co-ordinate space are related through the Jacobian as shown below [47].

$$\begin{Bmatrix} \frac{\partial \phi}{\partial \xi} \\ \frac{\partial \phi}{\partial \eta} \end{Bmatrix} = \begin{bmatrix} \frac{\partial x}{\partial \xi} & \frac{\partial y}{\partial \xi} \\ \frac{\partial x}{\partial \eta} & \frac{\partial y}{\partial \eta} \end{bmatrix} \begin{Bmatrix} \frac{\partial \phi}{\partial x} \\ \frac{\partial \phi}{\partial y} \end{Bmatrix} \tag{4.88}$$

$$\begin{Bmatrix} \frac{\partial \phi}{\partial \xi} \\ \frac{\partial \phi}{\partial \eta} \end{Bmatrix} = [J] \begin{Bmatrix} \frac{\partial \phi}{\partial x} \\ \frac{\partial \phi}{\partial y} \end{Bmatrix} \tag{4.89}$$

where the Jacobian [J] can be expressed as

$$[\mathrm{J}] = \begin{bmatrix} \frac{\partial x}{\partial \xi} & \frac{\partial y}{\partial \xi} \\ \frac{\partial x}{\partial \eta} & \frac{\partial y}{\partial \eta} \end{bmatrix} = \begin{bmatrix} \sum_{i=1}^{4} \frac{\partial}{\partial \xi} n_{i,\xi} x_i & \sum_{i=1}^{4} \frac{\partial}{\partial \xi} n_{i,\xi} y_i \\ \sum_{i=1}^{4} \frac{\partial}{\partial \eta} n_{i,\eta} x_i & \sum_{i=1}^{4} \frac{\partial}{\partial \eta} n_{i,\eta} y_i \end{bmatrix} \tag{4.90}$$

Equation (4.88) can also be expressed as

$$\begin{Bmatrix} \frac{\partial \phi}{\partial x} \\ \frac{\partial \phi}{\partial y} \end{Bmatrix} = [J]^{-1} \begin{Bmatrix} \frac{\partial \phi}{\partial \xi} \\ \frac{\partial \phi}{\partial \eta} \end{Bmatrix} \tag{4.91}$$

Where the inverse of Jacobian matrix can be expressed as,

$$[J]^{-1} = \frac{1}{|J|} \begin{bmatrix} J_{22} & -J_{12} \\ -J_{21} & J_{11} \end{bmatrix} \tag{4.92}$$

Where $|J|$ is the determinant of the Jacobian matrix.

For the rectangular element under consideration, the Jacobean reduces to a simplified form as given below.

$$[J] = \frac{1}{4} \begin{bmatrix} 2l & 0 \\ 0 & 2b \end{bmatrix} = \begin{bmatrix} l/2 & 0 \\ 0 & b/2 \end{bmatrix} \tag{4.93}$$

$$[J]^{-1} = \begin{bmatrix} 2/l & 0 \\ 0 & 2/b \end{bmatrix} \tag{4.94}$$

Where *l* and *b* are the length and width of the element in Cartesian coordinate space.

The relation between the differential areas in Cartesian co-ordinate space to natural co-ordinate space is given below. The following relation is useful during the integration of element characteristic matrices.

$$dA = dx\, dy = |J| d\xi . d\eta \tag{4.95}$$

(B) INTERPOLATION

The chosen primary field variables within the element are interpolated in terms of the corresponding nodal displacements and they are mapped to the sandwich element nodal displacement. For example, u_1, the longitudinal displacement of the base plate is purely a function of the nodal axial displacement of the base plate in X-direction and has only four interpolation functions. Similarly every primary field variable is interpolated in terms of corresponding four nodal variables. The derived displacements and rotations of the viscoelastic layer are functions of all the primary variables. Hence, interpolation functions of all the primary variables are mapped to the entire nodal displacement vector of the sandwich plate element. The detailed formulations of all the interpolation functions are given in Appendix-`I'.

The longitudinal displacement of the base plate in x-direction are interpolated and expressed as

$$\{u_1\} = [N_1]\{U_e\}^T \tag{4.96}$$

where $[N_1]$ is the interpolation for longitudinal displacement of base plate in x-direction.

The longitudinal displacement of the base plate in y-direction can be interpolated and expressed as

$$\{v_1\} = [N_2]\{U_e\}^T \tag{4.97}$$

where $[N_2]$ is the interpolation for longitudinal displacement of base layer in y-direction.

The longitudinal displacement of the constraining layer in x-direction can be written as

$$\{u_3\} = [N_3]\{U_e\}^T \tag{4.98}$$

where, $[N_3]$ is the interpolation for longitudinal displacement of constraining layer in x-direction.

The longitudinal displacement of the constraining layer in y-direction can be written as

$$\{v_3\} = [N_4]\{U_e\}^T \tag{4.99}$$

where, $[N_4]$ is the interpolation for longitudinal displacement of constraining layer in y-direction.

The transverse displacement of all the three layer in z- direction can be written as

$$\{w\} = [N_5]\{U_e\}^T \tag{4.100}$$

Where, $[N_5]$ is the interpolation for transverse displacement of all the three layers.

The rotation of the base layer in x-direction can be written as

$$\{\alpha_1\} = [N_6]\{U_e\}^T \tag{4.101}$$

Where,$[N_6]$ is the interpolation for transverse rotation of base layer in x- direction.

The rotation of the base layer in y-direction can be written as

$$\beta_1 = [N_7]\{U_e\}^T \tag{4.102}$$

Where, $[N_7]$ is the interpolation for rotation of base layer in y-direction.

The rotation of the constraining layer in x-direction can be written as

$$\alpha_3 = [N_8]\{U_e\}^T \tag{4.103}$$

Where, $[N_8]$ is the interpolation for rotation of constraining layer in x-direction.

$$\beta_3 = [N_9]\{U_e\}^T \tag{4.104}$$

Where, $[N_9]$ is the interpolation for rotation of constraining layer in y-direction.

The strains components and curvatures in different layers are functions of gradients of displacements in Cartesian space, whereas the displacements within the sandwich plate element are in natural co-ordinate space. Hence, inverse Jacobian relation mentioned in equation (4.91) is used to express the strain components as functions of gradient of displacements in natural co-ordinate space.

The strain vector corresponds to longitudinal displacements of base plate$\{\mathcal{E}_{bp}\}$ can be expressed as,

$$\{\mathcal{E}_{bp}\} = \begin{Bmatrix} \dfrac{\partial u_1}{\partial x} \\ \dfrac{\partial v_1}{\partial y} \\ \dfrac{\partial u_1}{\partial y} + \dfrac{\partial v_1}{\partial x} \end{Bmatrix} \tag{4.105}$$

The gradients of displacement field mentioned in the above equation are in Cartesian co-ordinate space. To express the above gradients in natural co-ordinates space, the inverse Jacobean relation expressed in equation (4.90)is used by introducing primary field variables u_1 and v_1 in place of ϕ as given below,

$$\begin{Bmatrix} \frac{\partial u_1}{\partial x} \\ \frac{\partial u_1}{\partial y} \end{Bmatrix} = [J]^{-1} \begin{Bmatrix} \frac{\partial u_1}{\partial \xi} \\ \frac{\partial u_1}{\partial \eta} \end{Bmatrix} \tag{4.106}$$

Similarly,

$$\begin{Bmatrix} \frac{\partial v_1}{\partial x} \\ \frac{\partial v_1}{\partial y} \end{Bmatrix} = [J]^{-1} \begin{Bmatrix} \frac{\partial v_1}{\partial \xi} \\ \frac{\partial v_1}{\partial \eta} \end{Bmatrix} \tag{4.107}$$

For the rectangular element of length *l* and *b*, the inverse Jacobian can be expressed as,

$$[J]^{-1} = \begin{bmatrix} 2/l & 0 \\ 0 & 2/b \end{bmatrix} \tag{4.108}$$

Introducing appropriate terms of equations (4.106), (4.107) and (4.108) in equation (4.105), the strain due to longitudinal displacement of base plate can be expressed in natural co-ordinates as given below.

$$\{\mathcal{E}_{bp}\} = \begin{Bmatrix} \frac{2}{l}\frac{\partial u_1}{\partial \xi} \\ \frac{2}{b}\frac{\partial v_1}{\partial \eta} \\ \frac{2}{l}\frac{\partial u_1}{\partial \eta} + \frac{2}{b}\frac{\partial v_1}{\partial \xi} \end{Bmatrix} \tag{4.109}$$

Substituting interpolation functions as given in equations (4.96) and (4.97) for u_1 and $v_1$in the above equation, it can be expressed as follows.

$$\{\mathcal{E}_{bp}\} = \begin{Bmatrix} \frac{2}{l}\frac{\partial}{\partial \xi}[N_1]\{U_e\}^T \\ \frac{2}{b}\frac{\partial}{\partial \eta}[N_2]\{U_e\}^T \\ \frac{2}{l}\frac{\partial}{\partial \eta}[N_1]\{U_e\}^T + \frac{2}{b}\frac{\partial}{\partial \xi}[N_2]\{U_e\}^T \end{Bmatrix} \tag{4.110}$$

Now the strain vector corresponds to longitudinal displacements of the base plate can be expressed as,

$$\{\mathcal{E}_{bp}\} = \left[\mathrm{B_{bp}}\right]\{U_e\}^T \tag{4.111}$$

Where, $\left[B_{bp}\right]$ is the coupling matrix between the strain between longitudinal displacement of the base plate and nodal displacements of the sandwich plate and it can be expressed as :

$$\{B_{bp}\} = \begin{Bmatrix} \frac{2}{l}\frac{\partial[N_1]}{\partial\xi} \\ \frac{2}{b}\frac{\partial[N_2]}{\partial\eta} \\ \frac{2}{l}\frac{\partial[N_1]}{\partial\eta} + \frac{2}{b}\frac{\partial[N_2]}{\partial\xi} \end{Bmatrix} \tag{4.112}$$

The strain vector$\{\mathcal{E}_{cp}\}$ due to longitudinal displacements of constraining layer can be expressed as,

$$\{\mathcal{E}_{cp}\} = \begin{Bmatrix} \frac{\partial u_3}{\partial x} \\ \frac{\partial v_3}{\partial y} \\ \frac{\partial u_3}{\partial y} + \frac{\partial v_3}{\partial x} \end{Bmatrix} \tag{4.113}$$

As it was considered in the previous case, the gradients of field variables of constraining layer in the above equation are transformed to the natural co-ordinate space using inverse Jacobian relationship as given below

$$\{\mathcal{E}_{cp}\} = \begin{Bmatrix} \frac{2}{l}\frac{\partial u_3}{\partial\xi} \\ \frac{2}{b}\frac{\partial v_3}{\partial\eta} \\ \frac{2}{l}\frac{\partial u_3}{\partial\eta} + \frac{2}{b}\frac{\partial v_3}{\partial\xi} \end{Bmatrix} \tag{4.114}$$

Substituting interpolation functions as given in equations(4.98) and (4.99) for 'u_3' and 'v_3'inthe above equation, it can be expressed as

$$\{\mathcal{E}_{cp}\} = \begin{Bmatrix} \frac{2}{l}\frac{\partial}{\partial\xi}[N_3]\{U_e\}^T \\ \frac{2}{b}\frac{\partial}{\partial\eta}[N_4]\{U_e\}^T \\ \frac{2}{l}\frac{\partial}{\partial\eta}[N_3]\{U_e\}^T + \frac{2}{b}\frac{\partial}{\partial\xi}[N_4]\{U_e\}^T \end{Bmatrix} \tag{4.115}$$

Now the strain vector corresponds to longitudinal displacements of the constraining layer can be expressed as,

$$\{\mathcal{E}_{cp}\} = \left[\mathrm{B_{cp}}\right]\{U_e\}^T \tag{4.116}$$

Where, $\left[B_{cp}\right]$ is the coupling matrix between strain due to longitudinal displacement of constraining layer and nodal displacements of sandwich plate and it can be expressed as given below.

$$[B_{cp}] = \begin{Bmatrix} \frac{2}{l}\frac{\partial[N_3]}{\partial\xi} \\ \frac{2}{b}\frac{\partial[N_4]}{\partial\eta} \\ \frac{2}{l}\frac{\partial[N_3]}{\partial\eta} + \frac{2}{b}\frac{\partial[N_4]}{\partial\xi} \end{Bmatrix} \tag{4.117}$$

The curvature due to transverse rotations of base plate can be represented as follows

$$\{\kappa_{bb}\} = \begin{Bmatrix} -\kappa_x^b \\ -\kappa_y^b \\ -\kappa_{xy}^b \end{Bmatrix} = \begin{Bmatrix} -\frac{\partial\alpha_1}{\partial x} \\ -\frac{\partial\beta_1}{\partial y} \\ -\frac{\partial\alpha_1}{\partial y} - \frac{\partial\beta_1}{\partial x} \end{Bmatrix} \tag{4.118}$$

The gradients in the above equation are transformed to the natural co-ordinate space using inverse Jacobian relationship and can be expressed as given below

$$\{\kappa_{bb}\} = \begin{Bmatrix} -\frac{2}{l}\frac{\partial\alpha_1}{\partial\xi} \\ -\frac{2}{b}\frac{\partial\beta_1}{\partial\eta} \\ -\frac{2}{l}\frac{\partial\alpha_1}{\partial\eta} - \frac{2}{b}\frac{\partial\beta_1}{\partial\xi} \end{Bmatrix} \tag{4.119}$$

Substituting interpolation functions as given in equation (4.101) and (4.102) for α_1 and β_1 in the above equation, it can be expressed as

$$\{\kappa_{bb}\} = \begin{Bmatrix} -\frac{2}{l}\frac{\partial}{\partial\xi}[N_6]\{U_e\}^T \\ -\frac{2}{b}\frac{\partial}{\partial\eta}[N_7]\{U_e\}^T \\ -\frac{2}{l}\frac{\partial}{\partial\eta}[N_6]\{U_e\}^T - \frac{2}{b}\frac{\partial}{\partial\xi}[N_7]\{U_e\}^T \end{Bmatrix} \tag{4.120}$$

The curvature due to transverse rotations of base plate can also be written as,

$$\{\kappa_{bb}\} = [B_{bb}]\{U_e\}^T \tag{4.121}$$

Where, $[B_{bb}]$ is the coupling matrix between curvature of base plate and nodal displacement of sandwich plate and it can be expressed as follows

$$[B_{bb}] = \begin{Bmatrix} -\frac{2}{\mathrm{l}}\left\{\frac{\partial[N_6]}{\partial\xi}\right\} \\ -\frac{2}{\mathrm{b}}\left\{\frac{\partial[N_7]}{\partial\eta}\right\} \\ -\frac{2}{\mathrm{l}}\left\{\frac{\partial[N_6]}{\partial\eta}\right\} - \frac{2}{\mathrm{b}}\left\{\frac{\partial[N_7]}{\partial\xi}\right\} \end{Bmatrix} \tag{4.122}$$

The curvature due to transverse rotations of constraining layer can be represented as follows

$$\{\kappa_{\mathrm{cb}}\} = \begin{Bmatrix} -\kappa_x^c \\ -\kappa_y^c \\ -\kappa_{xy}^c \end{Bmatrix} = \begin{Bmatrix} -\frac{\partial\alpha_3}{\partial x} \\ -\frac{\partial\beta_3}{\partial y} \\ -\frac{\partial\alpha_3}{\partial y} - \frac{\partial\beta_3}{\partial x} \end{Bmatrix} \tag{4.123}$$

The gradients in the above equation are transformed to the natural co-ordinate space using inverse Jacobian relationship and can be expressed as given below

$$\{\kappa_{\mathrm{cb}}\} = \begin{Bmatrix} -\kappa_x^c \\ -\kappa_y^c \\ -\kappa_{xy}^c \end{Bmatrix} = \begin{Bmatrix} -\frac{\partial\alpha_3}{\partial\xi} \\ -\frac{\partial\beta_3}{\partial\eta} \\ -\frac{\partial\alpha_3}{\partial\eta} - \frac{\partial\beta_3}{\partial\xi} \end{Bmatrix} \tag{4.124}$$

Substituting interpolation functions of equation (4.103) and (4.104) for α_3 and $\beta_3$in the above equation, it can be expressed as

$$\{\kappa_{\mathrm{cb}}\} = \begin{Bmatrix} -\frac{2}{l}\frac{\partial}{\partial\xi}[N_8]\{U_e\}^T \\ -\frac{2}{b}\frac{\partial}{\partial\eta}[N_9]\{U_e\}^T \\ -\frac{2}{l}\frac{\partial}{\partial\eta}[N_7]\{U_e\}^T - \frac{2}{b}\frac{\partial}{\partial\xi}[N_8]\{U_e\}^T \end{Bmatrix} \tag{4.125}$$

The above curvature $\{\kappa_{\mathrm{cb}}\}$due to transverse rotation of constraining layer can also be expressed as,

$$\{\kappa_{\mathrm{cb}}\} = [B_{cb}]\{U_e\}^T \tag{4.126}$$

Where, $[B_{cb}]$ is the coupling matrix between curvature of constraining layer and nodal vectors of sandwich plate and it can be expressed as follows

$$[\kappa_{cb}] = \begin{Bmatrix} -\frac{2}{l}\left\{\frac{\partial[N_8]}{\partial\xi}\right\} \\ -\frac{2}{\mathrm{b}}\left\{\frac{\partial[N_9]}{\partial\eta}\right\} \\ -\frac{2}{\mathrm{l}}\left\{\frac{\partial[N_8]}{\partial\eta}\right\} - \frac{2}{\mathrm{b}}\left\{\frac{\partial[N_9]}{\partial\xi}\right\} \end{Bmatrix} \tag{4.127}$$

The transverse shear strain component in vector form of base plate can be expressed as

$$\{\gamma_s^b\} = \begin{Bmatrix} \gamma_{xz}^b \\ \gamma_{yz}^b \end{Bmatrix} = \begin{Bmatrix} -\alpha_1 + \frac{\partial w}{\partial x} \\ -\beta_1 + \frac{\partial w}{\partial y} \end{Bmatrix} \tag{4.128}$$

By replacing the Cartesian gradient with the gradient in natural co-ordinate space, the above equation can be re-written as,

$$\{\gamma_s^b\} = \begin{Bmatrix} -\alpha_1 + \frac{2}{l}\frac{\partial w}{\partial \xi} \\ -\beta_1 + \frac{2}{\mathrm{b}}\frac{\partial w}{\partial \eta} \end{Bmatrix} \tag{4.129}$$

By substituting interpolation functions of equations (4.100), (4.101) and (4.102)for α_1, β_1 and w in the above equation, it can be expressed as

$$\{\gamma_s^b\} = \begin{Bmatrix} -[N_6]\{U_e\}^T + \frac{2}{l}\frac{\partial}{\partial\xi}[N_5]\{U_e\}^T \\ -[N_7]\{U_e\}^T + \frac{2}{b}\frac{\partial}{\partial\eta}[N_5]\{U_e\}^T \end{Bmatrix} \tag{4.130}$$

The above shear strain component can also be expressed as,

$$\{\gamma_s^b\} = [B_{bs}]\{U_e\}^T \tag{4.131}$$

Where, $[B_{bs}]$ is the coupling matrix due to shear strain of the base plate and nodal vectors of the sandwich plate and can be expressed as follows

$$[\mathrm{B_{bs}}] = \begin{bmatrix} -[N_6] + \frac{2}{l}\frac{\partial[N_5]}{\partial\xi} \\ -[N_7] + \frac{2}{b}\frac{\partial[N_5]}{\partial\eta} \end{bmatrix} \tag{4.132}$$

The transverse shear strain component in vector form for constraining layer can be expressed as,

$$\gamma_s^c = \begin{Bmatrix} \gamma_{xz}^c \\ \gamma_{xz}^c \end{Bmatrix} = \begin{Bmatrix} -\alpha_3 + \dfrac{\partial w}{\partial x} \\ -\beta_3 + \dfrac{\partial w}{\partial y} \end{Bmatrix} \tag{4.133}$$

By replacing the Cartesian gradient with the gradient in natural co-ordinate space, the above equation can be re-written as

$$\gamma_s^c = \begin{Bmatrix} -\alpha_3 + \dfrac{2}{l}\dfrac{\partial w}{\partial \xi} \\ -\beta_3 + \dfrac{2}{b}\dfrac{\partial w}{\partial \eta} \end{Bmatrix} \tag{4.134}$$

By substituting interpolation functions of equations (4.100) ,(4.103) and (4.104) for w, α_3 and $\beta_3$in the above equation, it can be expressed as

$$\{\gamma_s^c\} = \begin{Bmatrix} -[N_8]\{U_e\}^T + \dfrac{2}{l}\dfrac{\partial}{\partial \xi}[N_5]\{U_e\}^T \\ -[N_9]\{U_e\}^T + \dfrac{2}{b}\dfrac{\partial}{\partial \eta}[N_5]\{U_e\}^T \end{Bmatrix} \tag{4.135}$$

$$\{\gamma_s^c\} = [B_{cs}]\{U_e\}^T \tag{4.136}$$

Where, $[B_{bs}]$ is the coupling matrix between shear strain of the constraining layer and nodal vectors of the sandwich plate and it can be expressed as follows

$$[\mathrm{B_{cs}}] = \begin{bmatrix} -[N_8] + \dfrac{2}{l}\dfrac{\partial [N_5]}{\partial \xi} \\ -[N_9] + \dfrac{2}{b}\dfrac{\partial [N_5]}{\partial \eta} \end{bmatrix} \tag{4.137}$$

The transverse shear strain matrix of constrained (viscoelastic) layer can be expressed in terms of base and constraining layer nodal displacements as follows

$$\gamma_{xz}^v = \alpha_2 + \frac{\partial w}{\partial x} = \left[\left(\frac{u_3 - u_1}{t_v}\right) - \left(\frac{t_b\alpha_1 + t_c\alpha_3}{2t_v}\right)\right] + \frac{\partial w}{\partial x} \tag{4.138}$$

$$\gamma_{yz}^v = \beta_2 + \frac{\partial w}{\partial x} = \left[\left(\frac{v_3 - v_1}{t_v}\right) - \left(\frac{t_b\beta_1 + t_c\beta_3}{2t_v}\right)\right] + \frac{\partial w}{\partial y} \tag{4.139}$$

Where, $\gamma_{xz}^v, \gamma_{yz}^v$ are the transverse shear rotations in xz and yz planes of viscoelastic layer

$$\gamma_s^v = \begin{Bmatrix} \gamma_{xz}^v \\ \gamma_{yz}^v \end{Bmatrix} = [B_{vs}]\{U_e\}^T \tag{4.140}$$

$$[B_{vs}] = \begin{bmatrix} \left[([N_3] - [N_1])/t_v - \left((t_b[N_6] + t_c[N_8])/2t_v \right) \right] + \left\{ \frac{\partial [N_5]}{\partial \xi} \right\} \\ \left[([N_4] - [N_2])/t_v - \left((t_b[N_7] + t_c[N_9])/2t_v \right) \right] + \left\{ \frac{\partial [N_5]}{\partial \eta} \right\} \end{bmatrix} \quad (4.141)$$

The matrix relating stress –strain due to in-plane loads of base and constraining layer can be expressed as [47]

$$[D_{bp}] = \frac{E_b t_b}{(1-\nu_b^2)} \begin{bmatrix} 1 & \upsilon_b & 0 \\ \upsilon_b & 1 & 0 \\ 0 & 0 & (1-\upsilon_b)/2 \end{bmatrix} \quad (4.142)$$

$$[D_{cp}] = \frac{E_c t_c}{(1-\nu_c^2)} \begin{bmatrix} 1 & \upsilon_c & 0 \\ \upsilon_c & 1 & 0 \\ 0 & 0 & (1-\upsilon_c)/2 \end{bmatrix} \quad (4.143)$$

The matrix relating stress-strain due to bending loads of base and constraining layer can be written as

$$[D_{bb}] = \frac{E_b t_b^3}{12(1-\nu_b^2)} \begin{bmatrix} 1 & \upsilon_b & 0 \\ \upsilon_b & 1 & 0 \\ 0 & 0 & (1-\upsilon_b)/2 \end{bmatrix} \quad (4.144)$$

$$[D_{cb}] = \frac{E_c t_c^3}{12(1-\nu_c^2)} \begin{bmatrix} 1 & \nu_c & 0 \\ \nu_c & 1 & 0 \\ 0 & 0 & (1-\nu_c)/2 \end{bmatrix} \quad (4.145)$$

The rigidity matrix corresponding to shear strain of base and constraining layer can be written as

$$[D_{bs}] = G_b t_b \begin{bmatrix} 1 & 0 \\ 0 & 1 \end{bmatrix} \quad (4.146)$$

$$[D_{cs}] = G_c t_c \begin{bmatrix} 1 & 0 \\ 0 & 1 \end{bmatrix} \quad (4.147)$$

The rigidity matrix corresponds to shear strain of constrained layer can be written as

$$[D_{vs}^*] = G_v^* t_v \begin{bmatrix} 1 & 0 \\ 0 & 1 \end{bmatrix} \quad (4.148)$$

where G_v^* is the frequency dependent complex shear modulus of the viscoelastic layer

(C) STRAIN ENERGY OF SANDWICH PLATE ELEMENT

The strain energy of the sandwich plate has contributions due to longitudinal and transverse displacement of base and constraining layer and transverse shear deformation of the all three layers. The detailed expressions for the strain energy contributions are given below

The strain energy due to in plane displacement of base plate $[P_{bp}]$ can be expressed as follows:

$$[P_{bp}] = \frac{1}{2}\int_{-1}^{1}\int_{-1}^{1}\{\mathcal{E}_{bp}\}^T[D_{bp}]\{\mathcal{E}_{bp}\}|J|d\xi d\eta \tag{4.149}$$

substituting equation (4.111) for $\{\mathcal{E}_{bp}\}$ in the above equation, it can be re-written as

$$[P_{bp}] = \frac{1}{2}\{U_e\}^T\left[\int_{-1}^{1}\int_{-1}^{1}[B_{bp}]^T[D_{bp}][B_{bp}]|J|d\xi d\eta\right]\{U_e\} \tag{4.150}$$

The above equation can also be expressed as

$$[P_{bp}] = \frac{1}{2}\{U_e\}^T[K_{bp}]\{U_e\} \tag{4.151}$$

where $[K_{bp}]$ is the stiffness matrix due to longitudinal displacement of base plate and it can be expressed as

$$[K_{bp}] = |J|\int_{-1}^{1}\int_{-1}^{1}[B_{bp}]^T[D_{bp}][B_{bp}]d\xi d\eta \tag{4.152}$$

The strain energy due to in plane displacement of constraining layer $[P_{cp}]$ can be expressed as follows:

$$[P_{cp}] = \frac{1}{2}\int_{-1}^{1}\int_{-1}^{1}\{\mathcal{E}_{cp}\}^T[D_{cp}]\{\mathcal{E}_{cp}\}|J|d\xi d\eta \tag{4.153}$$

substituting equation (4.116) for $\{\mathcal{E}_{cp}\}$ in the above equation, it can be re-written as

$$[P_{cp}] = \frac{1}{2}\{U_e\}^T\left[\int_{-1}^{1}\int_{-1}^{1}[B_{cp}]^T[D_{cp}][B_{cp}]|J|d\xi d\eta\right]\{U_e\} \tag{4.154}$$

The above equation can also be expressed as

$$[P_{cp}] = \frac{1}{2}\{U_e\}^T[K_{cp}]\{U_e\} \tag{4.155}$$

where $[K_{cp}]$ is the stiffness matrix due to in-plane displacement of constraining layer and it can be expressed as

$$[K_{cp}] = |J| \int_{-1}^{1} \int_{-1}^{1} [B_{cp}]^T [D_{cp}][B_{cp}] d\xi d\eta \tag{4.156}$$

The strain energy due to in plane shear deformation of base plate $[P_{bs}]$ can be expressed as

$$[P_{bs}] = \frac{1}{2} \int_{-1}^{1} \int_{-1}^{1} \{\gamma_s^b\}^T [D_{bs}] \{\gamma_s^b\} |J| d\xi d\eta \tag{4.157}$$

substituting equation (4.131) for $\{\gamma_s^b\}$ in the above equation, it can be re-written as

$$[P_{bs}] = \frac{1}{2} \{U_e\}^T \left[\int_{-1}^{1} \int_{-1}^{1} [B_{bs}]^T [D_{bs}][B_{bs}] |J| d\xi d\eta \right] \{U_e\} \tag{4.158}$$

The above equation can also be expressed as

$$[P_{bs}] = \frac{1}{2} \{U_e\}^T [K_{bs}] \{U_e\} \tag{4.159}$$

where $[K_{bs}]$ is the stiffness matrix due in plane shear deformation of base layer and it can be expressed as

$$[k_{bs}] = |J| \int_{-1}^{1} \int_{-1}^{1} [B_{bs}]^T [D_{bs}][B_{bs}] d\xi d\eta \tag{4.160}$$

The strain energy due to in shear deformation of constraining layer $[P_{cs}]$ can be expressed as follows:

$$[P_{cs}] = \frac{1}{2} \int_{-1}^{1} \int_{-1}^{1} \{\gamma_s^c\}^T [D_{cs}] \{\gamma_s^c\} |J| d\xi d\eta \tag{4.161}$$

substituting equation (4.137) for $\{\gamma_s^c\}$ in the above equation, it can be re-written as

$$[P_{cs}] = \frac{1}{2} \{U_e\}^T \left[\int_{-1}^{1} \int_{-1}^{1} [B_{cs}]^T [D_{cs}][B_{cs}] |J| d\xi d\eta \right] \{U_e\} \tag{4.162}$$

The above equation can also be expressed as

$$[P_{cs}] = \frac{1}{2} \{U_e\}^T [K_{cs}] \{U_e\} \tag{4.163}$$

where $[K_{cs}]$ is the stiffness matrix due to shear deformation of base layer and it can be expressed as follows:

$$[K_{cs}] = |J| \int_{-1}^{1}\int_{-1}^{1} [B_{cs}]^T [D_{cs}][B_{cs}] d\xi d\eta \tag{4.164}$$

The strain energy due to bending of base beam $[P_{bb}]$can be expressed as

$$[P_{bb}] = \frac{1}{2} \int_{-1}^{1}\int_{-1}^{1} \{\kappa_{bb}\}^T [D_{bb}]\{\kappa_{bb}\}|J| d\xi d\eta \tag{4.165}$$

substituting equation (4.121) for $\{\kappa_{bb}\}$ in the above equation, it can be re-written as follows:

$$[P_{bb}] = \frac{1}{2}\{U_e\}^T \left[\int_{-1}^{1}\int_{-1}^{1} [B_{bb}]^T [D_{bb}][B_{bb}]|J| d\xi d\eta\right]\{U_e\} \tag{4.166}$$

The above equation can also be expressed as,

$$[P_{bb}] = \frac{1}{2}\{U_e\}^T [K_{bb}]\{U_e\} \tag{4.167}$$

where $[K_{bb}]$ is the stiffness matrix due bending of base layer and it can be expressed as follows:

$$[K_{bb}] = |J| \int_{-1}^{1}\int_{-1}^{1} [B_{bb}]^T [D_{bb}][B_{bb}] d\xi d\eta \tag{4.168}$$

The strain energy due to in bending of constraining layer $[P_{cb}]$ can be expressed as

$$[P_{cb}] = \frac{1}{2} \int_{-1}^{1}\int_{-1}^{1} \{\kappa_{cb}\}^T [D_{cb}]\{\kappa_{cb}\}|J| d\xi d\eta \tag{4.169}$$

substituting equation (4.127) in the above equation, it can be re-written as

$$[P_{cb}] = \frac{1}{2}\{U_e\}^T \left[\int_{-1}^{1}\int_{-1}^{1} [B_{cb}]^T [D_{cb}][B_{cb}]|J| d\xi d\eta\right]\{U_e\} \tag{4.170}$$

The above equation can also be expressed as

$$[P_{cb}] = \frac{1}{2}\{U_e\}^T [K_{cb}]\{U_e\} \tag{4.171}$$

where $[K_{cb}]$ is stiffness matrix due bending of base layer and it can be expressed as follows:

$$[K_{cb}] = |J| \int_{-1}^{1}\int_{-1}^{1} [B_{cb}]^T [D_{cb}][B_{cb}] d\xi d\eta \tag{4.172}$$

The strain energy due to shear deformation of viscoelastic layer $[P_{vs}^*]$ can be expressed as

$$[\mathrm{P}_{\mathrm{vs}}^{*}] = \frac{1}{2}\int_{-1}^{1}\int_{-1}^{1}\{\gamma_s^{v}\}^{\mathrm{T}}[\mathrm{D}_{\mathrm{vs}}^{*}]\{\gamma_s^{v}\}|\mathrm{J}|d\xi d\eta \tag{4.173}$$

substituting equation (4.141) for $\{\gamma_s^{v}\}$ in the above equation, it can be re-written as

$$[\mathrm{P}_{\mathrm{vs}}^{*}] = \frac{1}{2}\{\mathrm{U_e}\}^{\mathrm{T}}\left[\int_{-1}^{1}\int_{-1}^{1}[\mathrm{B_{vs}}]^{\mathrm{T}}[\mathrm{D}_{\mathrm{vs}}^{*}][\mathrm{B_{vs}}]|\mathrm{J}|d\xi d\eta\right]\{\mathrm{U_e}\} \tag{4.174}$$

The above equation can also be expressed as

$$[\mathrm{P}_{\mathrm{vs}}^{*}] = \frac{1}{2}\{\mathrm{U_e}\}^{\mathrm{T}}[\mathrm{K}_{\mathrm{vs}}^{*}]\{\mathrm{U_e}\} \tag{4.175}$$

where $[\mathrm{K}_{\mathrm{vs}}^{*}]$ is the strain matrix due transverse shear deformation of viscoelastic layer and it can be expressed as

$$[\mathrm{K}_{\mathrm{sv}}^{*}] = |\mathrm{J}|\int_{-1}^{1}\int_{-1}^{1}[\mathrm{B_{sv}}]^{\mathrm{T}}[\mathrm{D}_{\mathrm{vs}}^{*}][\mathrm{B_{sv}}]\mathrm{d}\xi\mathrm{d}\eta \tag{4.176}$$

The total strain energy of the sandwich plate can be expressed as

$$[P_e] = [P_{bp}] + [P_{bb}] + [P_{bs}] + [P_{cp}] + [P_{bc}] + [P_{cs}] + [\mathrm{P}_{\mathrm{vs}}^{*}] \tag{4.177}$$

By combining the individual contributions of strain energy, the total strain energy of the sandwich plate can be expressed as

$$P_e = \frac{1}{2}U_e^{T}[K_e^{*}]U_e \tag{4.178}$$

Where$[K_e^{*}]$ is the complex element stiffness matrix of sandwich plate and it can be expressed as

$$[K_e^{*}] = [K_{cp}] + [K_{cb}] + [K_{cs}] + [K_{vs}^{*}] + [K_{bp}] + [K_{bb}] + [K_{bs}] \tag{4.179}$$

(D) KINETIC ENERGY OF SANDWICH PLATE

The total kinetic energy of the sandwich plate has the contributions from in-plane and bending motion of all the three layers. The effect of rotary inertia of all the three layers is also taken into account. The contribution of kinetic energy corresponds to bending of all the three layers can be written as

$$T_b = \frac{1}{2}(\rho t)_{eq}\int_A \{\dot{\mathrm{w}}\}^{\mathrm{T}}\{\mathrm{w}\}dA \tag{4.180}$$

where,$(\rho t)_{eq} = \rho_1 \mathrm{t_b} + \rho_2 \mathrm{t_v} + \rho_3 \mathrm{t_c}$

By differentiating equation (4.100) with respect to time and substituting in the above equation, it can be expressed as,

$$[T_b] = \frac{1}{2}\{\dot{U}_e\}^T \left[(\rho t)_{eq} \int_{-1}^{1}\int_{-1}^{1} [\mathrm{N_5}]^{\mathrm{T}}[\mathrm{N_5}]|\mathrm{J}|d\xi d\eta\right]\{\dot{U}_e\} \tag{4.181}$$

The above equation can also be expressed as

$$[T_b] = \frac{1}{2}\{\dot{U}_e\}^T [M_b]\{\dot{U}_e\} \tag{4.182}$$

where $[M_b]$ is the element mass matrix due to bending of sandwich plate

$$[\mathrm{M_b}] = \left(\rho t\right)_{eq}\int_{-1}^{1}\int_{-1}^{1} [[\mathrm{N_5}]^{\mathrm{T}}[[\mathrm{N_5}]|\mathrm{J}|\mathrm{d}\xi\mathrm{d}\eta \tag{4.183}$$

The kinetic energy due to longitudinal motion of base layer [T_{bp}] can be expressed as

$$[T_{bp}] = \frac{1}{2}\int_A \rho_b t_b[\{\dot{u}_1\}^T\{\dot{u}_1\} + \{\dot{v}_1\}^T\{\dot{v}_1\}]dA \tag{4.184}$$

By substituting equation (4.96) and (4.97) in the above equation, it can be expressed as

$$[T_{bp}] = \frac{1}{2}\{\dot{U}_e\}^T \left[\rho_b t_b \int_{-1}^{1}\int_{-1}^{1}\{[\mathrm{N_1}]^{\mathrm{T}}[\mathrm{N_1}] + [\mathrm{N_2}]^{\mathrm{T}}[\mathrm{N_2}]\}|\mathrm{J}|d\xi d\eta\right]\{\dot{U}_e\} \tag{4.185}$$

The above equation can also be expressed as

$$[T_{bp}] = \frac{1}{2}\{\dot{U}_e\}^T [M_{bp}]\{\dot{U}_e\} \tag{4.186}$$

where $[M_{bp}]$ is the element mass matrix due to longitudinal motion of base plate

$$[\mathrm{M_{bp}}] = \rho_{\mathrm{b}}\mathrm{t_b}\int_{-1}^{1}\int_{-1}^{1}\left([\mathrm{N_1}]^{\mathrm{T}}[\mathrm{N_1}] + [\mathrm{N_2}]^{\mathrm{T}}[\mathrm{N_2}]\right)|\mathrm{J}|\mathrm{d}\xi\mathrm{d}\eta \tag{4.187}$$

The kinetic energy due to longitudinal motion of constraining layer $[T_{cp}]$ can be expressed as

$$[T_{cp}] = \frac{1}{2}\int_A \rho_c t_c[\{\dot{u}_3\}^T\{\dot{u}_3\} + \{\dot{v}_3\}^T\{\dot{v}_3\}]dA \tag{4.188}$$

By substituting equation (4.98) and (4.99) in the above equation, it can be expressed as

$$[T_{cp}] = \frac{1}{2}\{\dot{U}_e\}^T \left[\rho_c t_c \int_{-1}^{1}\int_{-1}^{1}\{[\mathrm{N_3}]^{\mathrm{T}}[\mathrm{N_3}] + [\mathrm{N_4}]^{\mathrm{T}}[\mathrm{N_4}]\}|\mathrm{J}|d\xi d\eta\right]\{\dot{U}_e\} \tag{4.189}$$

The above equation can also be expressed as

$$[T_{cp}] = \frac{1}{2}\{\dot{U}_e\}^T [M_{cp}]\{\dot{U}_e\} \tag{4.190}$$

where $[M_{cp}]$ is the element mass matrix due to in-plane motion of constraining layer.

$$\left[\mathrm{M_{cp}}\right] = \rho_c t_c \int_{-1}^{1}\int_{-1}^{1} ([\mathrm{N_3}]^{\mathrm{T}}[\mathrm{N_3}] + [\mathrm{N_4}]^{\mathrm{T}}[\mathrm{N_4}])\,|\mathrm{J}|\mathrm{d}\xi\mathrm{d}\eta \tag{4.191}$$

The contribution of kinetic energy due to shear deformation of viscoelastic layer can be expressed as

$$T_{vp} = \frac{1}{2}\int_A \rho_v t_v[\{\dot{u}_2\}^T\{\dot{u}_2\} + \{\dot{v}_2\}^T\{\dot{v}_2\}]dA \tag{4.192}$$

by substituting interpolations of sandwich plate in the above equation can be written as,

$$T_{vp} = \frac{1}{2}\{\dot{U}_e\}^T\left[\rho_v t_v \int_{-1}^{1}\int_{-1}^{1}\{[\mathrm{N}]^{\mathrm{T}}[\mathrm{C_v}][\mathrm{N}]\}|\mathrm{J}|d\xi d\eta\right]\{\dot{U}_e\} \tag{4.193}$$

where [N]= $\{[N_1]\quad[N_2]\quad[N_3]\quad[N_4]\quad[N_5]\quad[N_6]\quad[N_7]\quad[N_8]\quad[N_9]\}$

Equation (4.193) can also be expressed as,

$$[T_{vp}] = \frac{1}{2}\{\dot{U}_e\}^T[M_{vp}]\{\dot{U}_e\} \tag{4.194}$$

where, $[M_{vp}]$ is the element mass matrix due to longitudinal vibration of constrained (viscoelastic) layer.

$$\left[\mathrm{M_{vp}}\right] = \rho_v t_v|\mathrm{J}|\int_{-1}^{1}\int_{-1}^{1}\{[\mathrm{N}]^{\mathrm{T}}[\mathrm{C_v}][\mathrm{N}]\}d\xi d\eta \tag{4.195}$$

The constant $[\mathrm{C_v}]$ in the above equation is given in Appendix-'II'

The contribution of kinetic energy due to rotary inertia of base plate (T_{br}) can be expressed as

$$T_{br} = \frac{1}{2}\frac{\rho_b {t_b}^3}{12}\int_A \left[\{\dot{\alpha}_1\}^T\{\dot{\alpha}_1\} + \{\dot{\beta}_1\}^T\{\dot{\beta}_1\}\right]dA \tag{4.196}$$

$$T_{br} = \frac{1}{2}\{\dot{U}_e\}^T\left[\frac{\rho_b {t_b}^3}{12}\int_{-1}^{1}\int_{-1}^{1}\{[\mathrm{N_6}]^{\mathrm{T}}[\mathrm{N_6}] + [\mathrm{N_7}]^{\mathrm{T}}[\mathrm{N_7}]\}|\mathrm{J}|d\xi d\eta\right]\{\dot{U}_e\} \tag{4.197}$$

The above matrix can also be expressed as

$$[T_{br}] = \frac{1}{2}\{\dot{U}_e\}^T[M_{br}]\{\dot{U}_e\} \tag{4.198}$$

where $[M_{br}]$ is the element mass matrix due to rotational vibration of base layer and it can be expressed as

$$[\mathrm{M_{br}}] = \frac{\rho_b t_b^3}{12}\int_{-1}^{1}\int_{-1}^{1}\{[\mathrm{N_6}]^{\mathrm{T}}[\mathrm{N_6}] + [\mathrm{N_7}]^{\mathrm{T}}[\mathrm{N_7}]\}|\mathrm{J}|d\xi d\eta \tag{4.199}$$

The contribution of kinetic energy due to rotary inertia of constraining layer (T_{cr}) can be expressed as

$$T_{cr} = \frac{1}{2}\frac{\rho_c {t_c}^3}{12}\int_A \left[\{\dot{\alpha}_3\}^T\{\dot{\alpha}_3\} + \{\dot{\beta}_3\}^T\{\dot{\beta}_3\}\right] dA \tag{4.200}$$

$$T_{cr} = \frac{1}{2}\{\dot{U}_e\}^T\left[\frac{\rho_c {t_c}^3}{12}\int_{-1}^{1}\int_{-1}^{1}\{[\mathrm{N_8}]^{\mathrm{T}}[\mathrm{N_8}] + [\mathrm{N_9}]^{\mathrm{T}}[\mathrm{N_9}]\}|\mathrm{J}|d\xi d\eta\right]\{\dot{U}_e\} \tag{4.201}$$

The above matrix can also be expressed as

$$T_{cr} = \frac{1}{2}\{\dot{U}_e\}^T[M_{cr}]\{\dot{U}_e\} \tag{4.202}$$

where $[M_{cr}]$ is the element mass matrix due to rotational motion of constraining layer and it can be expressed as

$$[\mathrm{M_{cr}}] = \frac{\rho_c t_c^3}{12}\int_{-1}^{1}\int_{-1}^{1}\{[\mathrm{N_8}]^{\mathrm{T}}[\mathrm{N_8}] + [\mathrm{N_9}]^{\mathrm{T}}[\mathrm{N_9}]\}|\mathrm{J}|d\xi d\eta \tag{4.203}$$

The contribution of kinetic energy due to rotary inertia of viscoelastic layer (T_{vr}) can be expressed as

$$T_{vr} = \frac{1}{2}\{\dot{U}_e\}^T\left[\frac{\rho_v {t_v}^3}{12}\int_{-1}^{1}\int_{-1}^{1}\{[\mathrm{N}]^{\mathrm{T}}[\mathrm{I_v}][\mathrm{N}]\}\{\dot{U}_e\}d\xi d\eta\right]\{\dot{U}_e\} \tag{4.204}$$

The above matrix can also be expressed as

$$T_{vr} = \frac{1}{2}\{\dot{U}_e\}^T[M_{vr}]\{\dot{U}_e\} \tag{4.205}$$

where $[M_{vr}]$ is the element mass matrix due to rotational vibration of constrained layer and it can be expressed as

$$[\mathrm{M_{vr}}] = \frac{\rho_v t_v^3}{12}|\mathrm{J}|\int_{-1}^{1}\int_{-1}^{1}\{[\mathrm{N}]^{\mathrm{T}}[\mathrm{I_v}][\mathrm{N}]\}d\xi d\eta \tag{4.206}$$

The details of constant $[\mathrm{I_v}]$ is given in Appendix- 'II'.

The total kinetic energy of the sandwich plate can be written as

$$T_e = T_b + T_{bp} + T_{cp} + T_{vp} + T_{br} + T_{cr} + T_{vr} \tag{4.207}$$

By introducing equations (4.190), (4.194), (4.198),(4.202) and (4.205) for $T_b, T_{bp}, T_{cp}, T_{vp}, T_{br}, T_{cr} and\ T_{vr}$ in the above equation can also be expressed as follows:

$$T_e = \frac{1}{2}\{\dot{U}^e\}^T[M_e]\{\dot{U}^e\} \tag{4.208}$$

where$[M_e]$ is the element mass matrix for the sandwich plate and it can be expressed as

$$[M_e] = [\mathrm{M_b}] + [\mathrm{M_{bp}}] + [\mathrm{M_{cp}}] + [\mathrm{M_{vp}}] + [\mathrm{M_{br}}] + [\mathrm{M_{cr}}] + [\mathrm{M_{vr}}] \quad (4.209)$$

The size of the element mass matrix is 36 X 36.

By introducing the total potential energy equation (4.179) and total kinetic energy of equation (4.210) in equation (4.2), the element equation of motion can be obtained as

$$[M_e]\{\ddot{U}_e\} + [K_e^*]\{U_e\} = 0 \quad (4.210)$$

By assembling the elemental equations by ensuring continuity across the boundaries, the equation of motion can be obtain in the following form

$$[M]\{\ddot{U}\} + [K^*]\{U\} = 0 \quad (4.211)$$

By suppressing the degrees of freedom and the corresponding coefficients of the constraining layer, the unconstrained layer can be obtained from the model.

(E) FE FORMULATION OF SANDWICH PLATE STRUCTURE

The sandwich plate is modelled using Reissner –Mindlin plate theory to evaluate the dynamic properties. The plate is discretized using four noded plate element, with nine degrees of freedom (DOF) at each node. The constrained and constraining layer length is 240 mm compared to base plate length of 250mm.

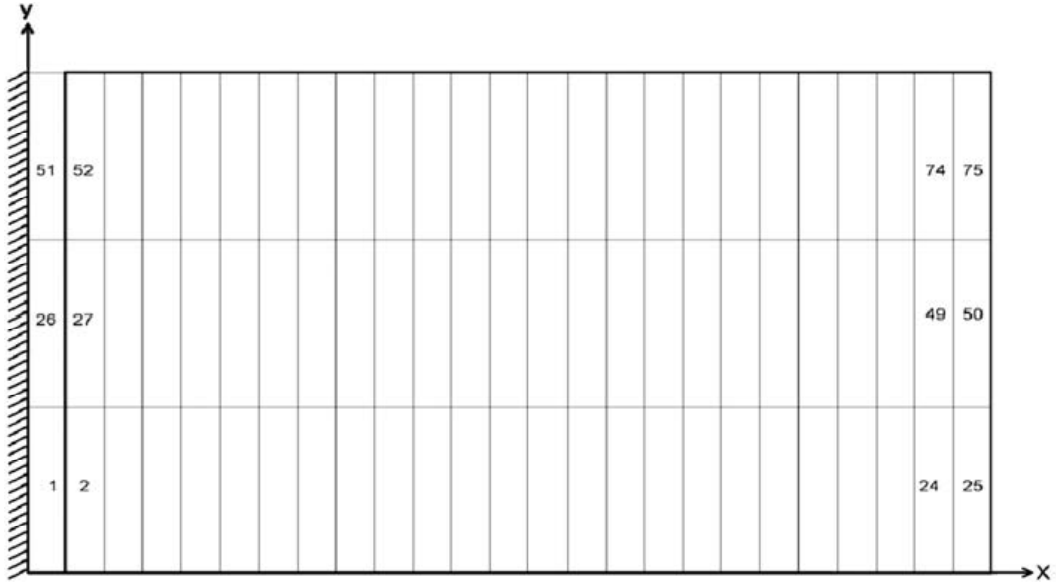

Figure 4.7 FE mesh of sandwich plate

The sandwich plate is discretized into 25 elements along X-direction and 3 elements along Y-direction directions as shown in Figure 4.6. The constrained and constraining layers are free at both edges. So, during FE formulation of sandwich plate, the material properties like Young's modulus, shear modulus and density of constrained and constraining layer are degraded to a low value for the elements 1, 26 and 51 respectively. The element mass matrix and complex stiffness matrix are assembled using standard assembly procedure to ensure continuity and compatibility across the element boundaries. The assembled dynamic equation of motion of sandwich beam is express in equation (4.211). All DOF's corresponding to clamped edges are constrained to simulate clamped at one edge and free at other three edge boundary condition (CFFF). The detailed procedure of solving dynamic equations of motion is described in chapter 5. Similar procedure is adopted for modelling of unconstrained layer by degrading the material properties of constraining layer to zero.

4.3 SUMMARY

Finite element based dynamic models are developed for sandwich beam and plate structures. The sandwich structure is discretized using finite element approximations and dynamic equations of motion are developed using Lagrangian method. Transverse shear deformation is considered for viscoelastic as well as base and constraining layers. The elements of the obtained stiffness matrix are complex and the real and imaginary parts are represented separately.

The main feature of the developed dynamic model is its capability to incorporate the frequency dependent properties of the viscoelastic layers. The model is also capable of handling unconstrained and constrained viscoelastic damping layers. The novel feature of the model is its suitability for developing an iterative computational scheme to solve the dynamic equations of motion presented in the next chapter.

.

CHAPTER 5

COMPUTATIONAL SCHEME FOR SANDWICH STRUCTURES WITH VISCOELASTIC LAYERS

5.1 INTRODUCTION

Equations of motion for the sandwich beam and plate structures with viscoelastic layers have been developed in the previous chapter. As already discussed in chapter 3, the material constants of viscoelastic layer are complex and frequency dependent. Due to this, the stiffness matrix in the developed FE based dynamic model consists of frequency dependent complex elements necessitating a special methodology to solve these equations of motion. An iterative computational scheme is proposed to solve these equations of motion and validated with experiment results. Dynamic equations of motion for sandwich structures developed in the previous chapter are modified for base excitation. The objective of the computational scheme is to find the loss factors of sandwich structure and evaluate the performance of viscoelastic materials for dynamic applications over a wide frequency band. This will help in carrying out simulations to design appropriate sandwich beam and plate structures.

5.2 EQUATIONS OF MOTION

The equations of motion developed for sandwich structures in the previous chapter are given below.

$$[M]\{\ddot{U}(t)\} + [K^*]\{U(t)\} = 0 \tag{5.1}$$

Where, [M] is the global mass matrix, [K^*] is the global complex stiffness matrix that varies with excitation frequency. The vectors U(t) and $\ddot{U}(t)$ are the generalized displacement and acceleration vectors respectively. The material properties of the viscoelastic layer are obtained using DMA for each discrete frequency and expressed in mathematical form using power-fit. The details of these equations are given chapter 3 as equations 3.22 to 3.25.

Equation (5.1) is solved for harmonic base excitation and the procedure is described below. The displacement and accelerations are partitioned into two groups namely the constrained and unconstrained generalized co-ordinates. The constrained generalized co-ordinates are those co-ordinates that lie on the base of the structure i.e. clamped to the exciter where the excitation is given as input. As per the partitioned generalized co-ordinates, the mass and stiffness matrices in equation 5.1 are also partitioned as given below.

$$\begin{bmatrix} M_{cc} & M_{cu} \\ M_{uc} & M_{uu} \end{bmatrix} \begin{Bmatrix} \ddot{U}_c(t) \\ \ddot{U}_u(t) \end{Bmatrix} + \begin{bmatrix} K^*_{cc} & K^*_{cu} \\ K^*_{uc} & K^*_{uu} \end{bmatrix} \begin{Bmatrix} U_c(t) \\ U_u(t) \end{Bmatrix} = 0 \tag{5.2}$$

The displacements in the above equations are partitioned for base excitation as, $\{U(x,t)\} = \{U_c(x,t)\ U_u(x,t)\}^T$, where $U_c(x,t)$ is the set of constrained generalised displacements and $U_u(x,t)$ is the set of unconstrained generalised displacements. The subscript 'cc' and 'uu' represent constrained and unconstrained part of global mass and global complex stiffness matrices. The subscript 'cu' represents the coupling terms between constrained and unconstrained degrees of freedom.

The equation (5.2) can also be written in the expanded form as follows

$$[M_{cc}]\{\ddot{U}_c(t)\} + [M_{cu}]\{\ddot{U}_u(t)\} + [K^*_{cc}]\{U_c(t) + [K^*_{cu}]\{U_u(t)\} = 0 \tag{5.3}$$

$$[M_{uc}]\{\ddot{U}_c(t)\} + [M_{uu}]\{\ddot{U}_u(t)\} + [K^*_{uc}]\{U_c(t) + [K^*_{uu}]\{U_u(t)\} = 0 \tag{5.4}$$

The set of unconstrained displacements can be decomposed into pseudo-static $\{U_s\}$ and dynamic parts $\{U_d\}$ as

$$U_u(x,t) = U_s(x,t) + U_d(x,t) \tag{5.5}$$

The pseudo-displacements can be obtained by excluding the first term on the left hand side of the equation (5.4) and by replacing $\{U_u\}$ by $\{U_s\}$:

$$\{U_s(x,t)\} = -[K_{uu}^*]^{-1}[K_{uc}^*]\{U_c(x,t)\} = [kk]\{U_c(x,t)\} \tag{5.6}$$

where, $[kk] = -[K_{uu}^*]^{-1}[K_{uc}^*]$ (5.7)

Substituting Eq. (5.6) in Eq. (5.5), it can be expressed as

$$\{U_u(x,t)\} = [kk]\{U_c(x,t)\} + \{U_d(x,t)\} \tag{5.8}$$

By substituting above equation in equation (5.4), it can be re-written as

$$[M_{uc}]\{\ddot{U}_c\} + [M_{uu}]\{[kk]\{\ddot{U}_c\} + \ddot{U}_d\} + [K_{uc}^*]\{U_c\} + [K_{uu}^*]\{[kk]U_c + U_d\} = 0 \tag{5.9}$$

The above equation can be further re-arranged as

$$[M_{uu}]\{\ddot{U}_d\} + [K_{uu}^*]\{U_d\} = -\{[M_{uc}] + [M_{uu}]\}[kk]\{\ddot{U}_c\} - \{[K_{uc}^*] + [K_{uu}^*][kk]\}\{U_c\} \tag{5.10}$$

The second terms in the right side of equation (5.10) reduces to zero after substituting equation (5.7). So equation (5.10) can be expressed as

$$[M_{uu}]\{\ddot{U}_d\} + +[K_{uu}^*]\{U_d\} = -\{[M_{uc}] + [M_{uu}]\}[kk]\{\ddot{U}_c\} \tag{5.11}$$

denoting $\Gamma = \{[M_{uc}] + [M_{uu}]\}[kk]$, the above equation becomes (5.12)

Adopting modal analysis approach, the response vector, U_d (x, t) can be written as,

$$\{U_d(x,t)\} = [P]\{q_m(t)\} \tag{5.13}$$

where, [P] is the modal matrix and $\{q_m(t)\}$ is the modal response vector. The modal matrix can be obtained by solving the eigenvalue problem as,

$$\left([K_{uu}^*\ ] - [M_{uu}]\omega^2\right)\{p\} = 0 \tag{5.14}$$

where {p} is the modal vector

As it is a well-known fact that, the major contribution in the dynamic response is contributed by first few modes, the equation of motion (5.12) is transformed in to first three modal co-ordinates. By transforming the equations of motion of Eq. (5.12) in to the modal co-ordinates using Eqn. (5.13).

$$[P]^T[M_{uu}][P]\{\ddot{q}_m(t)\} + [P]^T[K_{uu}{}^*][P]\{q_m(t)\} = [P][\Gamma]\{\ddot{U}_c(t)\} \tag{5.15}$$

This equation can be further simplified to

$$[M_m]\{\ddot{q}_m(t)\} + [K_m^*]\{q_m(t)\} = [\Gamma_m]\{\ddot{U}_c(t)\} \quad (5.16)$$

where, $[M_m]=[P]^T[M_{uu}][P]$ is the modal mass matrix, $[K_m^*]=[P]^T[K_{uu}^*][P]$ is the complex modal stiffness matrix, and $[\Gamma_m]=[P]^T\{\Gamma\}$ is the modal force vector. These equations are converted to frequency domain to obtain frequency response function (FRF) using state-space technique.

5.3 STATE SPACE FORMULATION

The equation of motion for the base excitation obtained in the previous section is in time domain. It is convenient to transform them to frequency domain to obtain Frequency Response Functions (FRFs). Hence, these equations are transformed using state space approach. The reduced dynamic model for base excitation of sandwich structure is presented below.

Considering the state vectors as,

$$\{z_1(t)\} = \{q_{mi}(t)\} \quad 5.17(a)$$

$$\{z_2(t)\} = \{\dot{q}_{mi}(t)\} \quad 5.17(b)$$

using the state equations, the reduced dynamic model equation of (5.16) can be written as

$$\begin{Bmatrix}\dot{z}_1(t)\\ \dot{z}_2(t)\end{Bmatrix} = \begin{bmatrix}[0]_{nxn} & [I]_{nxn}\\ -\{[M_m]^{-1}[K_m^R]\}_{nxn} & -\{[M_m]^{-1}[K_m^I]\}_{nxn}\end{bmatrix}\begin{Bmatrix}z_1(t)\\ z_2(t)\end{Bmatrix}_{2nx1} + \begin{bmatrix}[0]_{nx1}\\ [\Gamma_m]_{nx1}\end{bmatrix}\{\ddot{U}_c(t)\} \quad (5.18)$$

In this equation, the imaginary part of the stiffness matrix $[K_m^I]$ consists of loss factors of base plate, viscoelastic layer and constraining layer which represents the damping in the system. The loss factors for base and constraining layer are obtained from experiments while the loss factor of viscoelastic layer which is frequency dependent is obtained from DMA test and expressed as polynomial equations.

So, the equation (5.18) can be written in simplified form as

$$\{\dot{z}(t)\} = [A]\{z(t)\} + [B]\{\ddot{U}_c(t)\} \quad (5.19)$$

where, [A] is the state matrix and [B] is the input matrix

$$\{\ddot{q}_{mi}(t)\} = [\beta_s]\{\dot{z}(t)\} \quad (5.20)$$

where $[\beta_s] = [0 \quad 1]$

substituting the above equation in (5.19)

$$\{\ddot{q}_m(t)\} = \beta_s\big([A]\{z(t)\} + [B]\{\ddot{U}_c(t)\}\big) \tag{5.21}$$

The above equation the modal transfer functions can be written as

$$[\mathrm{H}_m(s)] = [\beta_s[A][sI - A]^{-1}[B] \tag{5.22}$$

The overall transfer functions for first three modes at the desired location can be expressed as

$$[H(s)] \quad = \sum_{i=1}^{3} \{P\}_i \, [H_{mi}(s)] \tag{5.23}$$

Mode summation method is used to calculate the overall response of the beam at the desired location. The frequency response function (FRF) can be generated from the results of many discrete frequency calculations of equation (5.23) starting from 20 Hz to 1000 Hz in discrete steps of 1 Hz. The complex stiffness matrix of viscoelastic layer is updated at each frequency and the magnitude corresponding to each excitation frequency is stored and FRF is constructed at a given location. From the stored data of FRF the loss factors of sandwich structure are calculated for the first three modes. The details of calculating response at each excitation frequency is shown in Figure 5.1 as flow chart.

5.4 SUMMARY

The dynamic equations of motion are altered for base excitation. The iterative computational scheme is developed to handle the frequency dependent moduli and loss factors of the viscoelastic material. The guidelines for extending the scheme to handle generic boundary conditions and force excitations are also presented.

The iterative scheme presented is a novel approach that helps to predict the dynamic response of sandwich structures with viscoelastic damping layers, whose properties are frequency dependent. The response is predicted in frequency domain which can be processed further to estimate the damping loss factors. This leads to a viable approach to predict the damping in sandwich structures in place of costly experimental methods.

FLOW CHART

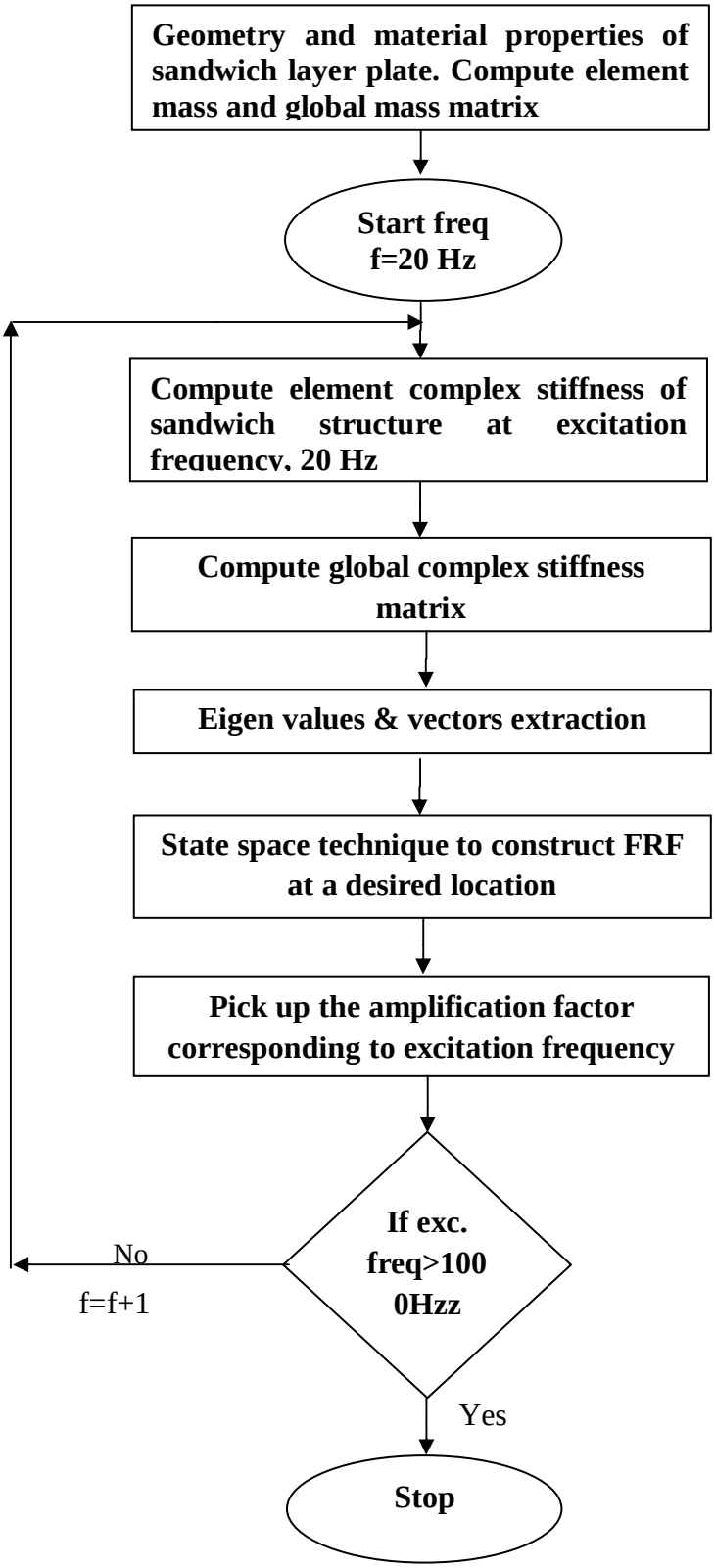

Figure 5.1 Flow chart

CHAPTER 6

EXPERIMENTAL STUDIES ON SANDWICH STRUCTURES

6.1 INTRODUCTION

In the previous chapters, the dynamic modelling of sandwich structure and the computational scheme to solve the dynamic equation of motion for base excitation has been discussed. In real working conditions, the experimental evaluation of damping becomes necessary to validate the developed dynamic model. The objective of the present chapter is to experimentally determine the natural frequencies, amplification and damping ratios of the sandwich structures. The details are presented in this chapter. The loss factors are calculated using FRFs obtained from experiments. Experiments are carried out with base excitation to eliminate the contribution of armature dynamics of the shaker to the response of the sandwich structure.

6.2 DESCRIPTION OF EXPERIMENTS

Experiments are carried out extensively on sandwich beam and plate structures with different viscoelastic materials. The details of instrumentation, clamping arrangement, preparation of test specimens, test setup and experimental procedure are presented below.

6.2.1 DETAILS OF INSTRUMENTATION

The instruments used in the experiments are briefly described below

(A) Electro-dynamic shaker

(B) Accelerometers

(C) Low noise microdot cables

(D) Signal output card

(E) LMS SCADAS-III programmable Quad Amplifier, PQA (Input module)

(F) LMS SCADAS-III hardware with LMS Test. Lab software

(A) ELECTRO-DYNAMIC SHAKER

It is an electro-mechanical device which transforms electrical A.C signal into mechanical vibration. The photograph of electrodynamic shaker is shown in Figure 6.1. The specifications of electro-dynamic shaker used in the experiments are given below.

i.	Force rating	:	20000 N
ii.	Frequency range	:	5-2000 Hz
iii.	Maximum bare table acceleration	:	100 g
iv.	Maximum displacement	:	± 25 mm
v.	First armature resonance	:	2500 Hz

Figure 6.1 Electrodynamic shaker

(B) ACCELEROMETERS

Miniature uniaxial accelerometers with built in signal conditioners are used during experiments. Figure 6.2 shows a typical miniature accelerometer. The accelerometer mounted on clamping plate measures base acceleration and accelerometers mounted at different locations on the sandwich structure measure the response. The specifications of the accelerometers are given below.

i.	Type	:	ICP® Accelerometer
ii.	Construction	:	Delta shear
iii.	Sensitivity	:	10 mV/g
iv.	Amplitude range	:	500 g
v.	Frequency range	:	1-9000 Hz

Figure 6.2 Miniature Accelerometer
Model No.352C41 (PCB make)

(C) LOW NOISE MICRODOT CABLES

The accelerometers with built in signal conditioners operate through a two wire circuit with signal/power on one lead and other lead being ground. Though, the output signals from these accelerometers are low impedance, low noise microdot cables as shown in Figure 6.3 are used to minimise the electrical noise. These cables are in tightly wrapped construction to minimize the triboelectric noise. The triboelectric noise is the charge-generated due to separation and movement of dielectric and shield in the cables which alters the output signal. The cable motion is restricted by anchoring at appropriate locations to reduce the electrical noise.

Figure 6.3 Low noise microdot cable

(D) SIGNAL OUTPUT CARD (QDAC)

The signal output card is also called as Quad Digital to Analog Convertor (QDAC) card. A built in Digital Signal Processing (DSP) chip in the QDAC supports the generation of variety of standard excitation signals such as burst random with variable burst length, impulse, sine and stepped sine signals up to a bandwidth of 40 kHz. The signal output card (DAC) provides the voltage output to the power amplifier. The associated software 'Test.lab' generates a sinusoidal frequency with given amplitude and frequency and send it to the power

amplifier through signal output card. The photograph of signal output card is shown in Figure 6.4. The specifications of signal output card are

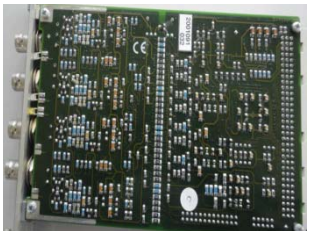

Figure 6.4 Signal output card (DAC)

i. Ultra-low noise and ultra low distortion
ii. 24-bit Digital to analog convertor for a dynamic range of 108 dB
iii. Bandwidth up to 40 kHz
iv. Output voltage of ±10 Volts
v. Full-colour coded LED indicator
vi. Uncorrelated baseband noise generation
vii. Sine and stepped signal with amplitude, phase and sweep control
viii. Continuous output of previously measured signals
ix. Slow start/stop
x. Smooth transition algorithm for transient free amplitude control

(E) LMS SCADAS-III PROGRAMMABLE QUAD AMPLIFIER, PQA (INPUT LMS **MODULE)**

SCADAS-III programmable Quad amplifier consists of signal conditioning card and signal processing card. The signal conditioner module provides the interface between accelerometer signal and signal processing card. The signal conditioner provides the power supply to the accelerometers. The module has an ICP cable check circuit to detect an open loop in the sensor cable. The signal processing module converts analog signals to digital signals. The photograph of the voltage input differential module is shown in Figure 6.5. The signal processing board provides real time data acquisition and digital signal processing. The signal processing provides the connection between one or more stacked signal conditioner cards. It has four 5-pole anti aliasing filters with equal time delay and four 16-bit delta sigma analog to digital converter.

Figure 6.5 Input module (ADC)

The specifications of the voltage/ICP input differential module are

i. Single ended input (BNC connector)
ii. Voltage and ICP modes selectable per channel
iii. Analog anti-alias and digital re-sampling filter
iv. 24-bit ∑- Δ ADC with up to 204.8 kHz sampling frequency
v. Alias free bandwidth of 92 kHz
vi. ICP sensor supply (3.5 milli Ampere)
vii. Cable check with full colour coded LED indicator
viii. AC coupling with 0.5 Hz or 7 Hz high pass filters
ix. Input range up to ±10 Volts

(F) LMS SCADAS-III HARDWARE WITH TEST. LAB SOFTWARE

The data acquisition and controller used in the experiments is Leuven Measurement System [48] manufactured by LMS, Belgium. It consists of four channel general purpose signal output card (Digital to Analog Convertor, DAC) and 64 channel voltage/ICP input module (Analog to Digital Convertor, ADC). SCADAS stands for supervisory controller and data acquisition system. The photograph of LMS SCADAS-III system is shown in Figure 6.6.

Figure 6.6 SCADAS-III: Controller and data acquisition system

6.2.2 CLAMPING ARRANGEMENT

The schematic of clamping arrangement is shown in Figure 6.7. The sandwich beam or plate is rigidly clamped at its base in between two clamping plates. The dimensions of each clamping plate are 200 X100 X 20 mm and they are made of mild steel. This clamping arrangement will also act as an interface fixture between sandwich structure and vibrating base of the electrodynamic shaker. The vibrating base of the shaker has a standard pattern of holes and these patterns of holes are replicated on the clamping plate.

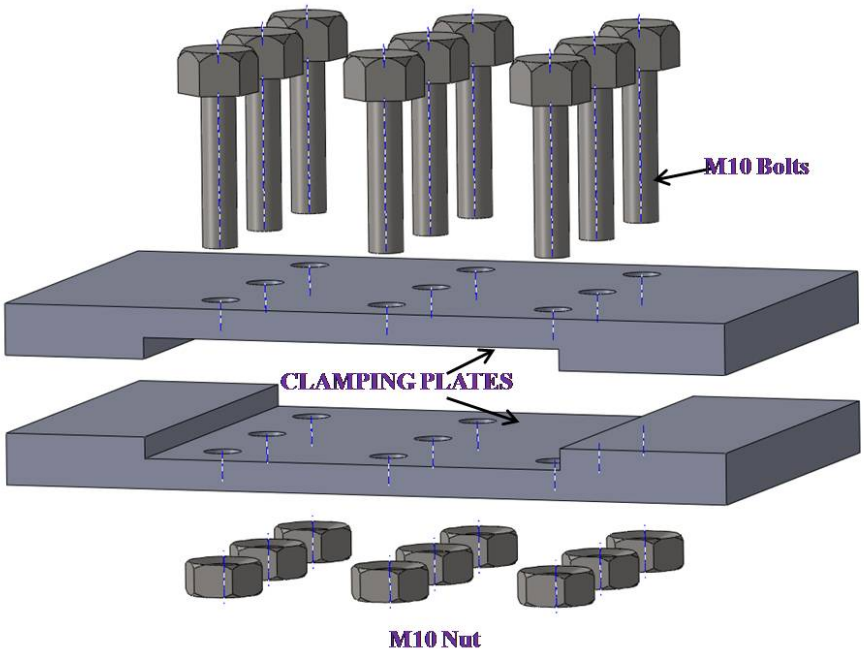

Figure 6.7 Schematic of clamping arrangement

6.2.3 PREPARATION OF TEST SPECIMEN

The details of test specimens of sandwich beam and plate structures are presented below. For both beam and plate structures, specimens are made with two viscoelastic materials in unconstrained and constrained layer configurations.

(A) SANDWICH BEAM

The dimensions of base beam, unconstrained and constrained layer sandwich beams are presented in Table 6.1.

Table 6.1 Geometry and Material properties of sandwich beam

Sandwich structure	**Length (mm)**	**Width (mm)**	**Thickness (mm)**	**Material Properties Density(ρ) kg/m3**	**Young's modulus(MPa) Shear Modulus (MPa) Poisson's ratio (υ)**	
Base Beam	L= 300	b=30	t_b=6.0	2740	E=71000 G=23300	$\upsilon = 0.30$
Constrained layer	L_c= 290	b=30	t_v=1.00	1220(EAP-2) 1260(EAP-43)	$E_v^* = E_v(f)\{1 + i\eta_v^t(f)\} *$	
					$G_v^* = G_v(f)\{1 + i\eta_v^s(f)\} *$	
Constraining layer	L_v= 290	b=30	t_c=1.00	2740	E=71000 G=23300	$\upsilon = 0.30$

** equations 3.22 and 3.27 of chapter 3.*

The following beam specimens are prepared for the experimental study.

i. Only Base beam
ii. Unconstrained layer beam with 1mm thickness of EAP-2
iii. Constrained layer beam with 1mm thickness of EAP-2
iv. Unconstrained layer beam with 1 mm thickness of EAP-43
v. Constrained layer beam with 1 mm thickness of EAP-43

During preparation of these test specimens the following procedure is adopted. The base beam is cleaned with isopropyl alcohol to remove grease and dust particles. The viscoelastic layer is bonded on the base beam using an adhesive. The chemical composition of the adhesive is polysulphide with epoxy adhesive and titanium dioxide as a filler material. After bonding the viscoelastic layer on the base beam, adequate pressure is applied on the specimen and it is cured at room temperature for 24 hours. This completes the specimen preparation for unconstrained layer treatment. In case of specimens with constraining layer treatment, the same procedure is followed and a constraining layer is bonded on the top of the viscoelastic layer in the same way.

The schematic diagrams and photograph of base, unconstrained and constrained layer beams are presented in the following Figures. 6.8 to 6.12.

Figure 6.8 Schematic setup of base beam with clamping plate arrangement

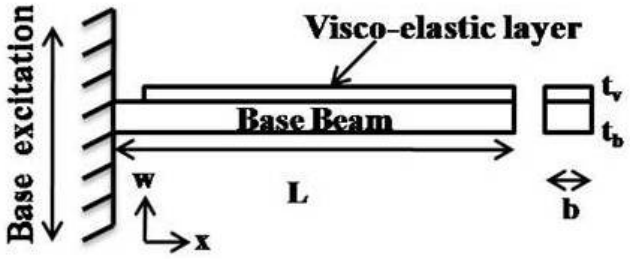

Figure 6.9 Schematic test setup of unconstrained layer sandwich beam

Figure 6.10 Photograph of unconstrained layer sandwich beam with EAP-2

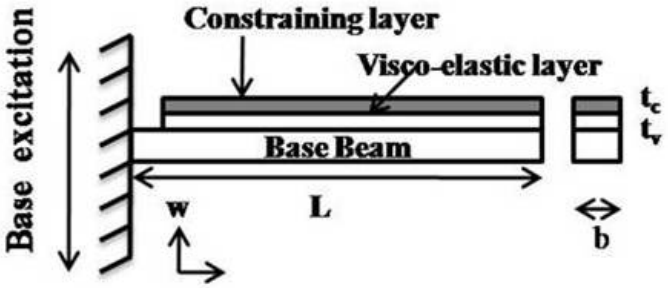

Figure 6.11 Schematic test setup of constrained layer sandwich beam

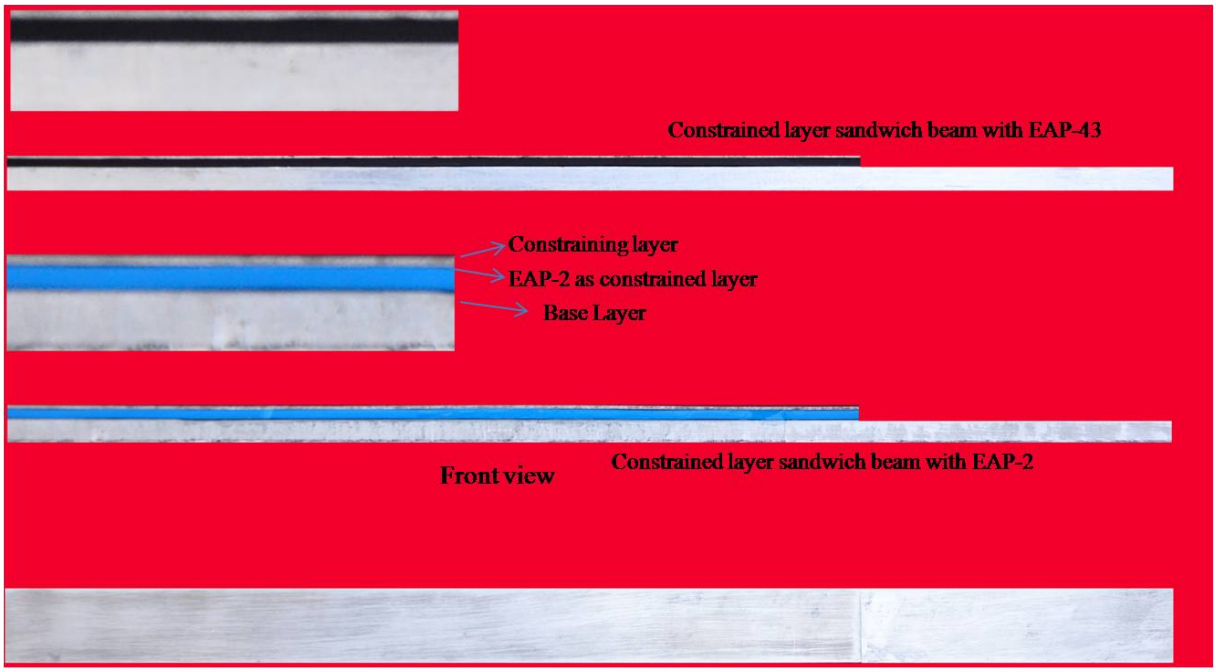

Figure 6.12 Photograph of constrained layer sandwich beam

(B) SANDWICH PLATE

The dimensions of base plate, unconstrained and constrained layer sandwich plate are presented in Table 6.2.

Table 6.2 Geometry and Material properties of sandwich plate

Sandwich structure	**Length (mm)**	**Width (mm)**	**Thickness (mm)**	**Material Properties Density(ρ) kg/m3**	**Young's Modulus (MPa) , Shear Modulus (MPa)**
Base Beam	L_{xb}= 250	L_y=150	t_b=6.00	2740	E=71000 ; G=23300
Constrained layer	L_{xv}= 240	L_y=150	t_v=1.00	1220(EAP-2) 1260(EAP-43)	$E_v^* = E_v(f)\{1 + i\eta_v^t(f)\}^*$
					$G_v^* = G_v(f)\{1 + i\eta_v^s(f)\}^*$
Constraining layer	L_v= 240	L_y=150	t_c=1.00	2740	E=71000 ; G=23300

**The constrained layer material properties are measured experimentally and expressed in mathematical form using power fit and presented in the respective equations 3.22 to 3.27 of chapter 3.*

For preparation of these specimens, similar procedure as explained for sandwich beams is adopted. The schematic and photographs of base plate, unconstrained and constrained layer plates are presented in the Figures 6.13 to 6.18.

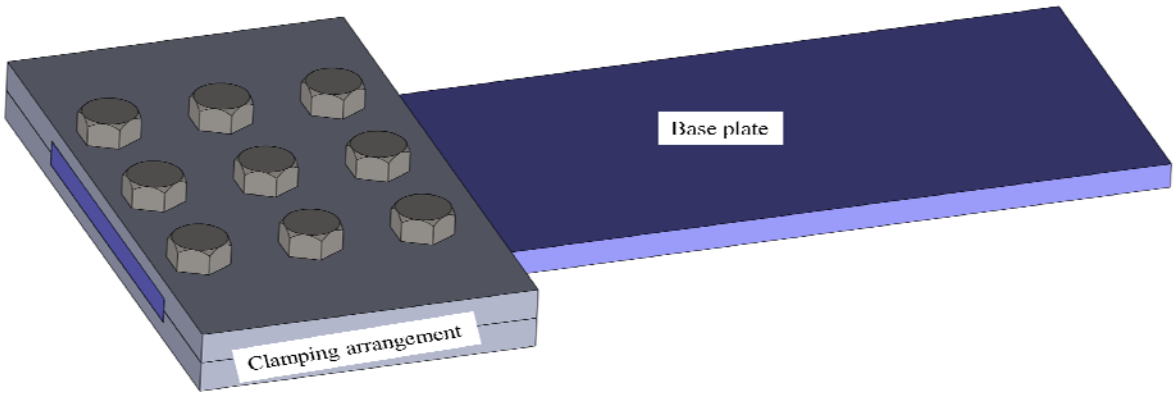

Figure 6.13 Schematic of base plate with clamping arrangement

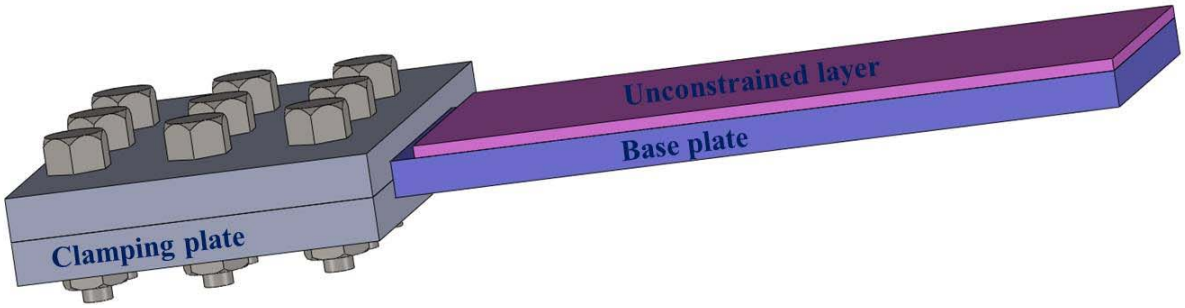

Figure 6.14 Schematic of unconstrained layer plate with clamping arrangement

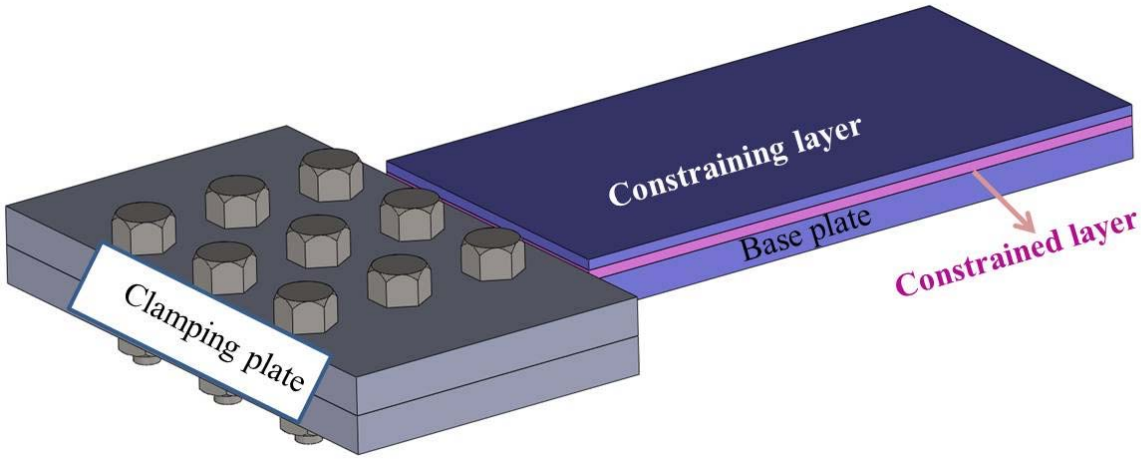

Figure 6.15 Schematic setup of constrained layer plate

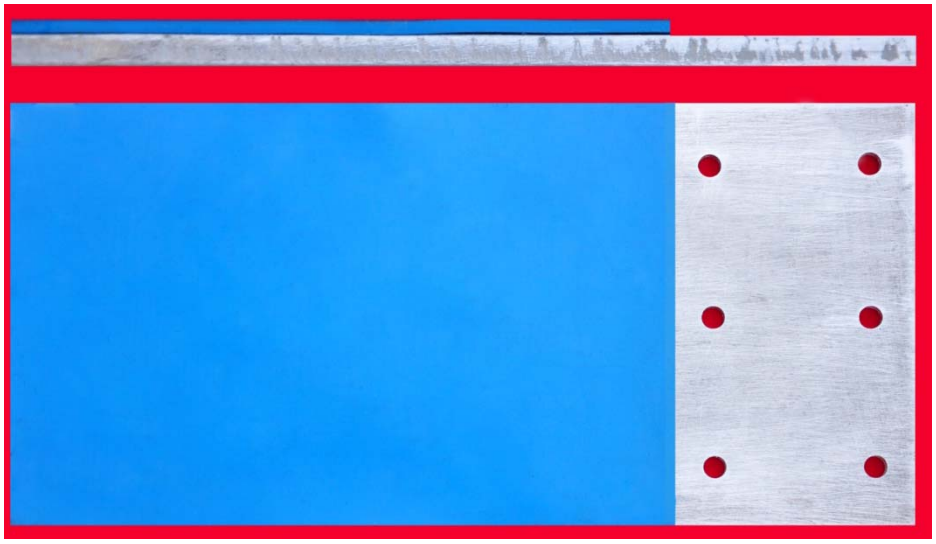

Figure 6.16 Photograph of unconstrained layer plate with EAP-2

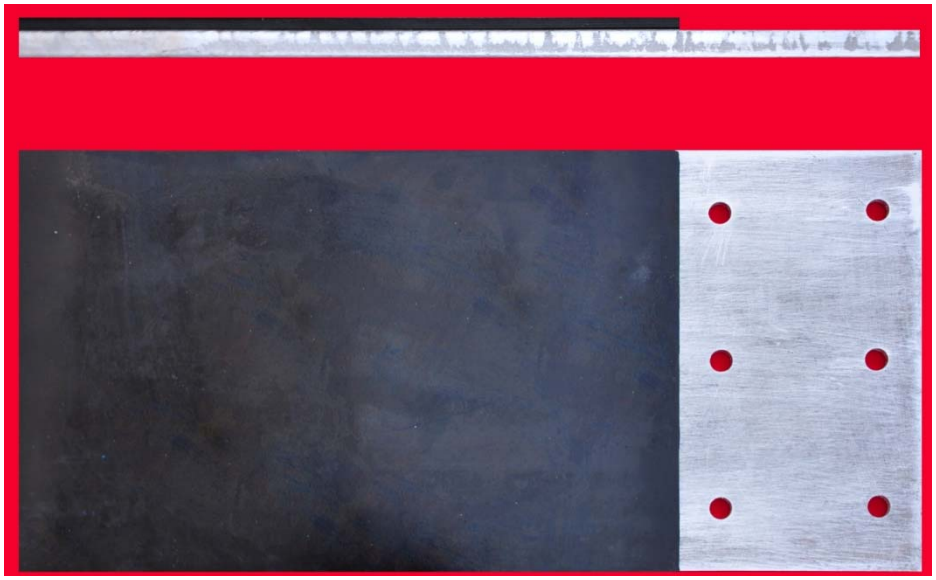

Figure 6.17 Photograph of unconstrained layer plate with EAP-43

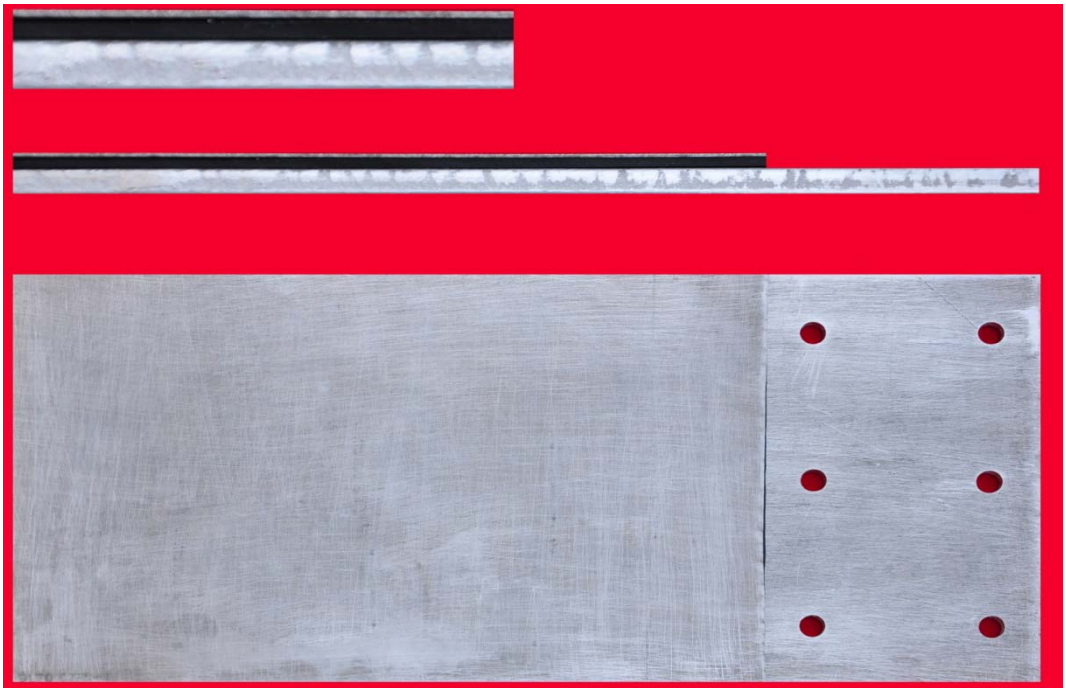

Figure 6.18 Photograph of constrained layer plate with EAP-43

6.2.4 EXPERIMENTAL SETUP

The schematic test and instrumentation setup of sandwich structure is shown in Fig. 6.19. The sandwich structure is held in between the clamping arrangement and in turn fixed to the vibrating base of the electrodynamic shaker. An accelerometer mounted on the clamping plate measures the base acceleration input and accelerometers mounted on the sandwich structure measures the responses. The accelerometers are selected in such a way that their total weight is less than one tenth of the sandwich structure [11]. Base excitation is chosen in the experiments to eliminate the participation of armature dynamics. This precautionary measure ensures the minimization of the mass loading of armature of the shaker and accelerometers. The voltage output signal of LMS controller is fed through signal output card to the power amplifier input and the amplified current output signal is fed to the armature of the shaker which provides necessary base acceleration to the sandwich structure.

Ten accelerometers are mounted on the sandwich beam and 15 accelerometers are mounted on the sandwich plate to measure the responses. The accelerometers are located at appropriate locations to capture the first three modes. The information about the nodes and antinodes obtained through theoretical modal analysis is used to mount the accelerometers at

appropriate locations. All the accelerometer outputs are connected to PQA module (voltage input) of LMS controller and data acquisition system using low noise microdot cables.

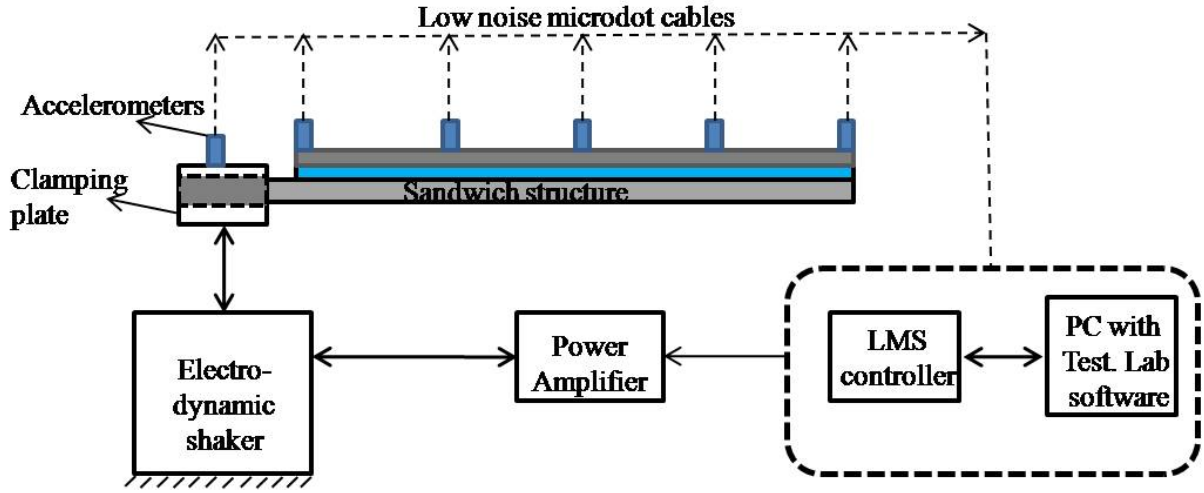

Figure 6.19 Schematic test and instrumentation setup of sandwich structure

6.2.5 EXPERIMENTAL PROCEDURE

The test specimens are subjected to harmonic acceleration input at the base. Base harmonic acceleration is given through the clamping device and the vibration responses of the specimen and the base acceleration input are acquired through the LMS system. The base of the specimen is subjected to stepped sine excitation for each frequency in the chosen frequency range. The details are summarized below.

i. The frequency of excitation starts from 20 Hz.

ii. A sine wave is generated at that frequency (say 20 Hz)in the digital computer and sent through the signal generation card (DAC).The voltage output of the signal generation card is fed to the power amplifier using co-axial cable. The amplified current output signal is fed to the armature of the shaker.

iii. After reaching the steady state condition, the responses of the accelerometers from all channels are acquired by PQA (input module) and processed in SCADAS-III hardware to obtain magnitude and phase information at that particular excitation frequency.

iv. Steps (i) to (iii) are repeated for each frequency up to 1000 Hz in steps of 1Hz and the FRFs are constructed.

The specimens are tested using sine sweep tests with sufficient dwell time for data acquisition and processing for a frequency band of 20 to 1000 Hz with an increment of 1 Hz. The time domain base acceleration input and response at different locations of the sandwich structure are transformed to frequency domain using Fast Fourier Transform (FFT). Frequency Response Functions (FRFs) are obtained from the responses of the sandwich structure to base acceleration input. The peak in the FRF is identified as the amplification factors and the corresponding frequency is the natural frequency. After identifying the resonance frequencies, with a fine frequency sweep in steps of 0.01 Hz and corresponding responses, damping ratios are estimated using half power point. Once the peak response and resonance are located for the chosen i^{th} mode, the half power points are determined where the acceleration amplitude is 0.707 times the peak amplitude and the corresponding frequencies f_1 and f_2 on either side of the resonance frequency are also determined. The damping ratio for the i^{th} mode ξ_{mi} can be estimated using the half-power point method using the following expression [49].

$$\xi_{mi} = \frac{f_{2i} - f_{1i}}{2f_i} \tag{6.1}$$

For structural damping, loss factor is considered as twice the damping ratio at resonance frequency. Hence the loss factor for the i^{th} mode, η_i can be expressed as

$$\eta_{mi} = \frac{f_{2i} - f_{1i}}{f_i} \tag{6.2}$$

Using this methodology, the damping ratios and loss factors are estimated for the first three modes of the test specimen. Further details of calculating damping ratio and loss factor are presented through a sample calculation in the next section.

(A) BASE BEAM

Base excitation experiments are carried out in cantilever boundary condition. The photograph of experimental setup for base beam is shown in Fig. 6.20. Stepped sine excitation is applied at the clamping plate locations and all 10 accelerometer responses on the base beam are acquired. Frequency response functions are obtained by transforming the input and response signals from time domain to frequency domain through Fast Fourier Transformation. A typical FRF obtained at the free end of the base beam is shown in Figure 6.21. The first three natural frequencies are identified from the FRF plot and they are found to be 51.00 Hz,

319.00 Hz and 909.10 Hz. The frequency response functions around the resonance frequencies are expanded by repeating the experiment around resonance with a frequency step of 0.01 Hz. The expanded frequency response function around the first mode is shown in Fig. 6.22. A sample calculation of loss factor for the first mode is given below.

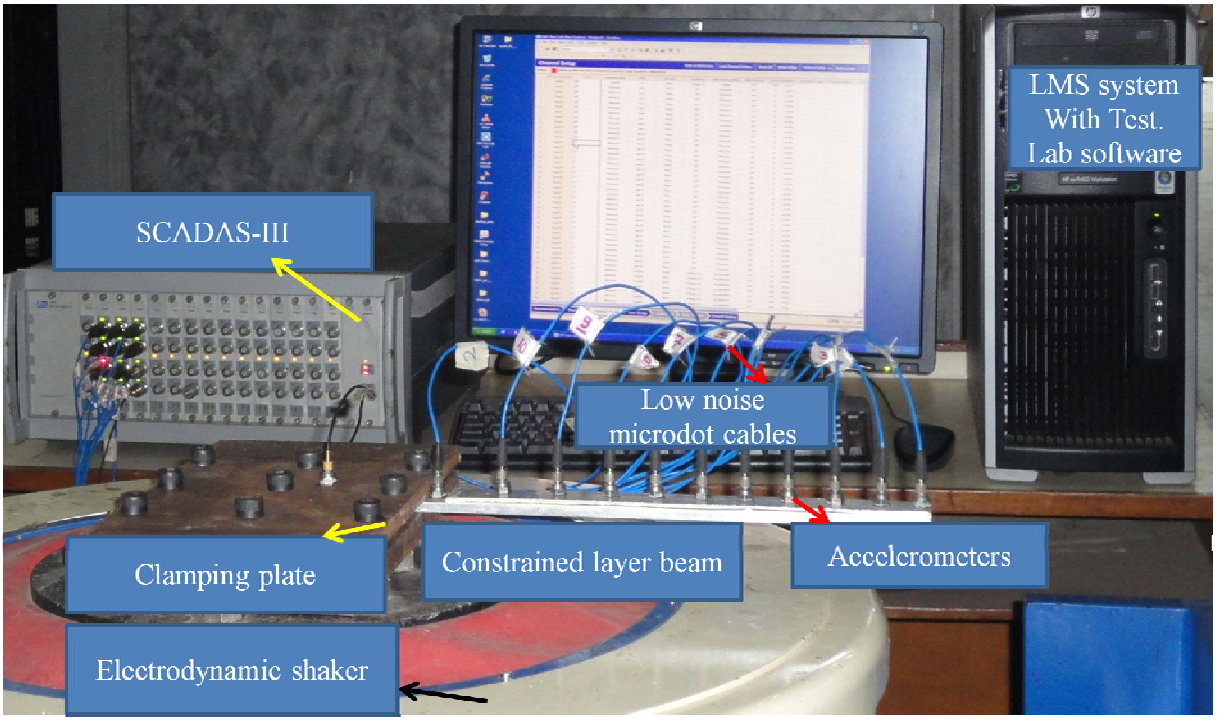

Figure 6.20 Photograph of experimental setup

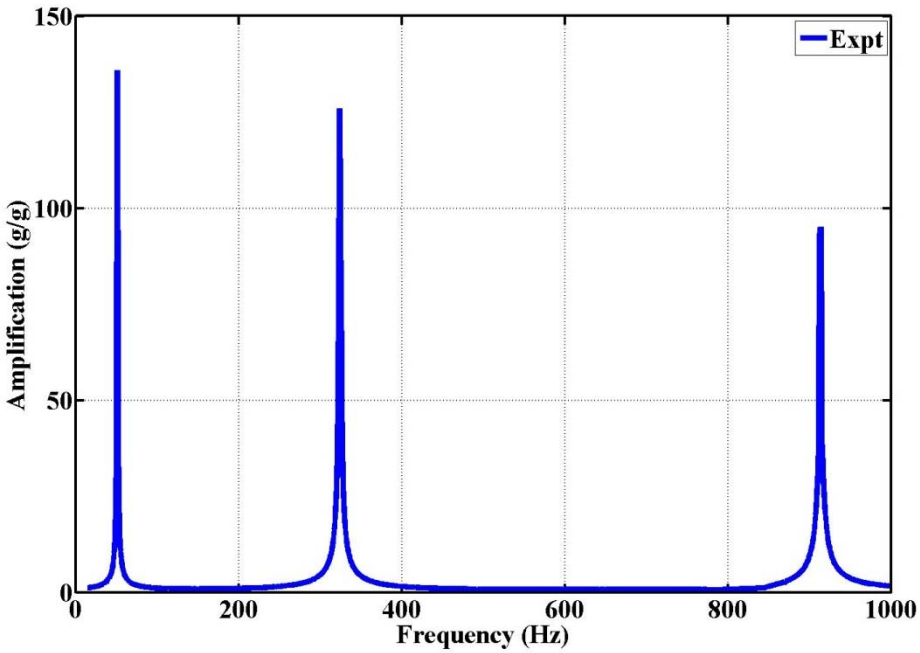

Figure 6.21 Frequency response function at tip of the base beam (experiment results)

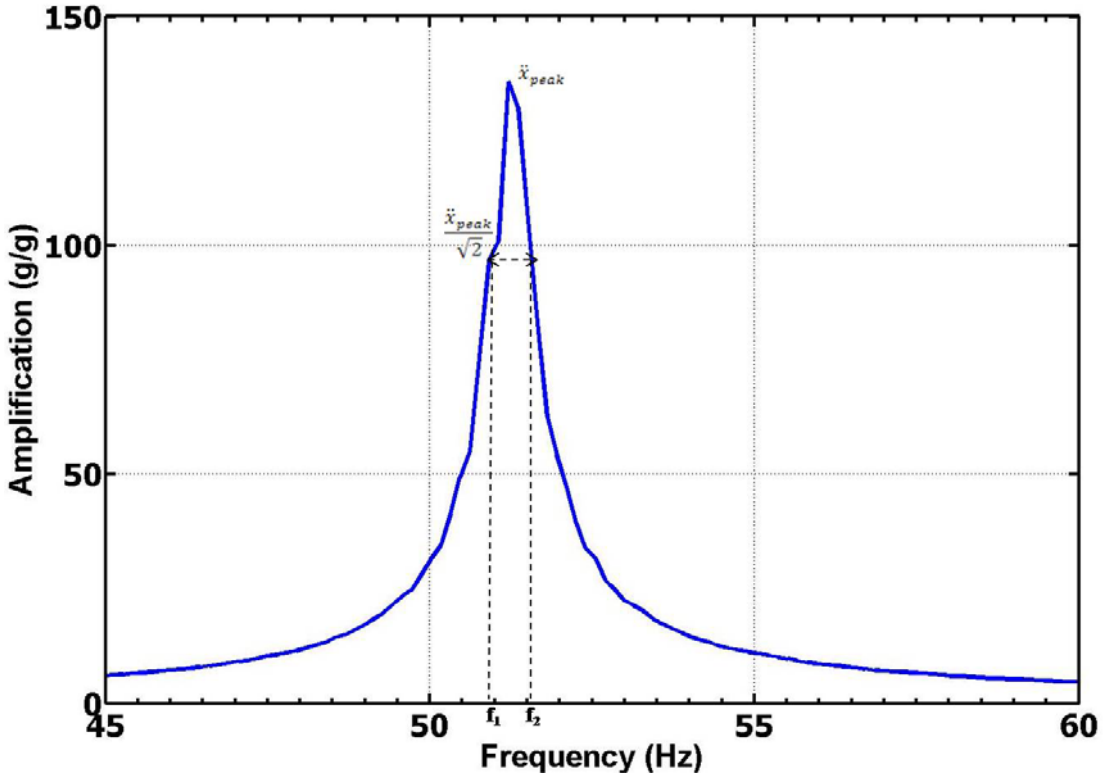

Figure 6.22 Frequency response function at tip of the base beam around I[st] mode resonance

The identified peak amplitude is 139.8. The amplitude corresponding to half power points is 99.8. The frequencies corresponding to half power points are 50.85 Hz and 51.65 Hz. The damping ratios and loss factors are calculated for the first mode using equation (6.1) as follows

$$\xi_{m1} = \frac{f_2 - f_1}{2f_n} = \frac{51.65 - 50.85}{2 * 51} = 0.0030$$

Loss factor η_s= 0.0030*2= 0.0060

Similarly, the loss factors at resonance are obtained for the second and third modes and they are 0.0065 and 0.0073 respectively.

The FRFs obtained from all the ten accelerometers are used to plot experimental mode shapes. The first three normalized mode shapes of base beam are shown in Figure 6.23.

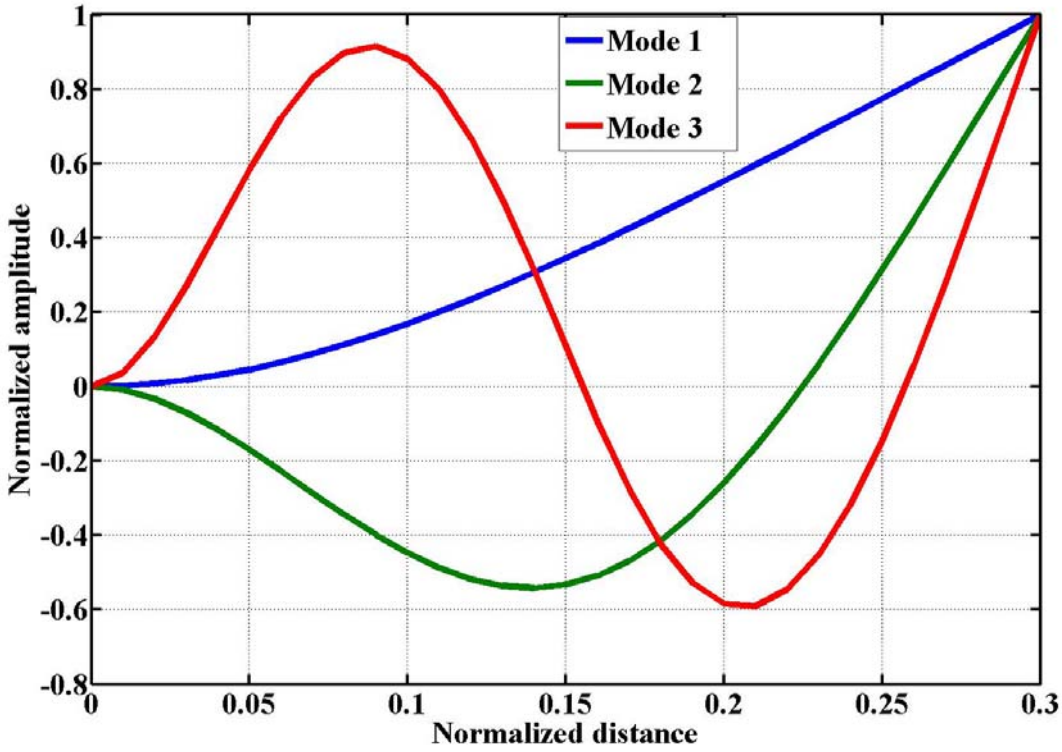

Figure 6.23 Normalized mode shapes of the cantilever beam

(B) UNCONSTRAINED LAYER SANDWICH BEAM

Similar procedure as explained for the base beam is adopted for unconstrained layer beam. A typical experimental FRF at the free end of unconstrained layer beam with 1mm thick EAP-43 viscoelastic layer is presented in Figure 6.24. The first three experimental natural frequencies obtained from FRF are 49.37 Hz, 310 Hz and 871 Hz. It can be observed that the natural frequencies of the unconstrained viscoelastic layered beam have slightly decreased due to additional mass and damping contribution of viscoelastic layer. Comparison of amplification factors is made by considering the respective first, second and third modes of base beam as reference. The attenuation levels are calculated using the following equation

$$dB = 20log_{10}\frac{x_{ui}}{x_{bi}} \tag{6.3}$$

Where x_{ui} is the magnitude of i^{th} natural mode of unconstrained layer sandwich beam and x_{bi} is the magnitude of i^{th} natural mode of the base beam. By comparing the FRF of unconstrained layer beam (refer Fig. 6.24) with base beam (refer Figure 6.21), an attenuation in amplification factors of 9.15 dB, 16.65 dB and 24.42 dB is observed for the first three modes respectively.

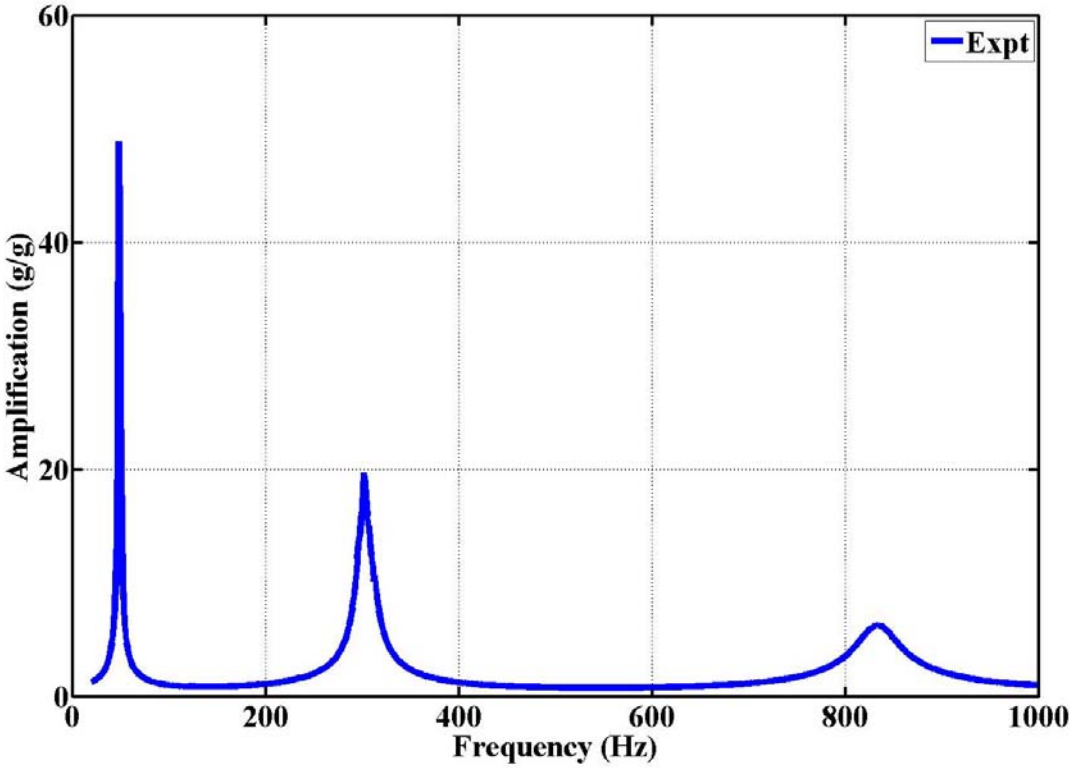

Figure 6.24 FRF at free end of the unconstrained layer beam with EAP-43

(C) CONSTRAINED LAYER SANDWICH BEAM

The typical frequency response function obtained at the free end of constrained layer beam is shown in Figure 6.25. The natural frequencies of the first three modes of constrained layer beam with EAP-43 are 47.00 Hz, 306 Hz and 850 Hz. It can be observed that the natural frequencies of the constrained layer sandwich beam have decreased due to the additional mass of viscoelastic and constraining layers and damping contribution of viscoelastic layer. The attenuation in amplification factors of unconstrained layer beam with EAP-43 are calculated using equation 6.3 by considering the respective base beam amplification factor as reference. The attenuation levels are 13.35 dB, 22.8 dB and 22.52 dB for the first three modes. It is found that higher attenuation is observed for all configurations. Constrained layer beam shows higher attenuation compared to unconstrained layer beam for all modes.

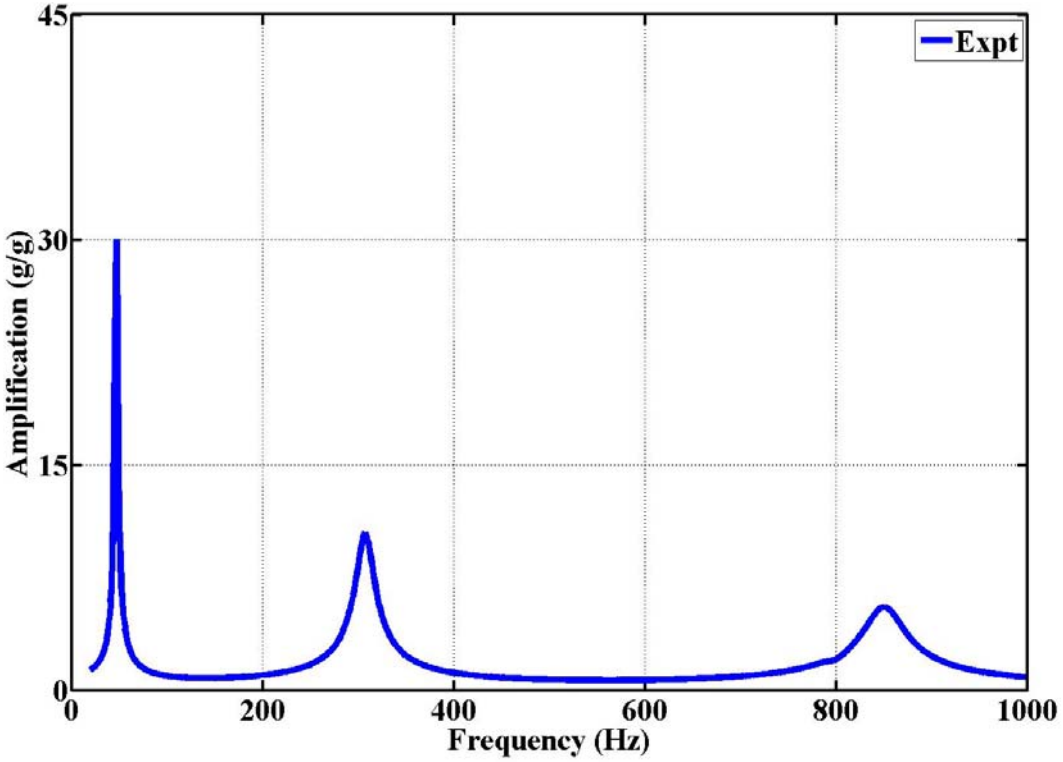

Figure 6.25 FRF at free end of the constrained layer beam with EAP-43

(D) BASE PLATE

Experiments are carried out with base plate fixed at one edge and free at other three edges (cantilever) boundary condition. The photograph of experimental setup for base plate is shown in Figure 6.26. The frequency response function at the free end of the base plate is shown in Figure6.27. The natural frequencies for the first three modes are found as 48.7 Hz, 302.3 Hz and 852 Hz respectively. The loss factors are calculated using half power point method as explained for beams. The loss factors for the first three modes are 0.0076, 0.0098 and 0.0120 respectively. The first three mode shapes obtained from the measured data during experiments are shown in Figures 6.28 to 6.30. These mode shapes are plotted using the responses obtained from fifteen accelerometers.

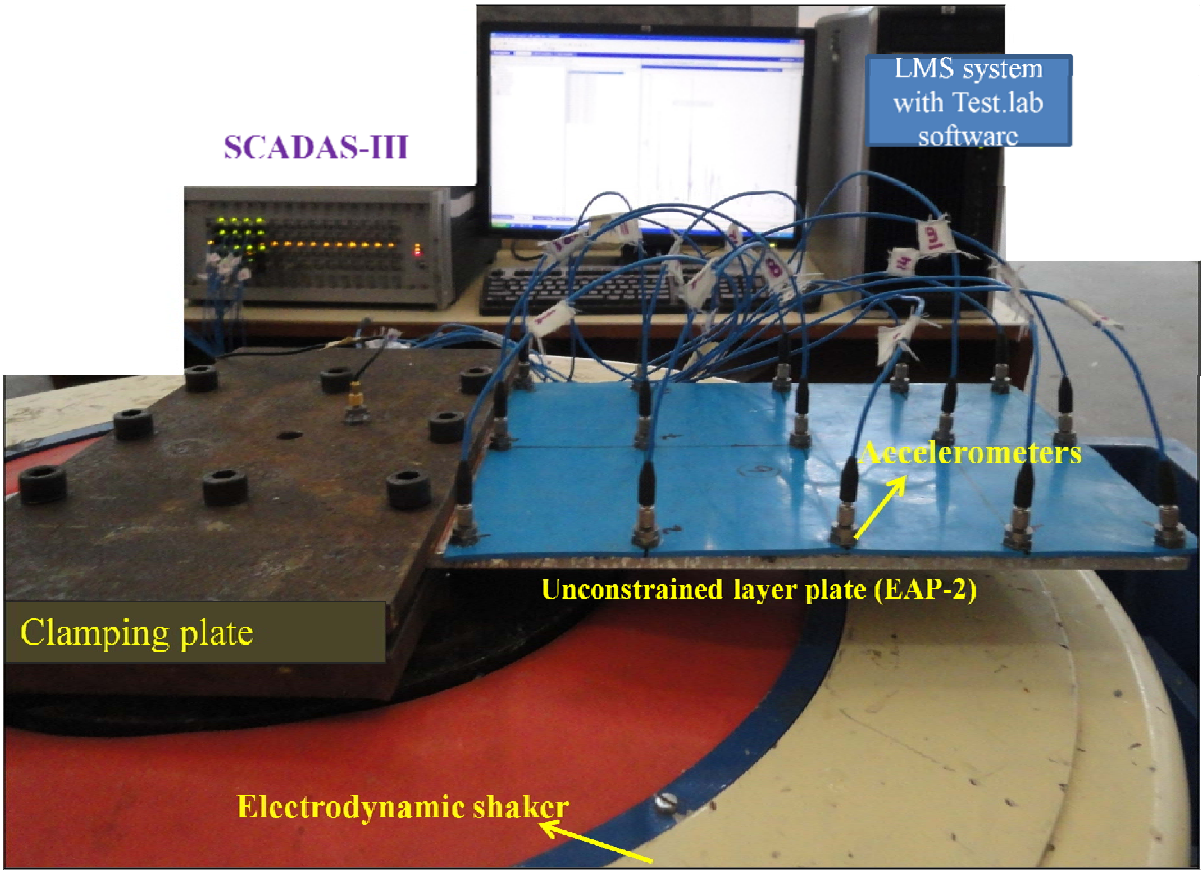

Figure 6.26 Photograph of experimental setup

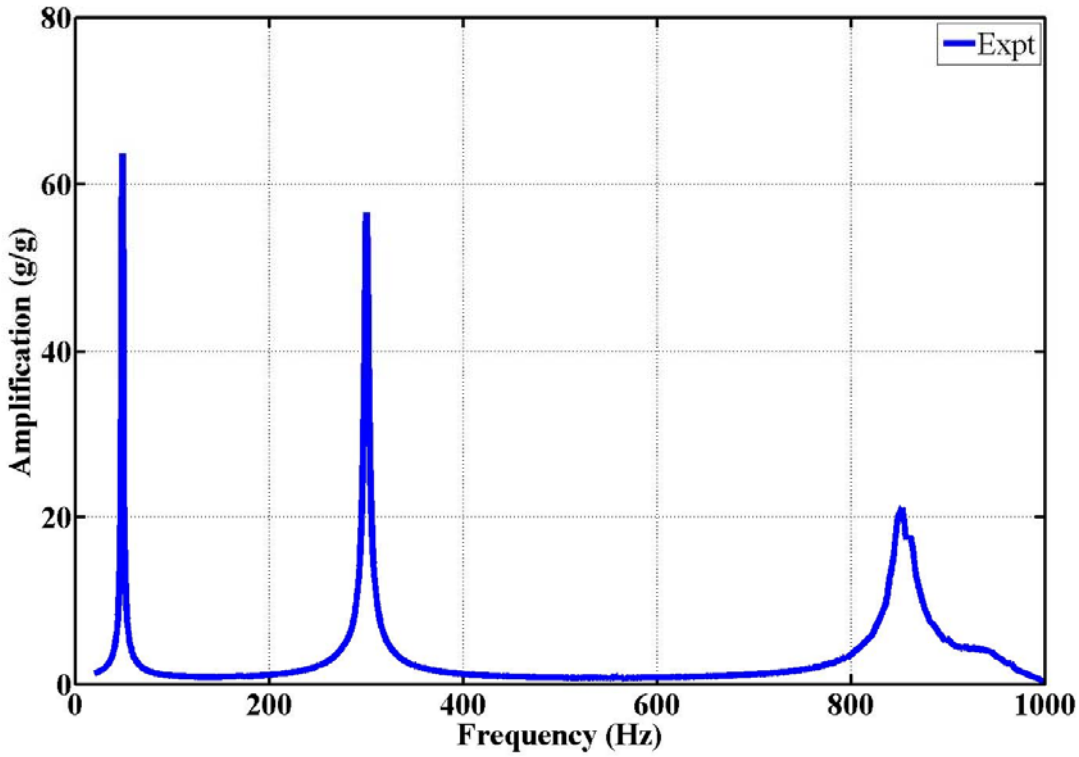

Figure 6.27 FRF at free end of the base plate

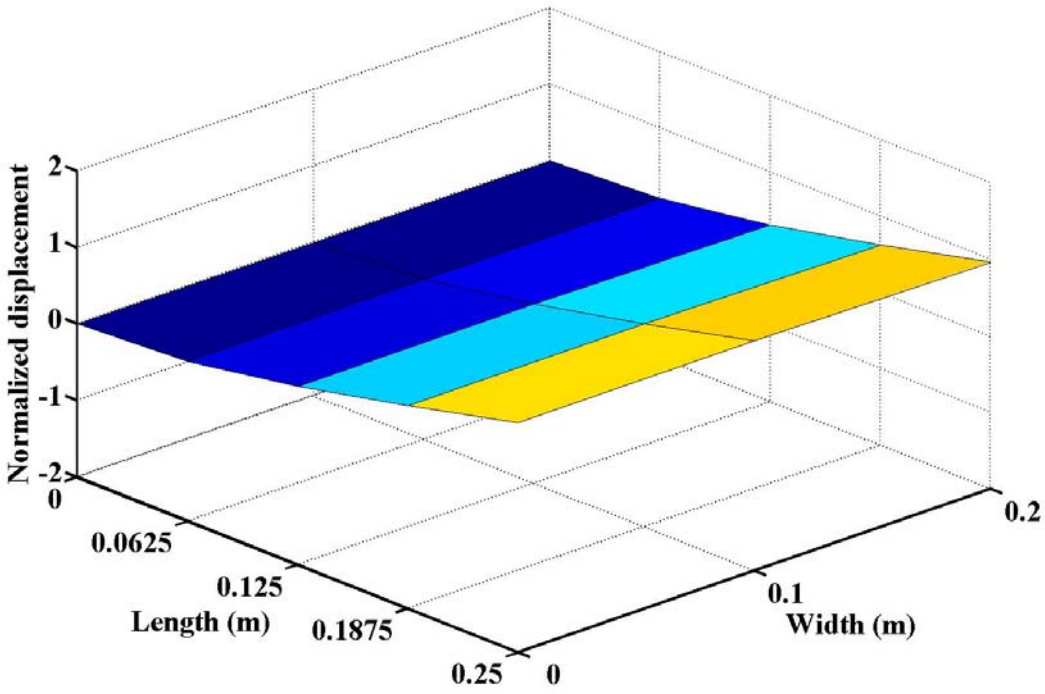

Figure 6.28 First bending mode of base plate (experimental)

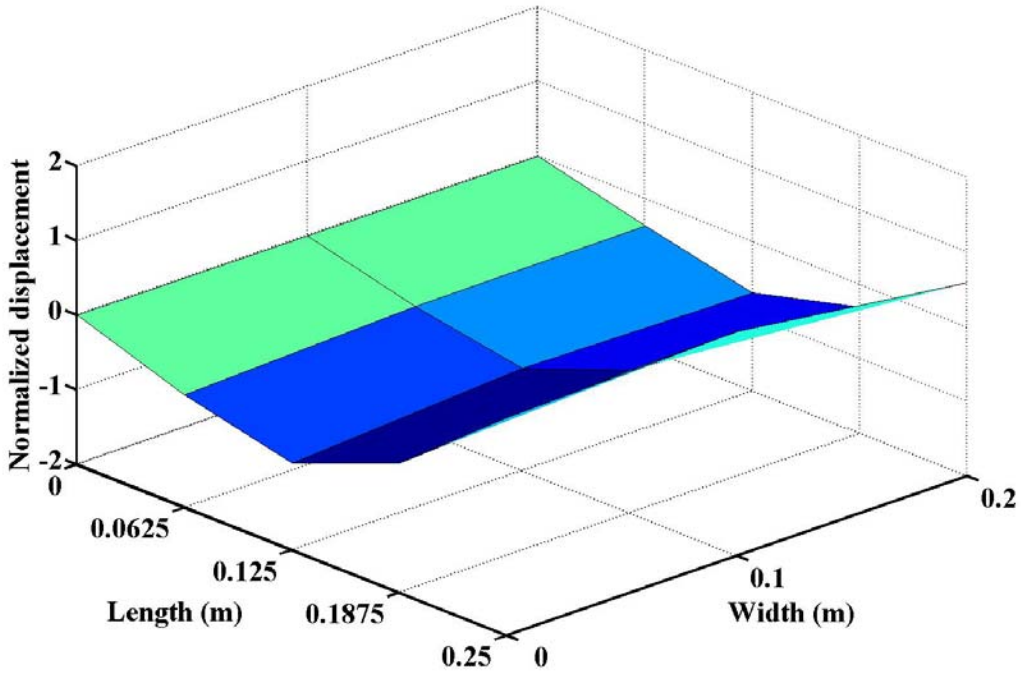

Figure 6.29 Second bending mode of base plate (experimental)

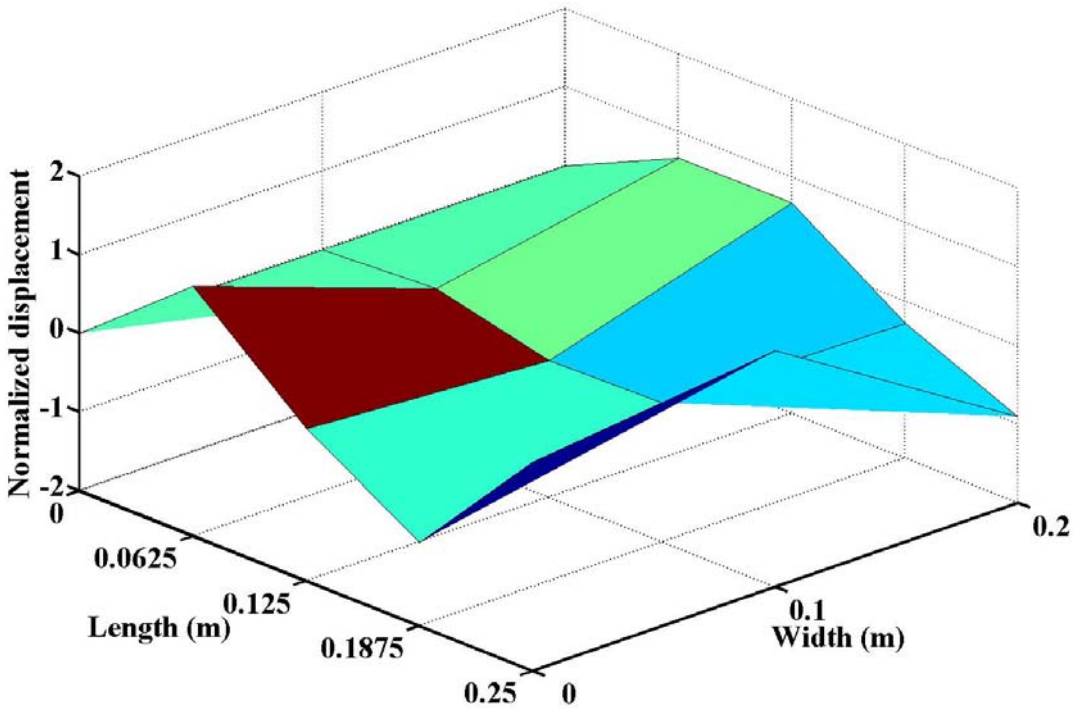

Figure 6.30 Third bending mode of base plate (experimental)

(E) UNCONSTRAINED LAYER SANDWICH PLATE

A typical FRF obtained from the experiment of the unconstrained layer sandwich plate with EAP-43 is shown in Figure 6.31. The experimental natural frequencies of the first three modes are measured as 45.89, 277.8 and 795 Hz respectively. It can be observed that the natural frequencies of the unconstrained viscoelastic layered plate have decreased due to additional weight and damping contribution of viscoelastic layer. The attenuation in amplification factors of unconstrained layer pate with EAP-43 are calculated using equation 6.3 by considering the respective base plate amplification factor as reference and they are 5.90, dB 6.89 dB and 12 dB for the first three modes respectively. It is also observed that higher attenuations are observed for higher modes. Similar behaviour is observed in unconstrained layer sandwich beam studies.

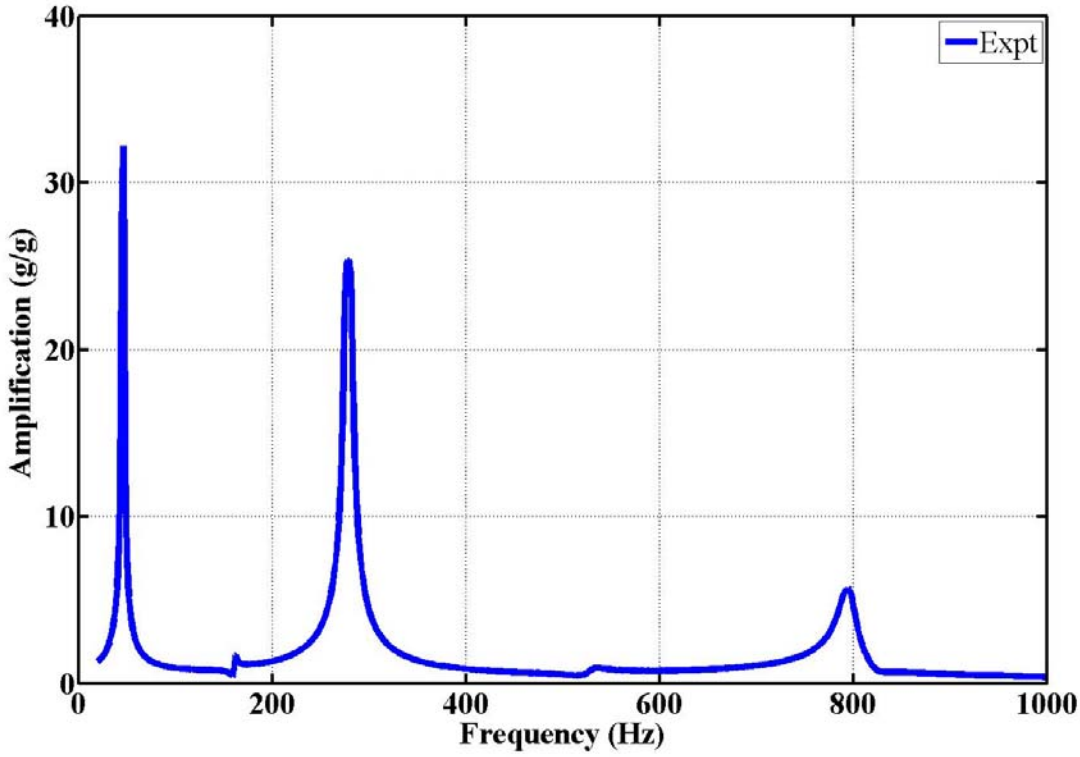

Figure 6.31 FRF of the unconstrained layer plate with EAP-43 at free end

(F) CONSTRAINED LAYER SANDWICH PLATE

The typical frequency response functions of the constrained layer plate with EAP-43 are obtained with similar experiments and are and shown in Fig.6.32. The experimental natural frequencies of the first three modes are measured as 43.07, 273.8 and 740.16 Hz respectively. It can be observed that the natural frequencies of the constrained layer sandwich plate have decreased due to the additional mass of viscoelastic layer and constraining layer plate and damping contribution of viscoelastic layer. Comparison of amplification factors are made by considering the respective first, second and third modes of base plate as reference and they are 12.92 dB, 23.45 dB and 21.98 dB for the first three modes respectively. From the FRF plots it is observed that constrained layer shows higher attenuation compared to unconstrained layer plate. Similar trend is observed during experiments of constrained layer sandwich beams.

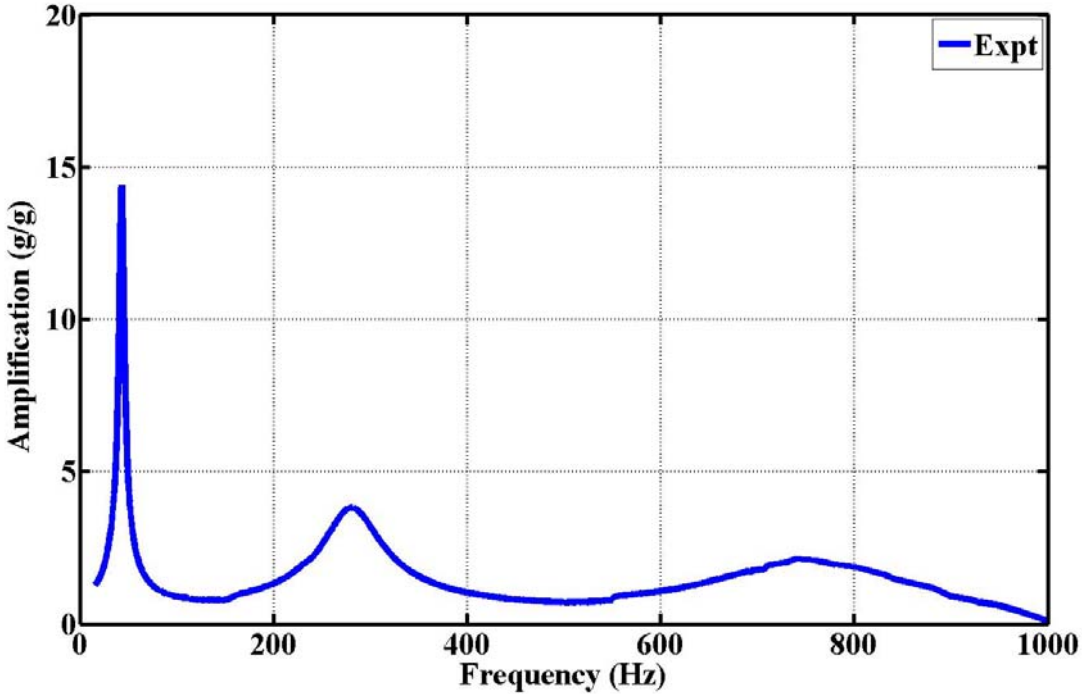

Figure 6.32 FRF of the constrained layer plate with EAP-43 at free end

6.3 SUMMARY

The detailed description of the instrumentation, sample preparation, test setup and experimental procedures are presented in this chapter. Experiments are carried out for 8 specimens; four of them are sandwich beams and remaining four are sandwich plates. FRF results for each case are presented. The dynamic models are validated and with the experimental results in the next chapter.

CHAPTER 7

VALIDATION OF THEORETICAL MODEL AND ANALYSIS OF SANDWICH STRUCTURES

7.1 INTRODUCTION

Finite element based dynamic models are developed in chapter 4. A computational scheme is developed in chapter 5 to solve the equation of motion for base excitation. The frequency response functions (FRFs) and loss factors are calculated using the computational scheme. The modal parameters are also obtained experimentally for uniform sandwich beams and plates in chapter 6. By comparing the computational and experimental results, the developed dynamic models are validated and the analysis of the results is carried out to understand the role of viscoelastic materials in improving damping. In most of the published literature, results are presented where it is assumed that the material properties of viscoelastic layer do not vary with excitation frequency. The viscoelastic materials considered in the present study have frequency dependent properties. Thus, computational studies are also carried out for sandwich beams and plate structures assuming constant material properties as given in literature and the results are compared with the present work. The theoretical results are validated with experiments for unconstrained and constrained configurations of beam and plates using different viscoelastic materials.

7.2 DYNAMIC BEAHVIOUR OF SANDWICH BEAMS

The geometric and material properties of the sandwich beam are given in Table 6.1 of the previous chapter. Two viscoelastic layers, EAP-2 and EAP-43, recently developed are considered in the present analysis. The material properties of these viscoelastic layers are presented in chapter 3. Before applying viscoelastic layer treatment on the beam, the loss factors of base beam are obtained. The attenuation levels using viscoelastic layers are expressed in decibels with the levels of base beam as a reference.

7.2.1 ANALYSIS OF BASE BEAM

The base beam is made of Aluminum and its dimension is given in Table 6.1. The Frequency Response Functions (FRFs)at the free end obtained from developed dynamic model and computational scheme are compared with experimental results of the base beam and are shown in Figure 7.1 and given in Table 7.1. Both the computational and experimental FRFs and frequencies are compared with theory and it is found that the errors are less than 3%. The loss factors for the first three modes are calculated from the experimental FRFs using half power method and they are 0.006, 0.0065 and 0.0073 respectively. These loss factors of the base beam are used in the FE model of unconstrained and constrained layer sandwich beam models. The loss factors obtained from the experiment are very low and it is due to the material damping of the aluminum beam.

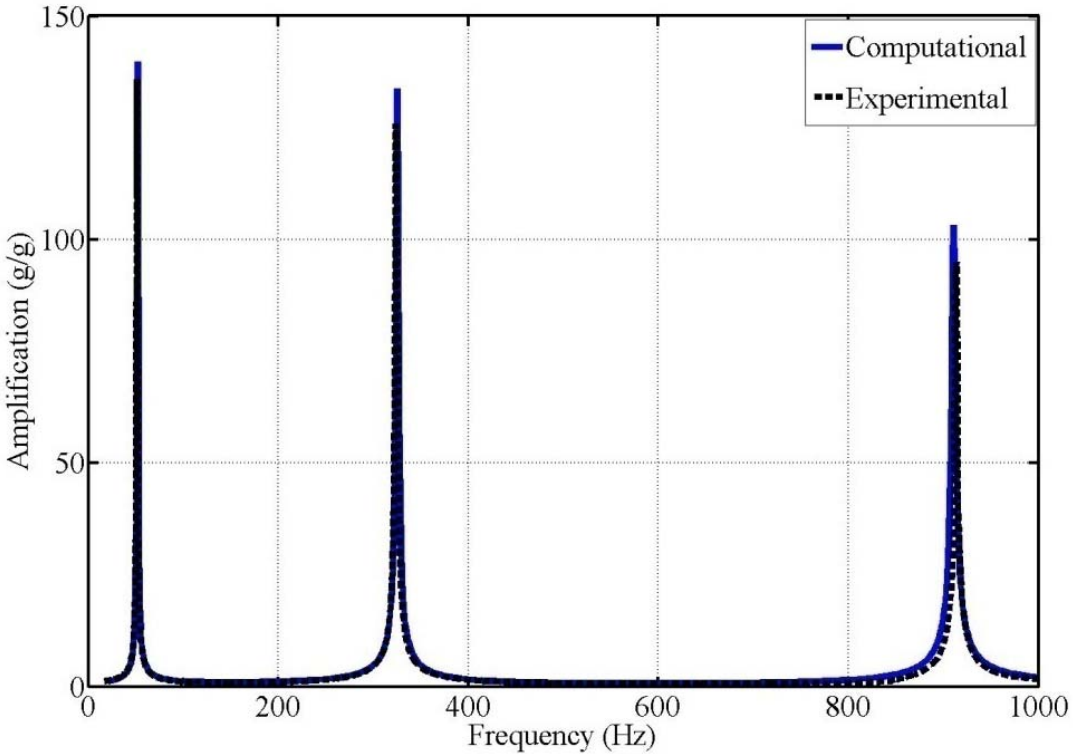

Figure.7.1 Comparison of numerical and experimental FRF at free end of cantilever beam

Table 7.1 Comparison of computational and Experimental frequencies for cantilever beam

	Natural Frequency (Hz)			
Mode	Theory (Hz) (Closed form)[49]*	FEM** (Hz) (Error)	Expt.(Hz) (Error)	Loss factor (Experiment)
I	52.05	51.96 (0.17%)	51.00 (2.02%)	0.0060
II	326.20	324.15 (0.60%)	319.00 (2.21%)	0.0065
III	913.39	910.76 (0.3%)	909.10 (0.53%)	0.0073

*Dimension of the beam are substituted in the formula for estimating natural frequencies
** Finite element method

7.2.2 ANALYSIS OF UNCONSTRAINED LAYER SANDWICH BEAM

The viscoelastic material is glued on the base beam to form an unconstrained layer sandwich beam configuration. Two viscoelastic materials namely EAP-2 and EAP-43 are used to get two different cases of unconstrained layer sandwich beam structures. Frequency Response Functions (FRFs) obtained at the free end using the dynamic model are compared

with experimental results for EAP-2 and EAP-43 are shown in Figures 7.2 and 7.3. The comparison of computational and experimental model frequencies, amplification and loss factors are presented in Tables 7.2 and 7.3. From the above figures and tables, it is found that computational results with frequency dependent material properties of viscoelastic layer and experimental results agree with experiments. By suppressing the variation of material properties in the dynamic models, computations are also carried and the results do not match well. Comparison of experimental amplification factors is made by considering the respective first, second and third modes of base beam as reference. The attenuation levels are calculated using the following expression.

$$dB = 20log_{10}\frac{x_{ui}}{x_{bi}} \tag{7.1}$$

Where x_{ui} is the amplification factor for ith natural mode of unconstrained layer sandwich beam and x_{bi} is the amplification factors for ith natural mode of the base beam.

An attenuation of 9.13 dB, 16.10 dB and 21.80 dB in amplitudes are observed for EAP-2 and an attenuation of 9.15 dB, 16.65 dB and 24.42 dB are observed for EAP-43 with respect to base beam for the first three natural modes respectively. The attenuation is observed to be higher for higher modes. Unconstrained layer beam with EAP-43 provides slightly higher vibration attenuation compared to EAP-2.

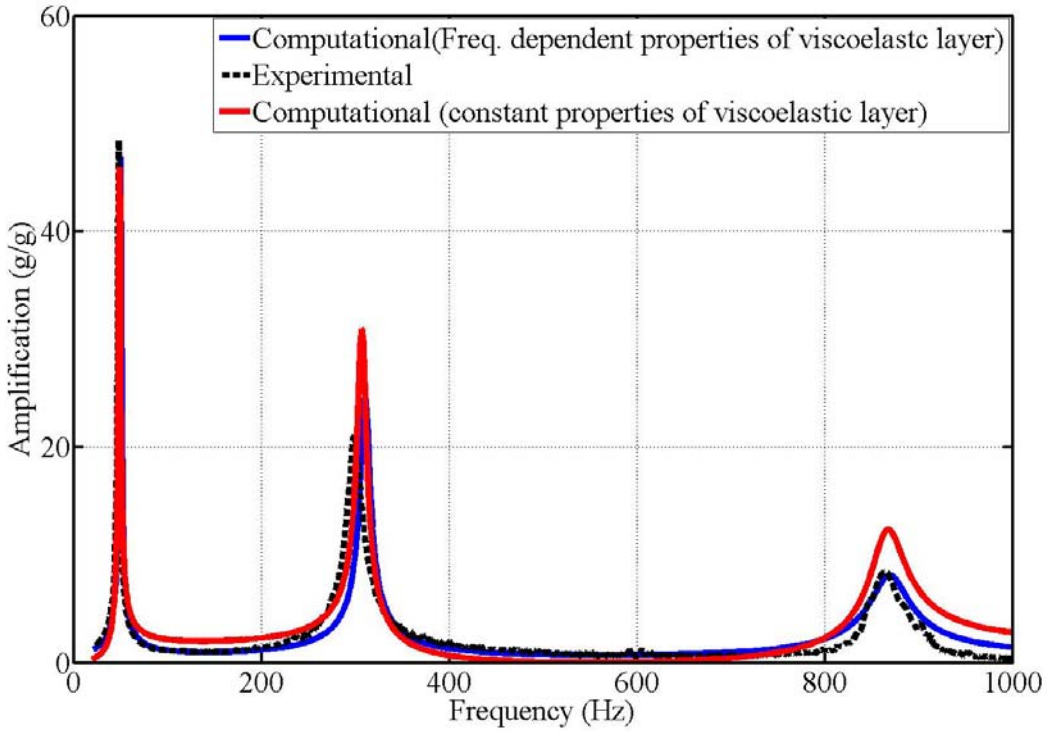

Figure 7.2 Comparison of FRF at free end of unconstrained layer cantilever sandwich beam with 1 mm thickness of EAP-2

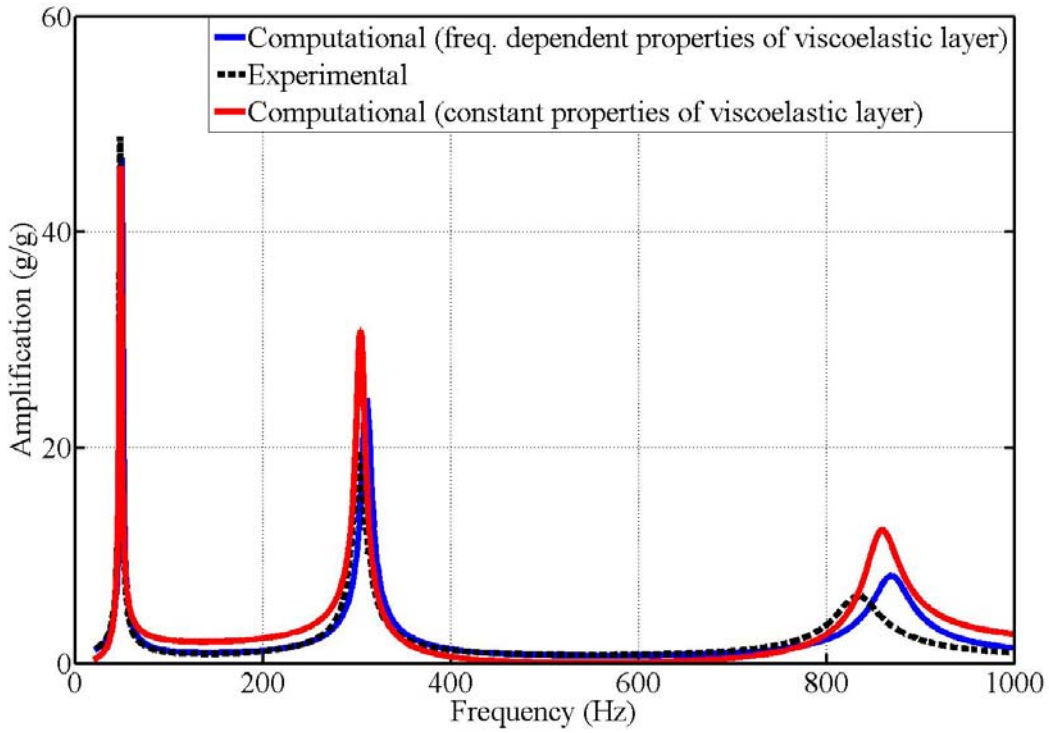

Figure 7.3 Comparison of FRF at free end of unconstrained layer cantilever sandwich beam with 1mm thickness of EAP-43

Table 7.2 Comparison of computational and Experimental results of unconstrained layer cantilever sandwich beam with 1mm thickness of EAP-2

	Frequency(Hz)			**Amplification (g/g)**			**Loss factors**		
	Comp(1)*	**Comp(2)***	**Expt.**	**Comp(1)**	**Comp(2)**	**Expt.**	**Comp(1)**	**Comp(2)**	**Expt.**
I	50.57	51.00	49.37	47.39	47.00	48.43	0.021	0.019	0.020
II	305.00	306.00	302.00	24.50	30.77	21.04	0.045	0.041	0.047
III	869.30	868.90	865.24	8.149	12.31	8.392	0.080	0.072	0.083

*Comp (1) computational results considering frequency dependent material properties of viscoelastic layer. Comp (2) computational results considering constant material properties of viscoelastic layer

Table 7.3 Comparison of computational and Experimental results of unconstrained layer cantilever sandwich beam with 1mm thickness of EAP-43

	Frequency(Hz)			**Amplification (g/g)**			**Loss factors**		
	Comp(1)*	**Comp(2)***	**Expt**	**Comp(1)**	**Comp(2)**	**Expt**	**Comp(1)**	**Comp(2)**	**Expt.**
I	50.00	50.60	49.00	47.39	47.20	46.09	0.022	0.020	0.023
II	302.00	304.00	301.00	23.70	30.20	19.68	0.053	0.046	0.055
III	869.00	862.00	836.00	8.069	12.31	6.21	0.099	0.078	0.108

*Comp (1) computational results considering frequency dependent material properties of viscoelastic layer. Comp (2) computational results considering constant material properties of viscoelastic layer

7.2.3 ANALYSIS OF CONSTRAINED LAYER SANDWICH BEAM

Two constrained layered sandwich beams are considered in the analysis. The first beam consists of EAP-2 as viscoelastic layer and the second beam consists of EAP-43. Frequency Response Functions (FRFs) obtained for the two beams at the free end using the dynamic model are compared with experimental results and are shown in Figures 7.4 and 7.5. The comparison of computational and experimental model frequencies, amplification and loss factors are given in Tables 7.4 and 7.5.

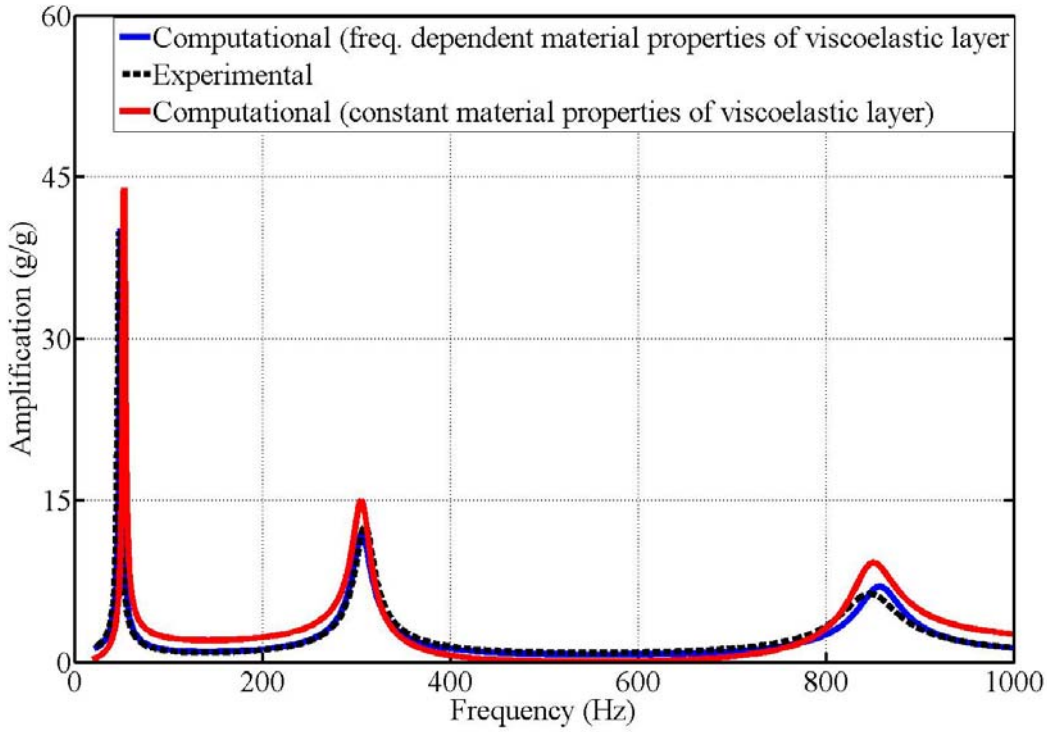

Figure 7.4 Comparison of FRF at free end of the constrained layer sandwich beam with 1 mm thickness of EAP-2

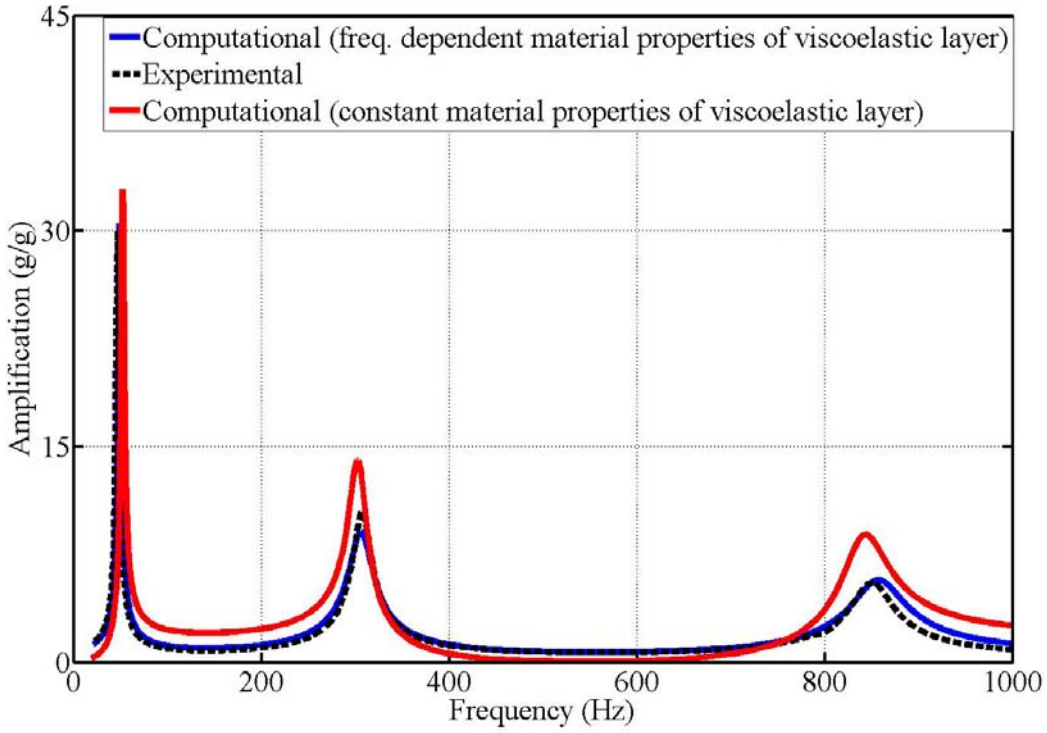

Figure 7.5 Comparison of FRF at free end of the constrained layer sandwich beam With1mm thickness of EAP-43

Table.7.4 Comparison of computational and Experimental results of constrained layer cantilever sandwich beam with 1mm thickness of EAP-2

	Frequency(Hz)			**Amplification (g/g)**			**Loss factors**		
	Comp(1)*	**Comp(2)***	**Expt**	**Comp(1)**	**Comp(2)**	**Expt**	**Comp(1)**	**Comp(2)**	**Expt.**
I	48.52	49.50	47.37	40.22	44.13	39.92	0.025	0.023	0.026
II	307.07	305.00	308.90	11.69	15.01	12.66	0.073	0.070	0.075
III	851.01	849.50	847.00	7.008	9.193	6.36	0.151	0.013	0.158

*Comp (1) computational results considering frequency dependent material properties of viscoelastic layer. Comp (2) computational results considering constant material properties of viscoelastic layer

Table.7.5 Comparison of computational and Experimental results of constrained layer cantilever sandwich beam of 1mm thickness of EAP-43

	Frequency(Hz)			**Amplification (g/g)**			**Loss factors**		
	Comp(1)*	**Comp(2)***	**Expt**	**Comp(1)**	**Comp(2)**	**Expt**	**Comp(1)**	**Comp(2)**	**Expt.**
I	48.11	49.00	47.00	30.56	32.12	30.05	0.033	0.025	0.034
II	307.00	302.40	306.00	9.047	14.04	10.17	0.093	0.073	0.096
III	857.00	842.00	850.00	5.707	8.859	5.472	0.151	0.182	0.191

From the above figures and tables, it is found that computational results with frequency dependent material properties of viscoelastic layer and experimental results agree with experiments. By suppressing the variation of material properties in the dynamic models, computations are also carried and the results do not match well. Comparison of amplification factors is made by considering the respective first, second and third modes of base beam as reference. Equation 7.1 is used to calculate the vibration attenuation of constrained layer sandwich beam. An attenuation of 10.89 dB, 20.48 dB and 24.42 dB in amplitudes are observed for EAP-2 with respect to base beam for the first three natural modes respectively. Similarly, an attenuation of 13.35 dB, 22.38 dB and 25.52 dB in amplitudes are observed for EAP-43 with respect to base beam for the first three natural modes respectively. From these figures and tables, it can be concluded that constrained layer sandwich beam with EAP-43 provides higher vibration attenuation compared to EAP-2.

The above comparative study of unconstrained layer and constrained layer sandwich beam results validates the developed dynamic model. The overall comparison of frequencies, amplification factors and vibration attenuation levels for base beam, unconstrained and constrained layer beam for EAP-2 and EAP-43 obtained from experiments are presented in Table 7.6.

Table 7.6 Comparison of amplification factors for EAP-2 and EAP-43 of cantilever sandwich beam (Experiment results)

Amplification, g/g (dB)							
	mode	**First**	**Second**	**Third**	**First**	**Second**	**Third**
Base beam (Base beam is considered as reference)	Freq (Hz)	51.96	324.15	910.76	51.96	324.15	910.76
	Amp.(g/g)	139.80	133.80	103.30	139.80	133.80	103.30
	dB	0	0	0	0	0	0
		EAP-2			**EAP-43**		
unconstrained layer sandwich beam (t_v/t=0.16)	Freq (Hz)	49.37	302.00	865.40	49.00	302.00	836.00
	Amp.(g/g)	48.86	21.04	8.40	48.75	19.68	6.21
	dB	-9.13	-16.10	-21.80	-9.15	-16.65	24.42
Constrained layer sandwich beam (t_v/t=0.16) & (t_c/t=0.16)	Freq (Hz)	47.37	308.90	847.00	47.00	306.00	850.00
	Amp.(g/g)	39.92	12.66	6.36	30.05	10.17	5.472
	dB	-11	-20.48	-24.40	-13.35	-22.38	-25.52

Based on these comparative results, it can be concluded that EAP-2 and EAP-43 provide higher attenuation at higher modes. The constrained layer sandwich structure provides higher attenuation compared to unconstrained layer sandwich structure. EAP-43 provides slightly higher attenuation in vibration levels compared to EAP-2.

7.3 DYNAMIC BEHAVIOUR OF SANDWICH PLATE

The results obtained from the dynamic model of sandwich plate are compared with experiments. The geometry and material properties of the sandwich plate are given in Table 6.2 of the previous chapter. Two viscoelastic materials, EAP-2 and EAP-43 are considered both in unconstrained and constrained configurations. The loss factors of the base plate made of aluminum are estimated from experimental results. The loss factors of the base plate are used in the computational model of the sandwich plate. These loss factors are considered as a reference for comparison of loss factors of sandwich plates of different configurations.

7.3.1 ANALYSIS OF BASE PLATE

The experimentally obtained FRF at the free end of the base plate is compared with analytical results and presented in Figure 7.6.

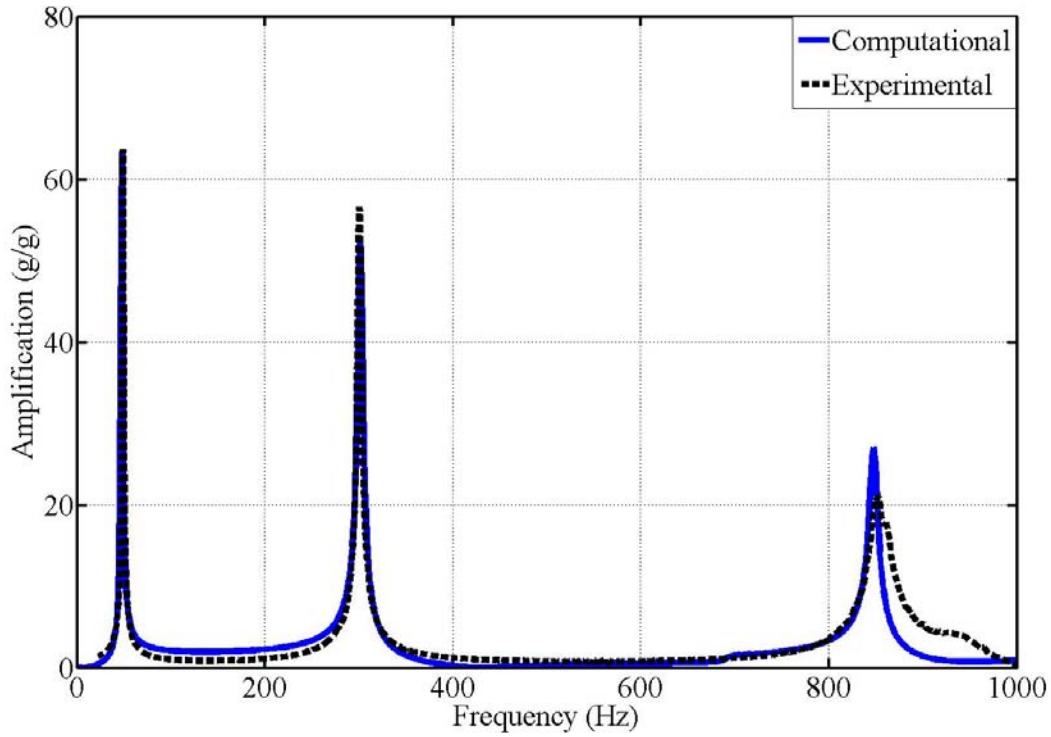

Figure7.6 Comparison of FRF of base plate at one of the free ends

The analytical and experimental natural frequencies, amplification factors and modal loss factors are tabulated in Table 7.7. It can be observed that the experimental and theoretical results are in good agreement. The damping present in the base plate is mainly due to the material damping.

Table 7.7 Comparison of Computational and experimental frequencies of base plate

	Natural Frequency (Hz)		Amplification (g/g)		
Mode	Comp.	Expt.	Comp.	Expt	Loss factor (experiment)
I	47.7	48.7	63.4	63.7	0.007
II	301.3	302.3	54.5	56.6	0.010
III	847.4	852.3	25.1	21.1	0.012

7.3.2 ANALYSIS OF UNCONSTRAINED LAYER SANDWICH PLATE

The viscoelastic material is glued on the base plate to form an unconstrained layer sandwich plate configuration. Two viscoelastic materials namely EAP-2 and EAP-43 are used to get two different cases of unconstrained layer sandwich plate structures. Frequency Response Functions (FRFs) obtained at the free end using the dynamic model are compared with experimental results for EAP-2 and EAP-43 as shown in Figures 7.6 and 7.7. The comparison of computational and experimental model frequencies, amplification and loss factors are presented in Tables 7.6 and 7.7. From the above figures and tables, it is found that computational results with frequency dependent material properties of viscoelastic layer agree with experiment results. By suppressing the variation of material properties in the dynamic models, computations are also carried and the results do not match well. It can also be observed from the tabulated data that higher attenuation levels are observed for higher modes. It can also be observed that EAP-43 provides higher loss factors and high attenuation compared to EAP-2.

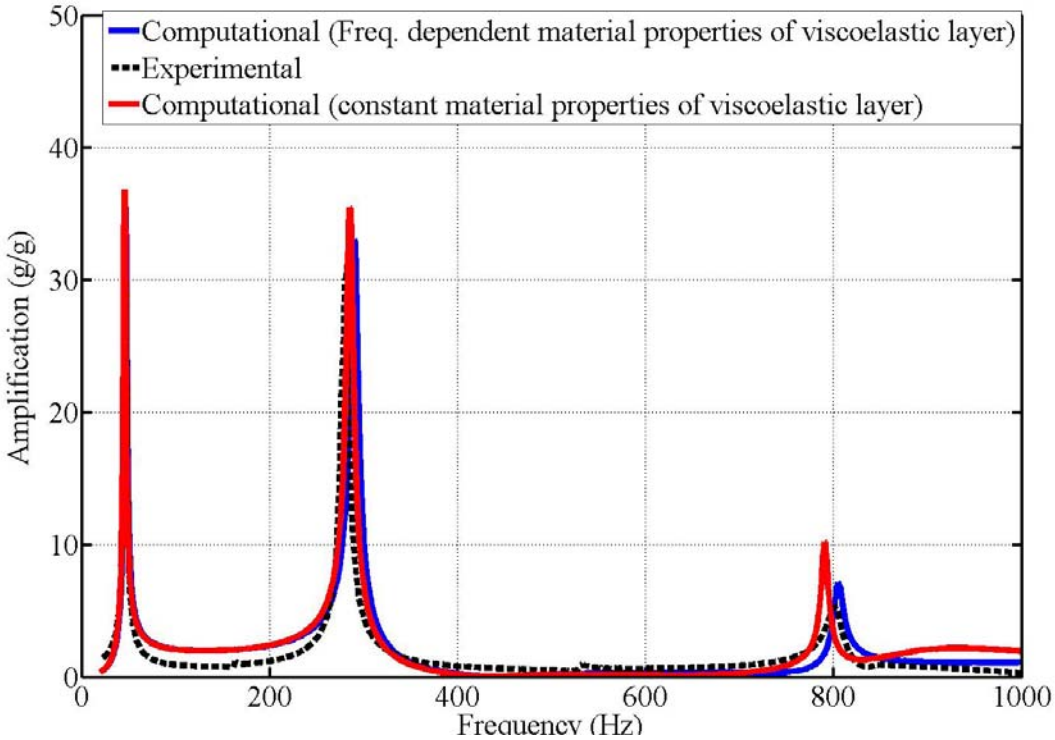

Figure 7.7 Comparison of FRF at one of the free end of unconstrained layer cantilever sandwich plate with 1mm thick EAP-2

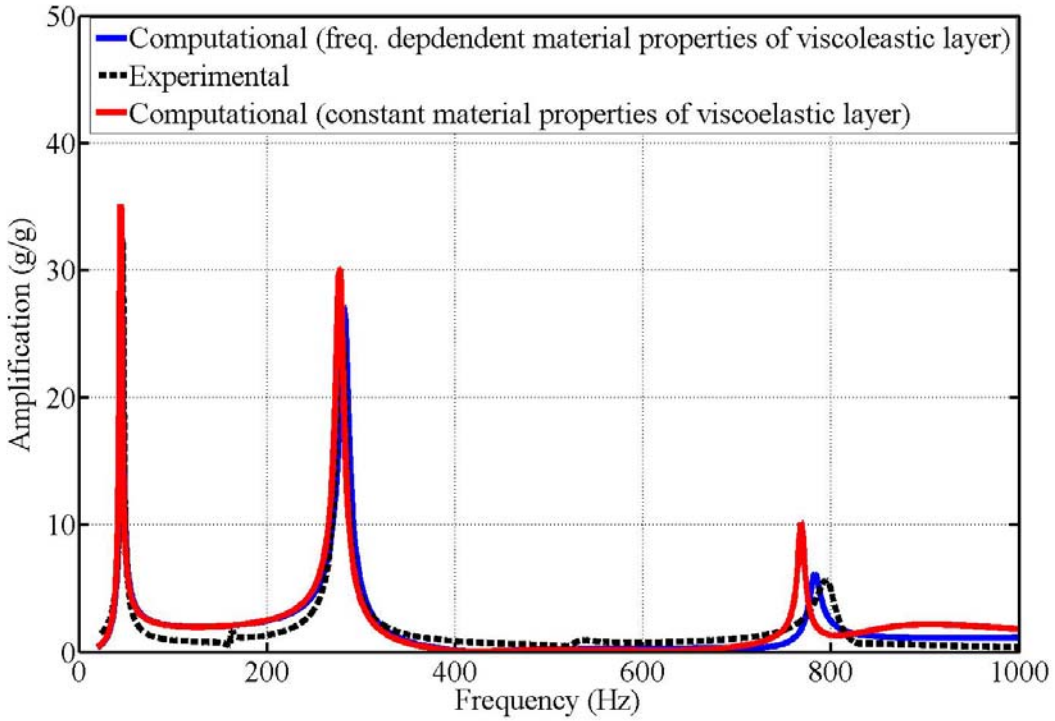

Figure 7.8 Comparison of FRF at one of the free end of unconstrained layer cantilever sandwich plate with 1mm thick EAP-43

Table 7.8 Comparison of computational and Experimental results of unconstrained layer cantilever sandwich plate with 1mm thickness of EAP-2

	Frequency(Hz)			Amplification (g/g)			Loss factors		
	Comp(1)*	Comp(2)*	Expt	Comp(1)	Comp(2)	Expt	Comp(1)	Comp(2)	Expt.
I	46.40	44.80	45.80	35.32	36.85	33.26	0.014	0.013	0.015
II	289.80	285.20	282.00	33.04	35.44	31.13	0.015	0.013	0.016
III	804.90	790.40	800.00	7.12	10.20	5.550	0.065	0.058	0.071

*Comp (1) computational results considering frequency dependent material properties of viscoelastic layer. Comp (2) computational results considering constant material properties of viscoelastic layer

Table 7.9 Comparison of computational and Experimental results of unconstrained layer cantilever sandwich plate with 1mm thickness of EAP-43

	Frequency(Hz)			Amplification (g/g)			Loss factors		
	Comp(1)*	Comp(2)*	Expt.	Comp(1)	Comp(2)	Expt.	Comp(1)	Comp(2)	Expt.
I	45.10	44.10	45.89	32.57	34.81	32.31	0.017	0.016	0.018
II	281.80	277.10	277.80	27.09	30.21	25.35	0.020	0.018	0.021
III	781.40	768.12	795.00	6.002	10.18	5.30	0.074	0.070	0.076

*Comp (1) computational results considering frequency dependent material properties of viscoelastic layer. Comp (2) computational results considering constant material properties of viscoelastic layer

7.3.3 ANALYSIS OF CONSTRAINED LAYER SANDWICH PLATE

The viscoelastic layer is sandwiched between aluminum base plate and constraining layer using epoxy adhesive to form a constrained layer plate structure. Two different viscoelastic layers namely EAP-2 and EAP-43 are used to obtain two different constrained layered plates for the purpose of validation and analysis. The FRFs, modal frequencies, amplification factors and modal loss factors are calculated using dynamic model and compared with experiments. The FRFs obtained at a free end of the plate by both methods is compared for validating the analytical model. The FRFs for the plate with EAP-2 and EAP-43 are shown in Figures 7.9 and 7.10. The corresponding data is tabulated in Table 7.9 and 7.10. From these figures and tabulated data, it is observed that the results of the theoretical model agree with the experiments. The table shows high attenuation levels for higher modes. The loss factors with EAP-43 sandwich plate are higher than loss factors of EAP-2 sandwich plate.

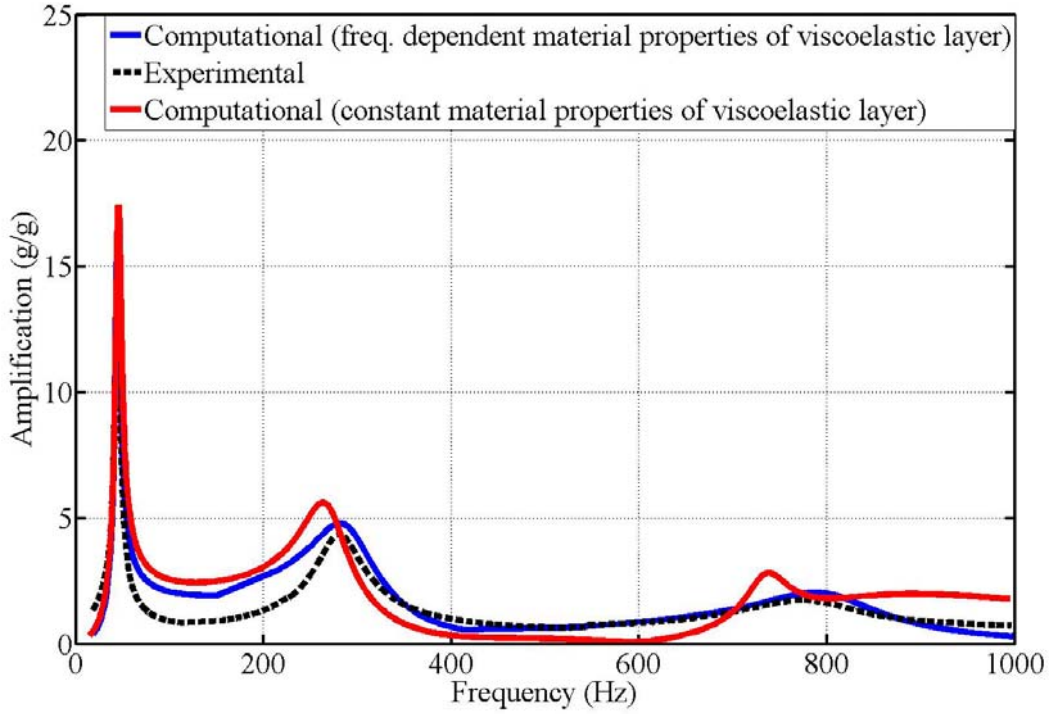

Figure 7.9 Comparison of FRF at one of the free end constrained layer cantilever sandwich plate with 1mm thick EAP-2

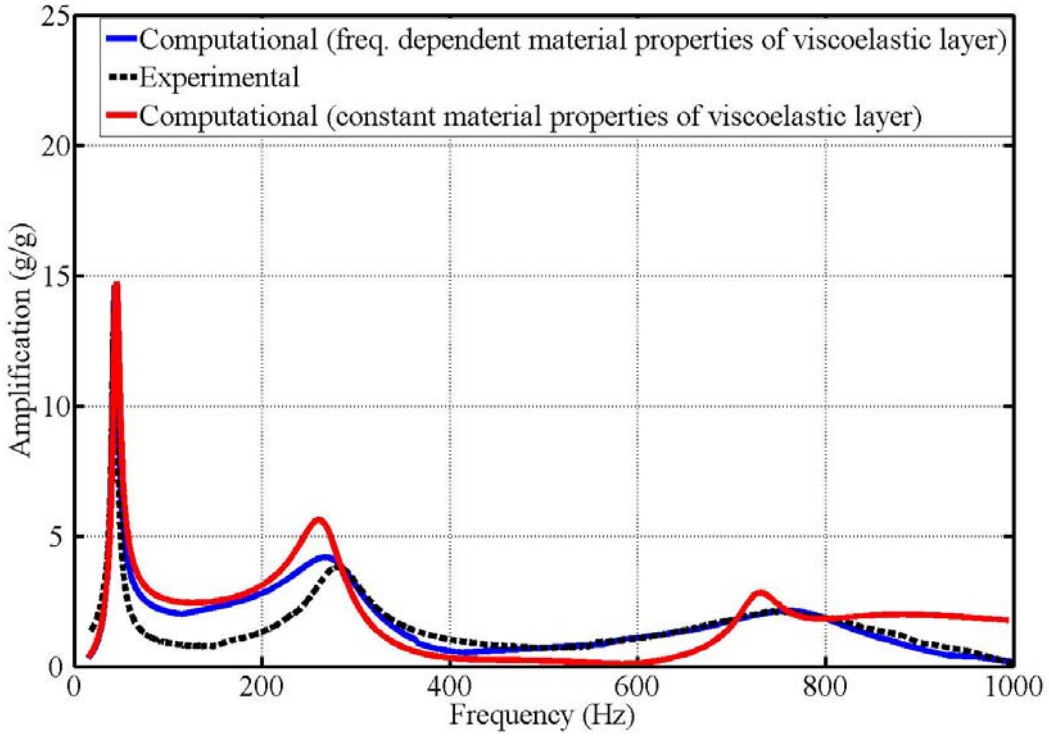

Figure 7.10 Comparison of FRF at one of the free end of constrained layer cantilever sandwich plate with 1mm thick EAP-43

Table 7.10 Comparison of computational and experimental results of constrained layer cantilever sandwich plate with 1mm thickness for EAP-2

	Frequency(Hz)			Amplification (g/g)			Loss factors		
	Comp(1)*	Comp(2)*	Expt	Comp(1)	Comp(2)	Expt	Comp(1)	Comp(2)	Expt.
I	44.50	45.40	44.20	16.20	17.40	15.70	0.042	0.040	0.044
II	282.90	260.90	282.00	4.80	5.69	4.40	0.071	0.068	0.074
III	786.70	737.40	777.20	2.20	2.82	1.80	0.095	0.083	0.101

*Comp (1) computational results considering frequency dependent material properties of viscoelastic layer. Comp (2) computational results considering constant material properties of viscoelastic layer

Table 7.11 Comparison of computational and experimental results of constrained layer cantilever sandwich plate with 1mm thickness for EAP-43

	Frequency(Hz)			Amplification (g/g)			Loss factors		
	Comp(1)*	Comp(2)*	Expt.	Comp(1)	Comp(2)	Expt.	Comp(1)	Comp(2)	Expt.
I	43.60	45.00	43.07	14.60	14.75	14.40	0.051	0.050	0.052
II	267.20	258.90	273.80	4.20	5.613	3.80	0.080	0.076	0.083
III	759.00	728.80	740.16	2.10	2.82	1.70	0.120	0.105	0.130

The overall comparison of amplification factors for bare plate, unconstrained and constrained layer plate for EAP-2 and EAP-43 are presented in Table 7.12.

Table 7.12 Comparison of Amplification factors for cantilever sandwich plate (Experimental results)

Amplification, g/g (dB),							
	Mode	First	Second	Third	First	Second	Third
Base plate, (Base plate is considered as reference)	Freq (Hz)	48.70	302.30	852.30	48.70	302.30	852.30
	Amp.(g/g)	63.70	56.60	21.10	63.70	56.60	21.10
	dB	0	0	0	0	0	0
		EAP-2			EAP-43		
unconstrained layer sandwich plate (t_v/t=0.16)	Freq (Hz)	45.80	282.00	800.00	45.89	277.80	795.00
	Amp.(g/g)	33.26	31.13	5.55	32.31	25.35	5.30
	dB	-5.66	-5.14	-11.37	-5.90	-6.89	-12.00
Constrained layer sandwich plate (t_v/t=0.16) & (t_c/t=0.16)	Freq (Hz)	44.20	282.00	777.20	43.07	273.80	740.16
	Amp.(g/g)	15.70	4.40	1.80	14.40	3.80	1.70
	dB	-12.17	-22.17	-21.38	-12.92	-23.45	-21.90

The above comparative study of unconstrained layer plate and constrained layer plate results obtained from the computation and experimental methods validates the developed dynamic model of sandwich plate and computational scheme. Based on these comparative studies, one can conclude that EAP-2 and EAP-43 shows higher attenuation at higher modes. The constrained layer sandwich structure shows higher attenuation compared to unconstrained layer. EAP-43 shows higher attenuation in vibration levels compared to EAP-2. The observations for sandwich plate structures are in line with the observations of the sandwich beam structures. By suppressing the variation of material properties in the dynamic models, computations are also carried and the results do not match well.

7.4 SUMMARY

The developed dynamic model for sandwich beam and plate structures and computational scheme are validated with several experimental results. The developed dynamic model and computational results with and without considering frequency dependent material properties of viscoelastic layer are also presented for eight configurations. From the computational results, it is concluded that the dynamic model considering frequency dependent material properties of viscoelastic layers are in close agreement with experimental results compared to dynamic model considering constant material properties of viscoelastic layer. The constrained viscoelastic layered structures provide higher damping when compared with unconstrained viscoelastic layered structures. Both the viscoelastic materials provide higher damping at higher modes. EAP-43 provides slightly higher damping compared to EAP-2.

CHAPTER 8

SIMULATION STUDIES ON SANDWICH PLATE STRUCTURES

8.1 INTRODUCTION

In the previous chapter, the developed dynamic models of sandwich beam and plate structures are validated with experiments. From the results it it understood that, sandwich structures with EAP-43 provides high attenuation than EAP-2. Further simulation studies are carried out on sandwich plate structures with EAP-3 using the validated dynamic model for different boundary conditions to identify optimal design parameters for high loss factors as a function of different layer thicknesses.

8.2 SIMULATION STUDIES ON SANDWICH PLATES

Simulations are carried out on constrained layer sandwich plate structure to determine the optimum layer thickness for various combinations of base plate (t_b), constraining layer (t_c) and viscoelastic layer thicknesses (t_v). The objective of these simulation studies is to obtain high loss factors for a given sandwich plate thickness (t). The viscoelastic layer thicknesses considered in the simulations are 0.5, 1, 1.5 and 2 mm. For each of the viscoelastic layer thickness, 15 combinations of base plate (t_b) and constraining layer (t_c) thicknesses are

considered in the simulation studies. The loss factors are computed for different ratios of (t_c/t) and (t_v/t). Neutral axis is computed for each of the above case and it is found that the neutral axis lies in the base layer when (t_c/t) is less than 0.41, in the constraining layer when this ratio is above 0.46, in the viscoelastic layer (constrained) when the ratio of (t_c/t) lies between 0.41 and 0.46.

Simulation studies are also carried out for the three different boundary conditions. The following are the three boundary conditions considered in the simulation studies.

a) Fixed at one edge and free at the three edges (CFFF).
b) Simple support on opposite edges and free at the other two opposite edges (SFSF).
c) Free–Free at all four edges (FFFF) boundary conditions.

(A) SANDWICH PLATE WITH CFFF BOUNDARY CONDITION

The sandwich structure is subjected to a harmonic force input. The FRFs are computed for a given location on the sandwich plate for fifteen combinations of base plate and constraining layer thicknesses keeping the viscoelastic layer thickness as constant. From the FRF, loss factors are calculated using half power method for the first three natural modes. The loss factors computed for each ratio of (t_c/t) and (t_v/t) are shown in Figures 8.1 to 8.3 and also given in Tables 8.1 to 8.3 for the first three modes respectively.

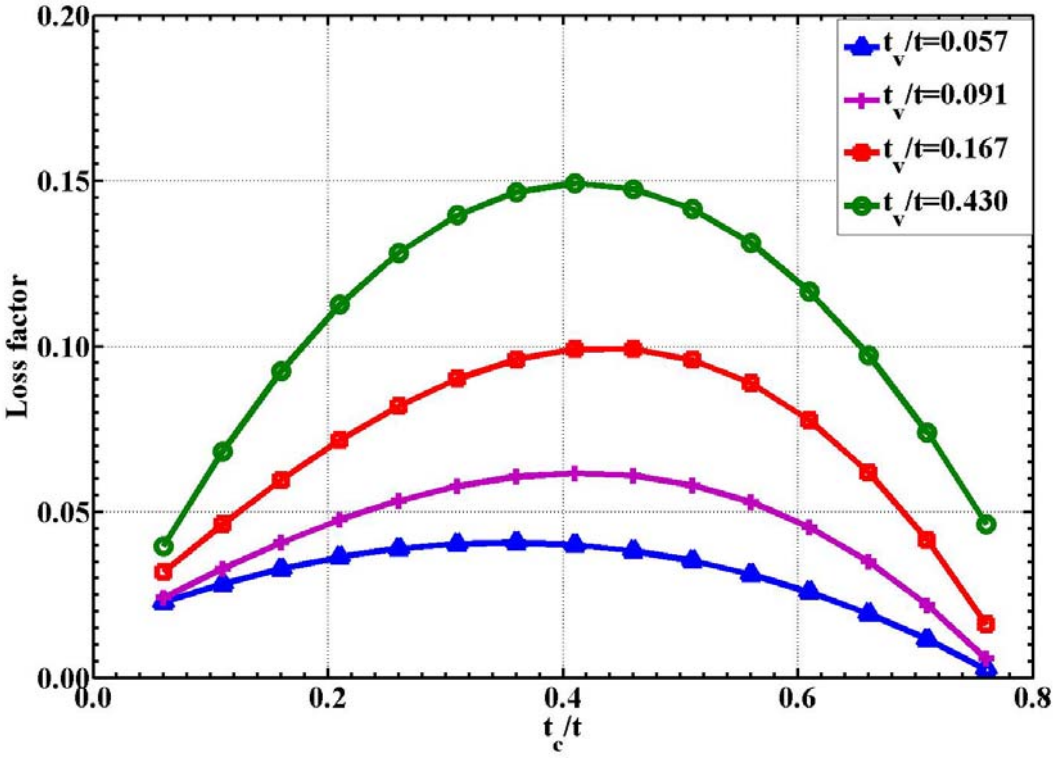

Figure 8.1 Variation of loss factor for CFFF boundary condition (Mode I) for different layer thicknesses

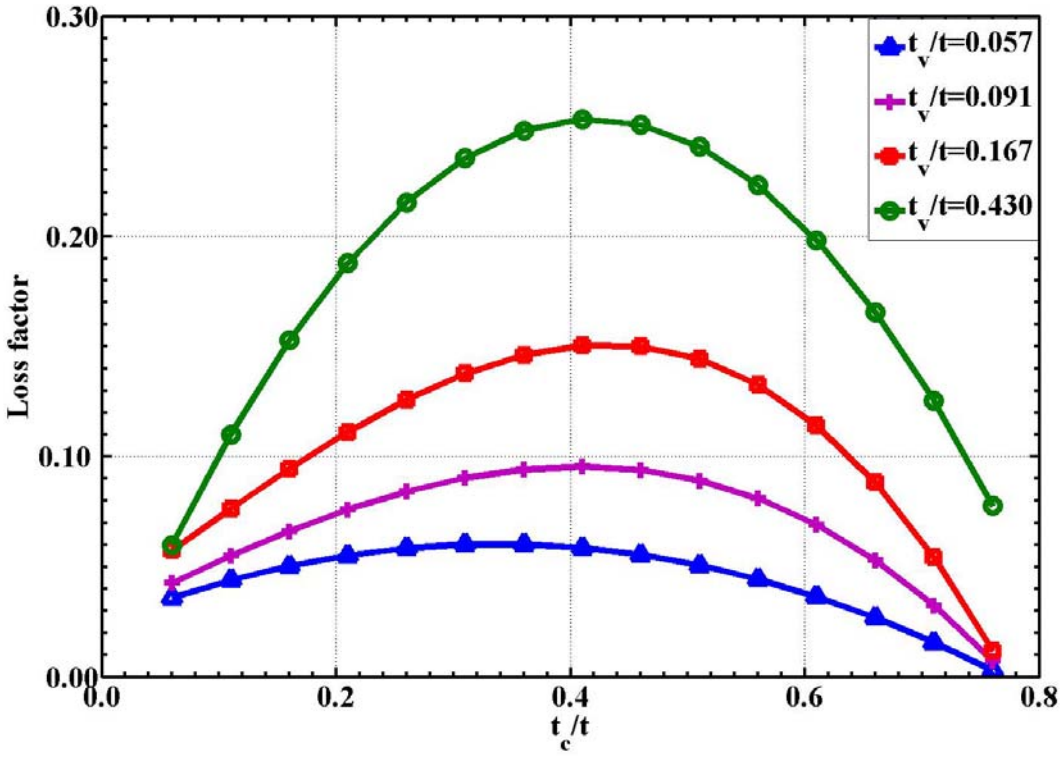

Figure 8.2 Variation of loss factor for CFFF boundary condition (Mode II) for different layer thicknesses

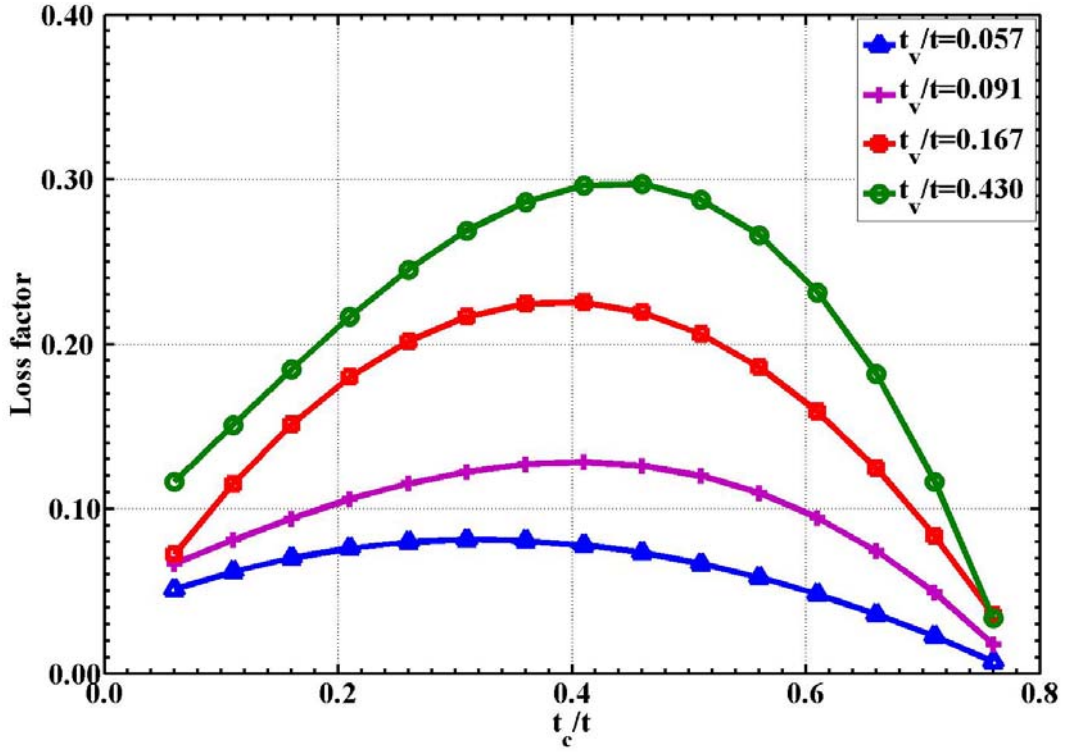

Figure 8.3 Variation of loss factor for CFFF boundary condition (Mode III) for different layer thicknesses

Table 8.1 Variation of loss factors for CFFF boundary condition (Mode I) for different layer thicknesses

	Loss Factors			
$\frac{t_c}{t}$	$\frac{t_v}{t} = 0.057$	$\frac{t_v}{t} = 0.091$	$\frac{t_v}{t} = 0.167$	$\frac{t_v}{t} = 0.430$
0.06	0.0228	0.0242	0.0320	0.0397
0.11	0.0283	0.0329	0.0463	0.0689
0.16	0.0329	0.0408	0.0597	0.0927
0.21	0.0363	0.0477	0.0717	0.1126
0.26	0.0389	0.0534	0.0819	0.1283
0.31	0.0404	0.0578	0.0902	0.1396
0.36	0.0408	0.0607	0.0961	0.1466
0.41	0.0401	0.0618	0.09919	0.1492
0.46	0.0383	0.0609	0.0995	0.1475
0.51	0.0353	0.0581	0.0958	0.1415
0.56	0.0312	0.0530	0.0888	0.1312
0.61	0.0259	0.0453	0.0776	0.1165
0.66	0.0193	0.0350	0.0619	0.0975
0.71	0.0116	0.0219	0.0416	0.0741
0.76	0.0025	0.0058	0.0161	0.0464

t_c = thickness of constraining layer, t_v= thickness of constrained layer;t_b= thickness of base plate; t= total thickness of constrained layer sandwich plate. i.e. $t=t_b+t_v+t_c$

Table 8.2 Variation of loss factors for CFFF boundary condition (Mode II) for different layer thicknesses

	Loss Factors			
$\frac{t_c}{t}$	$\frac{t_v}{t} = 0.057$	$\frac{t_v}{t} = 0.091$	$\frac{t_v}{t} = 0.167$	$\frac{t_v}{t} = 0.430$
0.06	0.0359	0.0426	0.0575	0.0599
0.11	0.0439	0.0549	0.0746	0.1101
0.16	0.0504	0.0662	0.0945	0.1528
0.21	0.0552	0.0759	0.1112	0.1879
0.26	0.0585	0.0841	0.1258	0.2155
0.31	0.0601	0.0903	0.1377	0.2356
0.36	0.0602	0.0942	0.1461	0.2448
0.41	0.0586	0.0955	0.1505	0.2532
0.46	0.0555	0.0939	0.1501	0.2507
0.51	0.0507	0.0892	0.1444	0.2407
0.56	0.0444	0.0810	0.1326	0.2231
0.61	0.0364	0.0692	0.1141	0.1981
0.66	0.0239	0.0529	0.0883	0.1655
0.71	0.0158	0.0326	0.0544	0.1254
0.76	0.0030	0.0075	0.0119	0.0777

t_c = thickness of constraining layer, t_v= thickness of constrained layer; t_b= thickness of base plate; t= total thickness of constrained layer sandwich plate. i.e $t=t_b+t_v+t_c$

Table 8.3 Variation of loss factors for CFFF boundary condition (Mode III) for different layer thicknesses

	Loss Factors			
$\frac{t_c}{t}$	$\frac{t_v}{t} = 0.057$	$\frac{t_v}{t} = 0.091$	$\frac{t_v}{t} = 0.167$	$\frac{t_v}{t} = 0.430$
0.06	0.0512	0.0668	0.0723	0.1165
0.11	0.0618	0.0811	0.1152	0.1509
0.16	0.0701	0.0943	0.1510	0.1848
0.21	0.0760	0.1058	0.1799	0.2167
0.26	0.0797	0.1154	0.2018	0.2452
0.31	0.0813	0.1226	0.2166	0.2690
0.36	0.0807	0.1270	0.2245	0.2865
0.41	0.0780	0.1283	0.2245	0.2964
0.46	0.0734	0.1262	0.2192	0.2973
0.51	0.0668	0.1201	0.2061	0.2877
0.56	0.0584	0.1097	0.1860	0.2662
0.61	0.0481	0.0947	0.1588	0.2315
0.66	0.0361	0.0746	0.1247	0.1812
0.71	0.0225	0.0491	0.0856	0.1166
0.76	0.0079	0.0177	0.0354	0.0335

t_c = thickness of constraining layer, t_v= thickness of constrained layer; t_b= thickness of base plate; t= total thickness of constrained layer sandwich plate. i.e. $t=t_b+t_v+t_c$

From the above results, it can be concluded that the high loss factors are observed when (t_c/t) lies between 0.41 and 0.46. For a given cross section of the sandwich plate structure, the shear strain is maximum at the neutral axis and decreases along the thickness on either side of the neutral axis. The dissipation of energy in constrained layer sandwich structure is through the shear deformation of viscoelastic layer. So, high loss factors are observed when the neutral axis of the sandwich structure falls in the viscoelastic layer. It is also observed from the above figures that the loss factors are higher for higher modes and increase as thickness of viscoelastic layer increases.

(B) SANDWICH PLATE WITH SFSF BOUNDARY CONDITION

Simulation studies are carried out for SFSF boundary condition. The FRFs are computed for a given location on the sandwich plate for the various base and constraining layer thicknesses. For each case, the loss factors are calculated from FRFs for the first three modes. The variation of loss factors with different (t_c/t) is shown in Figures 8.4 to and 8.6 and is also given in Tables 8.4 to 8.6 for the first three modes respectively.

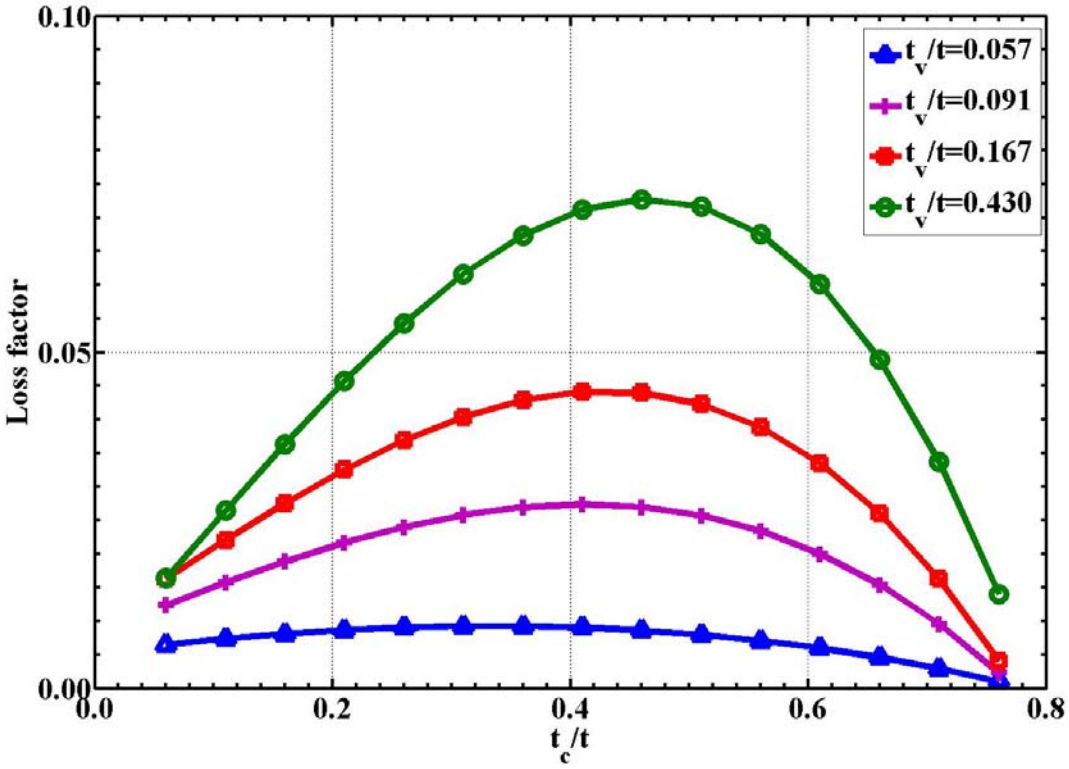

Fig. 8.4 Variation of loss factor for SFSF boundary condition (Mode I) for different layer thicknesses

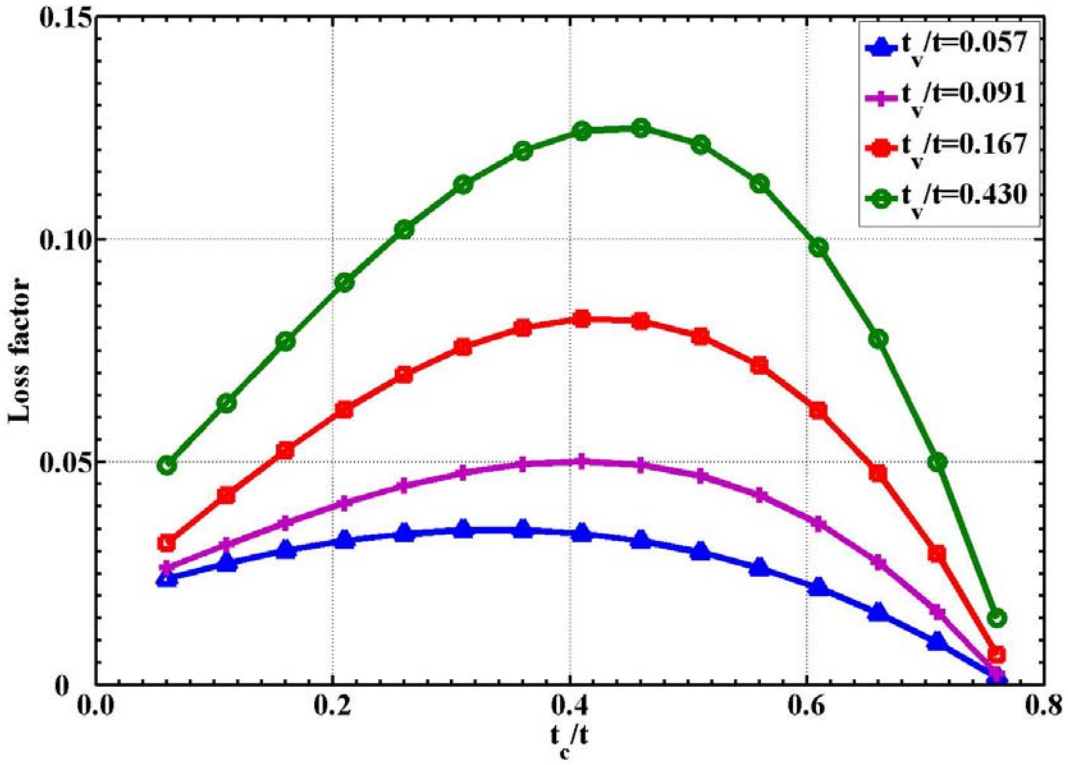

Figure 8.5 Variation of loss factor for SFSF boundary condition (Mode II) for different layer thicknesses

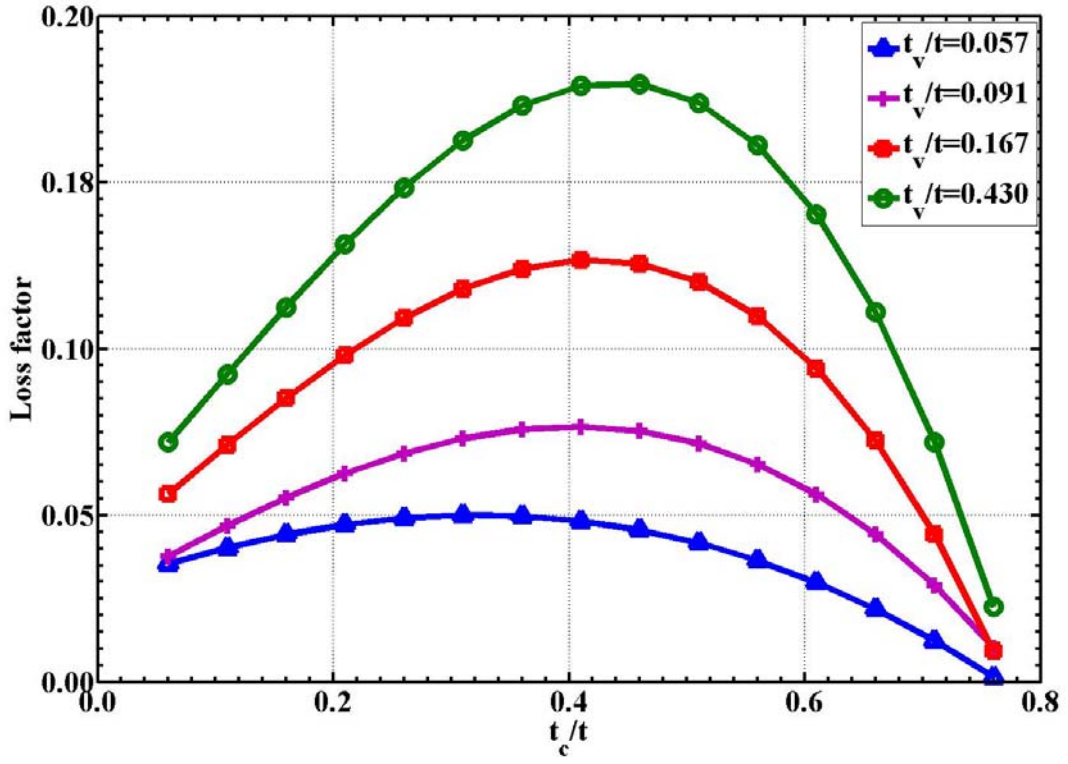

Figure 8.6 Variation of loss factor for SFSF boundary condition (Mode III) for different layer thicknesses

Table 8.4 Variation of loss factors for SFSF boundary condition (Mode I) for different layer thicknesses

	Loss Factors			
$\frac{t_c}{t}$	$\frac{t_v}{t} = 0.057$	$\frac{t_v}{t} = 0.091$	$\frac{t_v}{t} = 0.167$	$\frac{t_v}{t} = 0.430$
0.06	0.0065	0.0124	0.0163	0.0164
0.11	0.0074	0.0158	0.0221	0.0264
0.16	0.0081	0.0189	0.0276	0.0364
0.21	0.0087	0.0217	0.0326	0.0458
0.26	0.0091	0.0240	0.0369	0.0543
0.31	0.0093	0.0258	0.0404	0.0616
0.36	0.0093	0.0269	0.0428	0.0674
0.41	0.0090	0.0274	0.0441	0.0712
0.46	0.0086	0.0270	0.0440	0.0727
0.51	0.0080	0.0257	0.0423	0.0716
0.56	0.0071	0.0234	0.0388	0.0675
0.61	0.0060	0.0200	0.0335	0.0601
0.66	0.0046	0.0154	0.0260	0.0488
0.71	0.0030	0.0096	0.0163	0.0037
0.76	0.0010	0.0023	0.0041	0.0141

t_c = thickness of constraining layer, t_v= thickness of constrained layer; t_b= thickness of base plate; t= total thickness of constrained layer sandwich plate. i.e. $t=t_b+t_v+t_c$

Table 8.5 Variation of loss factors for SFSF boundary condition (Mode II) for different layer thicknesses

	Loss Factors			
$\frac{t_c}{t}$	$\frac{t_v}{t} = 0.057$	$\frac{t_v}{t} = 0.091$	$\frac{t_v}{t} = 0.167$	$\frac{t_v}{t} = 0.430$
0.06	0.0238	0.0263	0.0318	0.0494
0.11	0.0273	0.0314	0.0425	0.0632
0.16	0.0301	0.0364	0.0526	0.0771
0.21	0.0324	0.0408	0.0617	0.0903
0.26	0.0339	0.0446	0.0696	0.1022
0.31	0.0347	0.0476	0.0758	0.1123
0.36	0.0347	0.0495	0.0801	0.1199
0.41	0.0340	0.0502	0.0822	0.1243
0.46	0.0323	0.0494	0.0816	0.1250
0.51	0.0297	0.0469	0.0782	0.1213
0.56	0.0262	0.0426	0.0716	0.1125
0.61	0.0217	0.0362	0.0615	0.0982
0.66	0.0161	0.0275	0.0475	0.0776
0.71	0.0095	0.0614	0.0294	0.0501
0.76	0.0017	0.0025	0.0068	0.0151

t_c = thickness of constraining layer, t_v= thickness of constrained layer; t_b= thickness of base plate; t= total thickness of constrained layer sandwich plate. i.e. $t=t_b+t_v+t_c$

Table 8.6 Variation of loss factors for SFSF boundary condition (Mode III) for different layer thicknesses

	Loss Factors			
$\frac{t_c}{t}$	$\frac{t_v}{t} = 0.057$	$\frac{t_v}{t} = 0.091$	$\frac{t_v}{t} = 0.167$	$\frac{t_v}{t} = 0.430$
0.06	0.0353	0.0376	0.0563	0.0719
0.11	0.0403	0.0468	0.0711	0.0924
0.16	0.0442	0.0553	0.0852	0.1125
0.21	0.0472	0.0626	0.0987	0.1315
0.26	0.0492	0.0686	0.1092	0.1485
0.31	0.0500	0.0731	0.1180	0.1626
0.36	0.0497	0.0758	0.1240	0.1731
0.41	0.0483	0.0766	0.1267	0.1790
0.46	0.0456	0.0753	0.1256	0.1796
0.51	0.0417	0.0716	0.1210	0.1739
0.56	0.0364	0.0653	0.1097	0.1612
0.61	0.0298	0.0563	0.0940	0.1450
0.66	0.0213	0.0442	0.0724	0.1111
0.71	0.0123	0.0290	0.0443	0.0721
0.76	0.0014	0.0103	0.0092	0.0226

t_c = thickness of constraining layer, t_v= thickness of constrained layer; t_b= thickness of base plate; t= total thickness of constrained layer sandwich plate. i.e. $t=t_b+t_v+t_c$

From the above figures and tables, it is observed that high loss factors are observed when (t_c/t) lies between 0.41 and 0.46. The trend in the variation of loss factors for the first three modes is similar to that of CFFF boundary condition.

(C) SANDWICH PLATE WITH FFFF BOUNDARY CONDITION

The numerical studies are also extended for FFFF boundary condition. The variation of loss factors with different (t_c/t) and (t_v/t) are shown in Figures 8.7 to 8.9 and are also given in Tables 8.7 to 8.9 for the first three modes respectively.

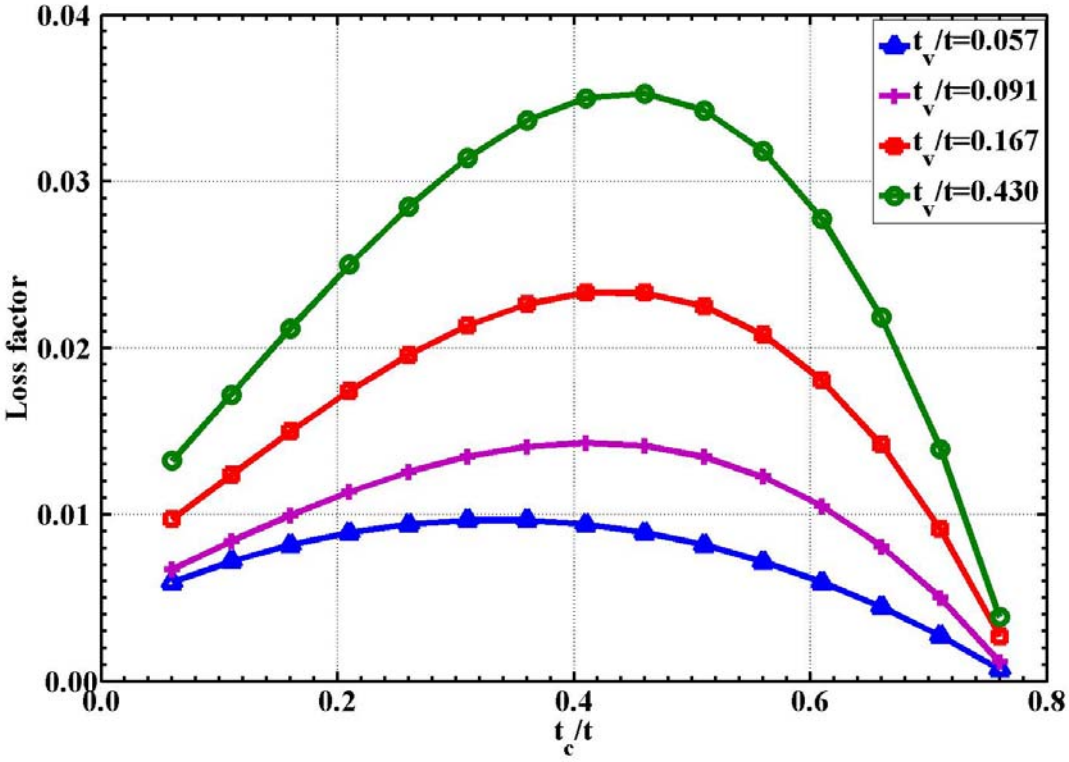

Figure 8.7 Variation of loss factor for FFFF boundary condition (Mode I) for different layer thicknesses

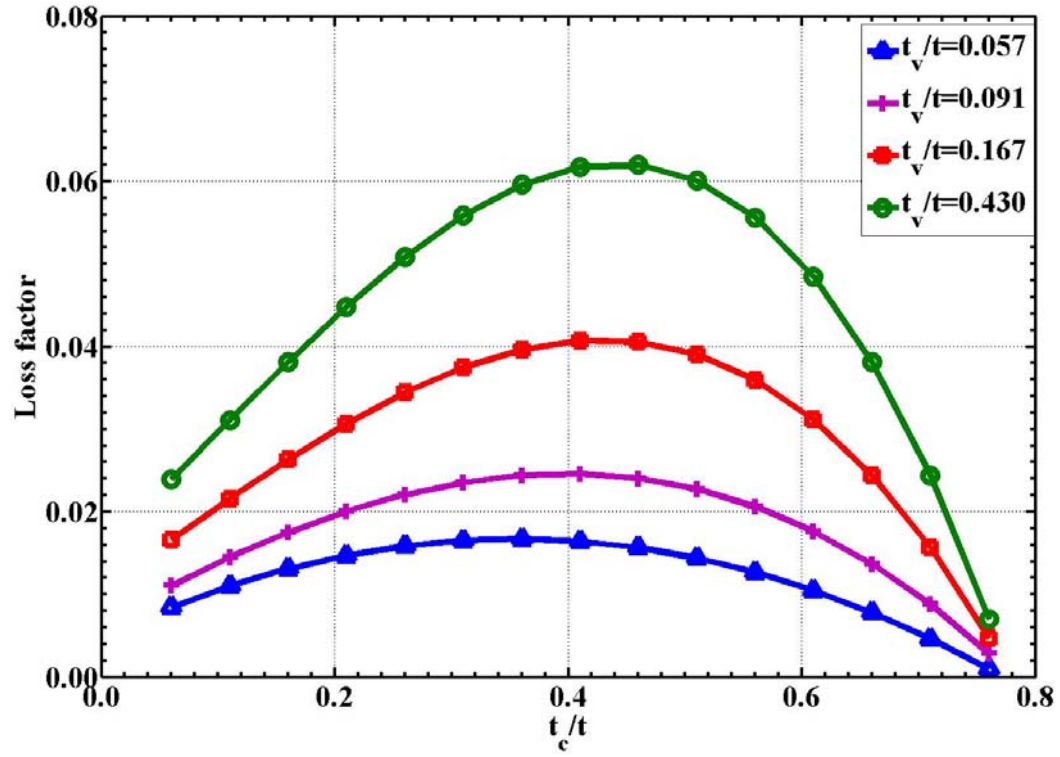

Figure 8.8 Variation of loss factor for FFFF boundary condition (Mode II) for different layer thicknesses

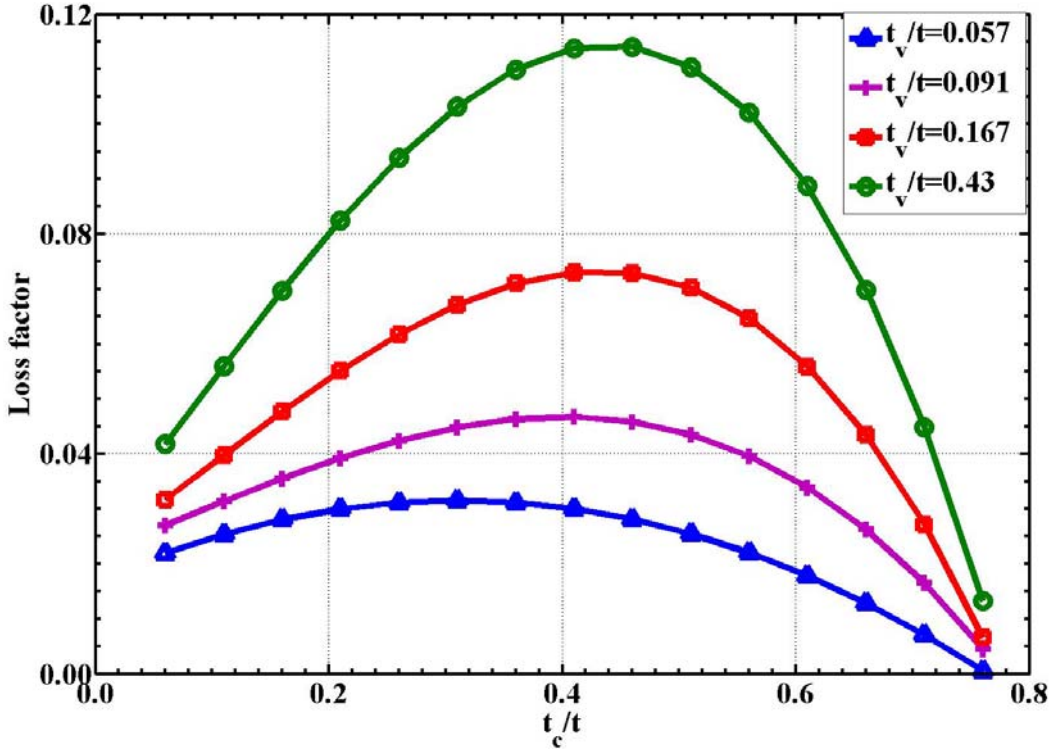

Figure 8.9 Variation of loss factor for FFFF boundary condition (Mode III) for different layer thickness

Table 8.7 Variation of loss factors for FFFF boundary condition (Mode I) for different layer thickness

	Loss Factors			
$\frac{t_c}{t}$	$\frac{t_v}{t} = 0.057$	$\frac{t_v}{t} = 0.091$	$\frac{t_v}{t} = 0.167$	$\frac{t_v}{t} = 0.430$
0.06	0.0059	0.0067	0.0097	0.0132
0.11	0.0072	0.0084	0.0124	0.0172
0.16	0.0082	0.0100	0.0150	0.0212
0.21	0.0089	0.0114	0.0173	0.0250
0.26	0.0094	0.0126	0.0196	0.0285
0.31	0.0097	0.0135	0.0213	0.0314
0.36	0.0097	0.0141	0.0226	0.0337
0.41	0.0094	0.0143	0.0233	0.0350
0.46	0.0081	0.0141	0.0233	0.0353
0.51	0.0082	0.0135	0.0225	0.0343
0.56	0.0072	0.0123	0.0208	0.0343
0.61	0.0059	0.0105	0.0180	0.0277
0.66	0.0044	0.0081	0.0142	0.0218
0.71	0.0027	0.0050	0.0911	0.0140
0.76	0.0007	0.0012	0.0027	0.0039

t_c = thickness of constraining layer, t_v= thickness of constrained layer; t_b= thickness of base plate; t= total thickness of constrained layer sandwich plate. i.e. $t=t_b+t_v+t_c$

Table 8.8 Variation of loss factors for FFFF boundary condition (Mode II) for different layer thickness

	Loss Factors			
$\frac{t_c}{t}$	$\frac{t_v}{t} = 0.057$	$\frac{t_v}{t} = 0.091$	$\frac{t_v}{t} = 0.167$	$\frac{t_v}{t} = 0.430$
0.06	0.0084	0.0111	0.0166	0.0239
0.11	0.0110	0.0145	0.0216	0.0311
0.16	0.0131	0.0175	0.0263	0.0382
0.21	0.0147	0.0206	0.0307	0.0448
0.26	0.0159	0.0221	0.0344	0.0508
0.31	0.0165	0.0236	0.0375	0.0558
0.36	0.0167	0.0244	0.0396	0.0596
0.41	0.0164	0.0246	0.0407	0.0617
0.46	0.0157	0.0241	0.0406	0.0620
0.51	0.0144	0.0228	0.0390	0.0601
0.56	0.0127	0.0206	0.0360	0.0556
0.61	0.0105	0.0176	0.0311	0.0484
0.66	0.0078	0.0137	0.0244	0.0381
0.71	0.0046	0.0088	0.0157	0.0244
0.76	0.0010	0.0029	0.0047	0.0078

t_c = thickness of constraining layer, t_v= thickness of constrained layer; t_b= thickness of base plate; t= total thickness of constrained layer sandwich plate. i.e. $t=t_b+t_v+t_c$

Table 8.9 Variation of loss factors for FFFF boundary condition (Mode III) for different layer thickness

	Loss Factors			
$\frac{t_c}{t}$	$\frac{t_v}{t} = 0.057$	$\frac{t_v}{t} = 0.091$	$\frac{t_v}{t} = 0.167$	$\frac{t_v}{t} = 0.430$
0.06	0.0219	0.0270	0.0317	0.0417
0.11	0.0254	0.0314	0.0398	0.0560
0.16	0.0281	0.0355	0.0477	0.0697
0.21	0.0300	0.0393	0.0551	0.0825
0.26	0.0311	0.0422	0.0617	0.0938
0.31	0.0315	0.0448	0.0671	0.1031
0.36	0.0312	0.0463	0.0710	0.1100
0.41	0.0300	0.0467	0.0730	0.1138
0.46	0.0281	0.0458	0.0729	0.1141
0.51	0.0254	0.0435	0.0702	0.1103
0.56	0.0220	0.0396	0.0646	0.1020
0.61	0.0178	0.0339	0.0558	0.0880
0.66	0.0128	0.0263	0.0435	0.0698
0.71	0.0071	0.0165	0.0272	0.0449
0.76	0.0005	0.0045	0.0066	0.0133

t_c = thickness of constraining layer, t_v= thickness of constrained layer; t_b= thickness of base plate; t= total thickness of constrained layer sandwich plate. i.e. $t=t_b+t_v+t_c$

From the above figures and tables, it is seen that the variation of loss factor for the sandwich plate structure with FFFF boundary condition is similar to the sandwich plate with CFFF and SFSF boundary conditions as discussed earlier.

A comparison of maximum loss factor for each (t_v/t) is given in table 8.10.The loss factor of the base plate in each mode is taken as reference value and the vibration attenuation levels are calculated in terms of decibels (dB) and presented below.

Table 8.10 Comparison of loss factor of base plate with maximum loss factors in CFFF, SFSF and FFFF boundary conditions

		Mode I	Mode II	Mode III
Base plate		0. 0076	0.0098	0.0120
CFFF t_c/t	$t_v/t = 0.057$	0.0408	0.0602	0.08130
	Attenuation(dB)	14.60	15.77	16.62
	$t_v/t = 0.091$	0.0618	0.0955	0.1283
	Attenuation(dB)	18.10	19.78	20.58
	$t_v/t = 0.167$	0.0995	0.1505	0.2245
	Attenuation(dB)	22.34	23.73	25.44
	$t_v/t = 0.430$	0.1492	0.2543	0.2964
	Attenuation(dB)	25.86	28.28	27.85
SFSF t_c/t	$t_v/t = 0.057$	0.0090	0.0347	0.050
	Attenuation(dB)	1.47	10.98	12.40
	$t_v/t = 0.091$	0.0274	0.0502	0.0731
	Attenuation(dB)	11.14	14.19	15.70
	$t_v/t = 0.167$	0.0441	0.0822	0.1180
	Attenuation(dB)	15.27	18.47	19.86
	$t_v/t = 0.430$	0.0727	0.1250	0.1626
	Attenuation(dB)	19.61	22.11	22.64
FFFF t_c/t	$t_v/t = 0.057$	0.0097	0.0167	0.0315
	Attenuation(dB)	2.12	4.66	8.40
	$t_v/t = 0.091$	0.0143	0.0246	0.0467
	Attenuation(dB)	5.49	7.99	11.80
	$t_v/t = 0.167$	0.0233	0.0407	0.0730
	Attenuation(dB)	9.73	12.38	15.68
	$t_v/t = 0.430$	0.0353	0.0620	0.1138
	Attenuation(dB)	13.34	16.02	19.54

By comparing the loss factors of base plate with the maximum loss factors obtained for different t_v/t in all three boundary conditions, it is concluded the loss factor increases with mode number and thickness of viscoelastic layer.

8.3 SUMMARY

The validated dynamic model and the computational scheme are extended to understand the behaviour of loss factors for various combinations of layer thicknesses. Simulation studies are also carried out for three different boundary conditions. From the simulations studies, it is concluded that high loss factors are observed when (t_c/t) lies between 0.41 and 0.46. This trend is independent of the natural modes and boundary conditions. The loss factors increase with increase in thickness of viscoelastic layer and mode number.

CHAPTER 9

SUMMARY AND CONCLUSIONS

9.1 SUMMARY

Two viscoelastic materials, EAP-2 and EAP-43 are characterized using Dynamic Mechanical Analyzer (DMA) for their frequency dependent material properties: Young's modulus, Shear Modulus, Poisson's ratio and loss factors. The experimental data obtained from DMA is expressed in mathematical form using power fit as continuous functions of frequencies in the range from 10^{-2} Hz to 10^{6} Hz. Through these equations, frequency dependent material properties of the viscoelastic layers are introduced in the dynamic models of sandwich structures.

Finite element based dynamic models are developed for sandwich beam and plate structures. The sandwich structure is discretized into finite elements and dynamic equations of motion are developed using Lagrangian method. The element mass and complex stiffness matrices for the sandwich beam and plate are developed considering the shear deformation of the viscoelastic layer. During FE formulation of the sandwich beam structure, longitudinal displacements of the base, constraining layer and transverse displacement of the sandwich beam are considered as primary field variables. The shear deformation of viscoelastic layer is derived from the longitudinal displacements of base and constraining layer. During formulation of sandwich plate structure, longitudinal displacements and rotations in x and y directions of the base and constraining layers, transverse displacement of the sandwich plate are considered as primary field variables.

A computational scheme is developed to solve the dynamic equations of motion of the sandwich structures. The developed dynamic equations of motion accommodate frequency dependent complex stiffness of the viscoelastic material. MATLAB codes are developed to solve the dynamic models for computing frequency response functions and loss factors.

Extensive experiments are carried out on sandwich beam and plate structures and frequency response functions (FRF's) are obtained. The FRF's and loss factors obtained from the experiments are compared with those obtained from computational scheme for eight different configurations. By suppressing the variation of material properties in the dynamic model, simulations are also carried out to confirm the need of introducing frequency dependent material properties.

The validated dynamic model and the developed code is used to compute loss factors for various thickness ratios and boundary conditions of the sandwich plate structure and optimal parameters are identified for vibration attenuation.

9.2 CONCLUSIONS

The following are the conclusions drawn from the present work:

i. Two viscoelastic materials, EAP-2 and EAP-43 are characterised for their frequency dependent material properties. Based on the experimental data, frequency dependent Young's modulus, shear modulus and loss factors are expressed in mathematical form using power fit as functions of frequency using the experimental data for both the viscoelastic materials.
ii. Finite Element based dynamic models are developed for sandwich structures considering the frequency dependent complex Young's and shear modulus of viscoelastic material.
iii. The performance of both the viscoelastic material, EAP-2 and EAP-43 in attenuating the vibration amplitudes are evaluated. It is concluded that both the viscoelastic materials provide higher vibration attenuation.
iv. By comparing both the viscoelastic materials, EAP-43 is found to be superior compared to EAP-2 for achieving higher vibration attenuations. The reason for higher

attenuation is attributed to carbon black used as filler in EAP-43 which provides better loss factors compared to the titanium dioxide in EAP-2.

v. Constraining layer sandwich structures provide higher damping and vibration attenuation compared to unconstrained layer sandwich structures.

vi. Unconstrained layer sandwich beams and plates with the thickness ratio ($t_v/t=0.20$) can be employed in real life structures, if the required vibration attenuation levels are around 5 to 10 dB.

vii. Constrained layer sandwich beams and plates with the thickness ratio ($t_v/t=0.16$) and (($t_c/t=0.16$) can be employed in real life structures, if the required vibration attenuation levels are more than 10 dB.

viii. There is a shift in natural frequency of unconstrained and constrained layer sandwich structures to a lower side compared to base structure alone. This is due to the additional mass and damping of viscoelastic layer.

ix. Based on the simulation studies on sandwich plate structure, it is concluded that

(a) For a given sandwich plate thickness (t), higher loss factors are obtained when the ratio of constraining layer thickness to total thickness of sandwich plate (t_c/t) lies between 0.41 to 0.46.

(b) Loss factor increases with increase in viscoelastic layer thickness.

(c) Irrespective of boundary conditions, loss factors increase with mode number.

9.3 SCOPE FOR FUTURE WORK

The following future work is proposed

i. During development of dynamic models for sandwich beam and plate structures, only the frequency dependent material properties of viscoelastic layers are considered at constant temperature. The proposed models can be extended by considering both frequency and temperature dependent material properties of viscoelastic layers.

ii. The developed dynamic models for sandwich beam and plate structure, assume perfect bonding between the layers. The developed dynamic model can be improved by modelling adhesive between the layers.

iii. In the present model the viscoelastic layers covers the entire surface of the base structure. The model can be extended for optimum location of viscoelastic patches instead of complete layer.

iv. The developed dynamic model consider passive constraining layer. The proposed model can be extended by replacing passive constraining layer with active constraining layer.

APPENDIX-`I'

INTERPOLATION FUNCTIONS OF SANDWICH PLATE

$[N_1] = [n_{11} \quad n_{12} \quad n_{13} \quad n_{14}]$ is the interpolation for in-plane displacement of base layer in x-direction and the individual terms are expressed as follows:

$$n_{11} = [n_1 \ 0 \ 0 \ 0 \ 0 \ 0 \ 0 \ 0 \ 0] \qquad n_{13} = [n_3 \ 0 \ 0 \ 0 \ 0 \ 0 \ 0 \ 0 \ 0]$$
$$n_{12} = [n_2 \ 0 \ 0 \ 0 \ 0 \ 0 \ 0 \ 0 \ 0] \qquad n_{14} = [n_4 \ 0 \ 0 \ 0 \ 0 \ 0 \ 0 \ 0 \ 0] \qquad \text{(A.1)}$$

$[N_2] = [n_{11} \quad n_{12} \quad n_{13} \quad n_{14}]$ is the interpolation for inplane displacement of base layer in y-direction and the individual terms are expressed as follows:

$$n_{21} = [0 \ n_1 \ 0 \ 0 \ 0 \ 0 \ 0 \ 0 \ 0] \qquad n_{23} = [0 \ n_3 \ 0 \ 0 \ 0 \ 0 \ 0 \ 0 \ 0] \qquad \text{(A.2)}$$
$$n_{22} = [0 \ n_2 \ 0 \ 0 \ 0 \ 0 \ 0 \ 0 \ 0] \qquad n_{24} = [0 \ n_4 \ 0 \ 0 \ 0 \ 0 \ 0 \ 0 \ 0]$$

$[N_3] = [n_{31} \quad n_{32} \quad n_{33} \quad n_{34}]$ is the interpolation for constraining layer in x-direction and the individual terms are expressed as follows:

$$n_{31} = [0 \ 0 \ n_1 \ 0 \ 0 \ 0 \ 0 \ 0 \ 0] \qquad n_{33} = [0 \ 0 \ n_3 \ 0 \ 0 \ 0 \ 0 \ 0 \ 0]$$
$$n_{32} = [0 \ 0 \ n_2 \ 0 \ 0 \ 0 \ 0 \ 0 \ 0] \qquad n_{34} = [0 \ 0 \ n_4 \ 0 \ 0 \ 0 \ 0 \ 0 \ 0] \qquad \text{(A.3)}$$

$[N_4] = [n_{41} \quad n_{42} \quad n_{43} \quad n_{44}]$ is the interpolation for constraining layer in y-direction and the individual terms are expressed as follows:

$$n_{41} = [0 \ 0 \ 0 \ n_1 \ 0 \ 0 \ 0 \ 0 \ 0] \qquad n_{43} = [0 \ 0 \ 0 \ n_3 \ 0 \ 0 \ 0 \ 0 \ 0]$$
$$n_{42} = [0 \ 0 \ 0 \ n_2 \ 0 \ 0 \ 0 \ 0 \ 0] \qquad n_{44} = [0 \ 0 \ 0 \ n_4 \ 0 \ 0 \ 0 \ 0 \ 0] \qquad \text{(A.4)}$$

$[N_5] = [n_{51} \quad n_{52} \quad n_{53} n_{54}]$ is the interpolation for transverse displacement for all three layers. where,

$$n_{51} = [0 \ 0 \ 0 \ 0 \ n_1 \ 0 \ 0 \ 0 \ 0] \qquad n_{53} = [0 \ 0 \ 0 \ 0 \ n_3 \ 0 \ 0 \ 0 \ 0]$$
$$n_{52} = [0 \ 0 \ 0 \ 0 \ n_2 \ 0 \ 0 \ 0 \ 0] \qquad n_{54} = [0 \ 0 \ 0 \ 0 \ n_4 \ 0 \ 0 \ 0 \ 0] \qquad \text{(A.5)}$$

$[N_6] = [n_{61} \quad n_{62} \quad n_{63} \quad n_{64}]$ is the interpolation for rotation of base layer in x direction and the individual terms are expressed as follows:

$$n_{61} = [0 \ 0 \ 0 \ 0 \ 0 \ n_1 \ 0 \ 0 \ 0] \qquad n_{63} = [0 \ 0 \ 0 \ 0 \ 0 \ n_3 \ 0 \ 0 \ 0]$$
$$n_{62} = [0 \ 0 \ 0 \ 0 \ 0 \ n_2 \ 0 \ 0 \ 0] \qquad n_{64} = [0 \ 0 \ 0 \ 0 \ 0 \ n_4 \ 0 \ 0 \ 0] \qquad \text{(A.6)}$$

$[N_7] = [n_{71} \quad n_{72} \quad n_{73} \quad n_{74}]$ is the interpolation for rotation of base layer in y-direction and the individual terms are expressed as follows:

$$n_{71} = [0 \ 0 \ 0 \ 0 \ 0 \ 0 \ n_1 \ 0 \ 0] \qquad n_{73} = [0 \ 0 \ 0 \ 0 \ 0 \ 0 \ n_3 \ 0 \ 0]$$
$$n_{72} = [0 \ 0 \ 0 \ 0 \ 0 \ 0 \ n_2 \ 0 \ 0] \qquad n_{74} = [0 \ 0 \ 0 \ 0 \ 0 \ 0 \ n_4 \ 0 \ 0] \qquad \text{(A.7)}$$

$[N_8] = [n_{81} \quad n_{82} \quad n_{83} \quad n_{84}]$ is the interpolation for rotation of constraining layer in x-direction. Where,

$$n_{81} = [0 \ 0 \ 0 \ 0 \ 0 \ 0 \ 0 \ n_1 \ 0] \qquad n_{83} = [0 \ 0 \ 0 \ 0 \ 0 \ 0 \ 0 \ n_3 \ 0]$$
$$n_{82} = [0 \ 0 \ 0 \ 0 \ 0 \ 0 \ 0 \ n_2 \ 0] \qquad n_{84} = [0 \ 0 \ 0 \ 0 \ 0 \ 0 \ 0 \ n_4 \ 0] \tag{A.8}$$

$[N_9] = [n_{91} \quad n_{92} \quad n_{93} \quad n_{94}]$ is the interpolation for rotation of constraining layer in y-direction.where,

$$n_{91} = [0 \ 0 \ 0 \ 0 \ 0 \ 0 \ 0 \ 0 \ n_1] \qquad n_{93} = [0 \ 0 \ 0 \ 0 \ 0 \ 0 \ 0 \ 0 \ n_3]$$
$$n_{92} = [0 \ 0 \ 0 \ 0 \ 0 \ 0 \ 0 \ 0 \ n_2] \qquad n_{94} = [0 \ 0 \ 0 \ 0 \ 0 \ 0 \ 0 \ 0 \ n_4] \tag{A.9}$$

APPENDIX-`II'

$$[\mathrm{C_v}] = \begin{bmatrix} 1/4 & 0 & 0 & 0 & 0 & 0 & 0 & 0 & 0 \\ 0 & 1/4 & 0 & 0 & 0 & 0 & 0 & 0 & 0 \\ 1/2 & 0 & 1/4 & 0 & 0 & 0 & 0 & 0 & 0 \\ 0 & 1/2 & 0 & 1/4 & 0 & 0 & 0 & 0 & 0 \\ 0 & 0 & 0 & 0 & 0 & 0 & 0 & 0 & 0 \\ t_b/4 & 0 & t_b/4 & 0 & 0 & t_b^2/16 & 0 & -t_b t_c/8 & 0 \\ 0 & t_b/4 & 0 & t_b/4 & 0 & 0 & t_b^2/16 & 0 & -t_b t_c/8 \\ -t_c/4 & 0 & -t_c/4 & 0 & 0 & -t_b t_c/8 & 0 & t_c^2/16 & 0 \\ 0 & -t_c/4 & 0 & -t_c/4 & 0 & 0 & -t_b t_c/8 & 0 & t_c^2/16 \end{bmatrix} \quad \text{(B.1)}$$

$$I_v = \frac{1}{t_v^2}\begin{bmatrix} 1 & 0 & 0 & 0 & 0 & 0 & 0 & 0 & 0 \\ 0 & 1 & 0 & 0 & 0 & 0 & 0 & 0 & 0 \\ -2 & 0 & 1 & 0 & 0 & 0 & 0 & 0 & 0 \\ 0 & -2 & 0 & 1 & 0 & 0 & 0 & 0 & 0 \\ 0 & 0 & 0 & 0 & 0 & 0 & 0 & 0 & 0 \\ t_b & 0 & -t_b & 0 & 0 & t_b^2/4 & 0 & t_b t_c/2 & 0 \\ 0 & t_b & 0 & -t_b & 0 & 0 & t_b^2/4 & 0 & t_b t_c/2 \\ t_c & 0 & -t_c & 0 & 0 & t_b t_c/2 & 0 & t_c^2/4 & 0 \\ 0 & t_c & 0 & -t_c & 0 & 0 & t_b t_c/2 & 0 & t_c^2/4 \end{bmatrix} \quad \text{(B.2)}$$

REFERENCES

[1] Alam, N. and Asnani, N.T., (1984), "Vibration and damping analysis of multilayered rectangular plates with constrained viscoelastic layers", Journal of Sound and Vibration, Vol. 97(4), pp. 597-614.

[2] Baber, T.T., Maddox, R.A. and Orozco, C.E., (1998), "A finite element model for harmonically excited viscoelastic sandwich beams," Computer and Structure, Vol. 66(1), pp. 105-113.

[3] Bagley, R.L. and Torvik, P.J., (1983), "Fractional calculus- a different approach to the analysis of viscoelastically damped structures", AIAA Journal, Vol. 21(5), pp.741-748.

[4] Bai, J.M., and Sun, C.T., (1995), "The effect of viscoelastic adhesive layers on structural damping of sandwich beams," Mechanics of Structures and Machines, Vol. 23(1), pp. 1–16.

[5] Barbosa, F.S. and Farage, M.C.R., (2008), "A finite element model for sandwich viscoelastic beams: experimental and numerical assessment", Journal of Sound and Vibration, Vol. 317, pp 91-111.

[6] Cook, R.D., Malkus, D.S., and Plesha, M.E., (1988), Chapter 6, Concepts and applications of finite element analysis, John Wiley & Sons, United Kingdom.

[7] Cupial, P. and Niziol, J., (1995),"Vibration and damping analysis of a three-layered composite plate with a viscoelastic mid layer", Journal of Sound and Vibration, Vol. 183(1), pp. 99-114

[8] DiTaranto, R.A., (1965), "Theory of vibratory bending for elastic and viscoelastic layered finite- length beams," Journal of Applied Mechanics, Transactions ASME Vol. 32(4), pp: 881-886.

[9] DiTaranto, R.A. and McGraw, J.R., (1969), "Vibratory bending of damped laminated plates," Journal of Manufacturing Science and Engineering, Vol. 91(4), pp.1081-1090.

[10] Douglas, B.E., and Yang, J.C.S., (1978), "Transverse compressional damping in the vibratory response of elastic-viscoelastic-elastic beams," AIAA Journal, Vol. 16(9), pp.925-930.

[11] Ewins, D.J., (1984), Modal testing: Chapter- 3 and 4, Theory and Practice, Research Studies Press Ltd.

[12] Fernando C., and Elejabarrieta, M.J., (2006), "Modelling of viscoelastic materials whose storage modulus is constant with frequency," International Journal of Solids and Structures, Vol. 43, pp.7721-7726.

[13] Fernando C., and Elejabarrieta, M.J., (2008) "Structural vibration of flexural beams with thick unconstrained layer damping," International Journal of Solids and Structures, Vol. 45, pp.5805-5813.

[14] Galucio, A.C., Deu, J.F., and Ohayon, R., (2004), "Finite element formulation of viscoelastic sandwich beams with fractional derivative operators," Computational Mechanics, Vol. 33(4), pp.282-291.

[15] Ganesan, N. and Nagaraja Rao, S., (1986), "Vibration of annular plates partially treated with unconstrained damping layer," Computers and Structures, Vol. 23(1), pp.87-93.

[16] Golla, D.F. and Hughes, P.C., (1985), "Dynamics of viscoelastic structures- A time-domain, finite element formulation," Journal of Applied Mechanics, Vol. 52(4), pp.897-906.

[17] Grewal, J.S., Sedaghati, R., and Esmailzadeh, E., (2013), "Vibration analysis and design optimization of sandwich beam with constrained viscoelastic core layer," Journal of Sandwich Structures and Materials, Vol. 15(2), pp.203-228.

[18] Ha, K.H., (1990), "Finite element analysis of sandwich plates: An over view", Computers and Structures, Vol. 37(4), pp.397-403.

[19] Hammmami, L., Zghal, B., Tahar, F., and Mohamed, H., (2005), "Characterization of modal damping of sandwich plates," Journal of Vibration and Acoustics, Transactions of ASME, Vol. 127, pp.431-440.

[20] Ioannides, E., and Grootenhuis, P., (1979), "A finite element analysis of the harmonic response of damped three-layer plates," Journal of Sound and Vibration, Vol. 67(2), pp. 203-218.

[21] Johnson, C.D., and Kienholz, D.A., (1982), "Finite element prediction of damping in structures with constrained viscoelastic layers," AIAA Journal, Vol. 20(9), pp.1284-1290.

[22] Jones, D.I.G., (2001), Chapter 2 and 6, Handbook of Viscoelastic Vibration Damping, John Wiley & Sons, Chichester, UK.

[23] Kamel, A. and Noureddine, A., (2009), "A new 3D finite element for sandwich beams with a viscoelastic core," Journal of Vibration and Acoustics, Vol. 131(2), pp.021010-1 to 021010-9

[24] Kerwin, E.M., (1959), "Damping of flexural waves by a constrained viscoelastic layer," Journal of the Acoustical Society of America, Vol. 31(7), pp. 952-962.

[25] Lee, L.J. and Fan Y.J., (1996), "Bending and vibration analysis of composite sandwich plates," Computers and Structures, Vol. 60(1), pp. 103-112

[26] Lesieutre, G.A. and Mingori, D.L., (1990), "Finite element modelling of frequency- dependent material damping using augmenting thermodynamic fields," Journal Guidance, Control and Dynamics, Vol. 13(6), pp. 1040-1050.

[27] Lesieutre, G.A. and Bianchini, E., (1995), "Time domain modelling of linear viscoelasticity using an-elastic displacement fields," Journal of Vibration and Acoustics, Vol. 117(4), pp. 424-430.

[28] Lofti, H., Bacem, Z.,Tahar, F. and Mohamed, H., (2005), "Characterization of modal damping of sandwich plates," Journal of Vibration and Acoustics, Vol. 127(5), pp.431-440.

[29] LMS, LMS Test.lab manual, LMS International, Belgium

[30] Lu, Y. P., Killian, J.W., and Everstine, G.C., (1979), "Vibrations of three layered damped sandwich plate composites," Journal of Sound and Vibration, Vol. 64(1), pp. 63-71.

[31] Mace, M., (1994), "Damping of beam vibrations by means of a thin constrained viscoelastic layer: Evaluation of a new theory," Journal of Sound and Vibration, Vol. 172(5), pp.557-591.

[32] Martinez, M. and Elejabarrieta, M.J., (2010), "Characterisation and modelling of viscoelastically damped sandwich structures," International Journal of Mechanical Sciences, Vol. 52(9), pp.1225-1233.

[33] Martinez, M. and Elejabarrieta, M.J., (2011), "Dynamic characterization of high damping viscoelastic materials from vibration test data," Journal of Sound and Vibration, Vol. 330(16), pp.3930-3943.

[34] Mead, D.J. and Markus, S., (1969), "The forced vibration of a three-layer, damped sandwich beams with arbitrary boundary conditions," Journal of Sound and Vibration, Vol. 10(2), pp.163-175.

[35] Mead, D.J. and Markus, S., (1970), “Loss factor and resonant frequencies of Encastre damped sandwich beam,” Journal of Sound and Vibration, Vol. 12(1), pp.99-112.

[36] Mead, D.J., (1982), “A comparison of some equations for the flexural vibration of damped sandwich beams,” Journal of Sound and Vibration, Vol. 83(3), pp.363-377.

[37] Mead, D.J., (1998), Chapter 9, Passive vibration control, John Wiley & Sons, United Kingdom.

[38] Nakra, B.C., (1976), “Vibration control with viscoelastic materials I,” Shock and Vibration Digest, Vol. 8(6), pp.3-12.

[39] Nakra, B.C., (1981), “Vibration control with viscoelastic materials II,” Shock and Vibration Digest, Vol. 13(1), pp.17-20.

[40] Nakra, B.C., (1984), “Vibration control with viscoelastic materials III,” Shock and Vibration Digest, Vol. 16(5), pp.17-22

[41] Nashif, A.D., Jones D.I. and Henderson J.P., (1985), Chapter 2, Vibration Damping, John Wiley and Sons, New York.

[42] Ross, D., Ungar, E., and Kerwin, E.M Jr. (1959), "Damping of flexural vibrations by means of Viscoelastic laminae," Structural Damping: Colloquium on Structural Damping, Sec.III, ASME Annual Meeting, New York, pp.49-88.

[43] Sadasiva Rao, Y.V.K. and Nakra, B.C., (1974), “Vibrations of unsymmetrical sandwich beams and plates with viscoelastic cores,” Journal of Sound and Vibration, Vol. 34(3), pp.309-326.

[44] Saeed, M., Hassan, H., and Hossein, M.N., (2012), “Free and forced random vibration analysis of sandwich plates with thick viscoelastic cores,” Journal of Vibration and Control, Vol. 19(14), pp.2223-2240.

[45] Sainsbury, M.G. and Zhang, Q.J., (1999), “The Galerkin element method applied to the vibration of damped sandwich beams,” Computers and Structures, Vol. 71(3), pp.239-256.

[46] Scotchdamp Vibration Control Systems, (1993), Product Information and Performance Data, 3M

[47] Soni, M.L. and Bogner, F.K., (1982), “Finite element vibration analysis of damped structures,” Journal of AIAA, Vol. 20(5), pp.700-707.

[48] Sun, C.T., and Lu, Y.P., (1995), Vibration damping of structural elements, prentice- Hall, Englewood Cliffs, New Jersey.

[49] Thomson, W.T., *Theory of Vibration with Applications*, 4th ed., Prentice-Hall, Englewood Cliffs, 1993.

[50] Torvik, P.J., and Runyon, B.D., (2007), "Estimating the loss factors of plates with constrained layer damping treatments," AIAA Journal, Vol. 45(7), pp.1492-1500.

[51] Trindade, M.A., Benjeddou, A. and Ohayon, R., (2001), "Finite element modelling of hybrid active-passive vibration damping of multilayer piezoelectric sandwich beams-Part I: Formulation," International Journal of Numerical Methods in Engineering, Vol. 51(7), pp.835-854.

[52] Tso-Liang, T. and Ning-Kang, H., (2001), "Analysis of damping characteristics for viscoelastic laminated beams," Journal of Computer Methods in Applied Mechanics and Engineering, Vol. 190, pp.3881-3892.

[53] Vasques, C.M.A., Moreira, R.A.S. and Dias Rodrigues, J., (2010), "Viscoelastic damping technologies – Part I: Modelling and finite element implementation," Journal of Advance Research in Mechanical Engineering, Vol. 1(2), pp.76-95.

[54] Wang, G. and Wereley, N.M., (2002), "Spectral finite element analysis of sandwich beams with passive constrained layer damping," Journal of Vibration and Acoustics, Vol. 124(3), pp. 376-386.

[55] Wang, G. and Wereley, N.M., and Chang, D.C., (2003), "Analysis of sandwich plates with viscoelastic damping using two dimensional plate modes," AIAA Journal, Vol. 41(5), pp.924-932.

[56] Won, S.G., Bae, S.H., Cho, J.R., Bae, S.R., and Jeong, W.B., (2013), "Three-layered damped beam element for forced vibration analysis of symmetric sandwich structures with a viscoelastic core," Finite Elements in Analysis and Design, Vol. 68, pp.39-51.

[57] Zapfe, J.A. and Lesieutre, G.A., (1999), "A discrete layer beam finite element for the dynamic analysis of composite sandwich beams with integral damping layers," Computers and Structures, Vol. 70(6), pp.647-666.

[58] Zhicheng, H., Zhaoye, Q., and Fulcei, C., (2014), "Vibration and damping characteristics of sandwich plates with viscoelastic core," Journal of Vibration and Control, DOI"10.1177/107754631454527.

OUTCOME OF THE PRESENT WORK

Part of the work is published as the following papers:

1. Kishore Kumar, K, Krishna Y, and Bangarubabu P (2010), "Vibration control of beams using viscoelastic layers," **Proceedings of the VIth International conference on Vibration Engg and technology of Machinery, VETOMAC** held at IIT, Delhi held during December 13-15, 2010.
2. Bangarubabu, P, Kishore Kumar, K and Krishna Y (2012), "Damping Effect of Viscoelastic Material on Sandwich Beams", **International Conference on Trends in Industrial and Mechanical Engineering (ICTIME 2012),** March 24-25, Dubai.
3. Kishore Kumar, K, Krishna Y, Bangarubabu, P., (2015), "Damping in beams using viscoelastic materials," **Institute of Mechanical Engineers**, Part-L, **Journal of Material, Design and Applications**, Vol.229 (2), pp.117-125.
4. Kishore Kumar, K, Krishna, Y and Bangarubabu, P, (2014), "Estimation of Loss factors of constrained layer plate using viscoelastic layers", **Institute of Mechanical Engineers, Part-L, Journal of Material, Design and Applications**, DOI:10-1177/1464420714532792

ACKNOWLEDGMENTS

I take this opportunity to express my sincere gratitude to my guides, Prof. P. Bangaru Babu and Dr. Y Krishna for their invaluable guidance, suggestions and support during my work.

I am grateful to my Doctorial Scrutiny Committee (DSC) members, Prof. S Srinivasa Rao, Department of Mechanical Engineering, Prof. D. Ramaseshu, Department of Civil Engineering, National Institute of Technology, Warangal, for their support and suggestions at every level from starting to completion of the work.

I am thankful to Prof. T. Srinivasa Rao, Director, National Institute of Technology Warangal and Prof. C.S.P. Rao, Chairman, DSC and Head of Mechanical Engineering Department, National Institute of Technology, Warangal, for their support and encouragement.

I am very much thankful to Prof. Prof. L.Krishnanand, Prof. G. R. N. Tagore, Prof. K. Madhumurthy and Prof. A.V.Narasimha Rao, Chairmen, DSC at various periods for extending their support in completing the research work.

I profoundly express my thanks to Dr. K. Jayaraman, Scientist 'H', Director, Defence Research and Development Laboratory, Mr. P. S. R. Anjaneyulu, Scientist 'G', Technology Director, Flight Structures, Shri. A. K. Kaushik, Emeritus Scientist, Shri. G. A. Srinivasa Murthy, Scientist `G', ANSP, Dr. D. Ramkrishna Scientist 'E', ANSP, Mrs. J. Swapna, Scientist 'E', Structural Test Facility for their valuable inputs during this work

I express my thanks to Director, NMRL, Dr. Chakraborthy, Scientist `H', Dr. M.R Patri, Scientist `G' and Praveen Sreenivasan, Scientist `D' for providing the viscoelastic material and allowing to carryout experiments at NMRL. I express my thanks our colleagues in Structural Test Facility for their valuable inputs and support extended during this work. My special thanks to the DRDL, Library.

I am very much obliged to my wife for her continuous support and encouragement right from beginning of the work to ending for instigating the zeal to materialize this dream.

Last but not the least; I am grateful to my parents, my children, family members and well-wishers for their continuous and unswerving support.

Date: July 2015 **K Kishore Kumar**

Biographical Sketch of the Author

The author K Kishore Kumar was born on May 13, 1967 as youngest son to late Shri Kalahasti Mallikarjunam and late Smt. Kalahasti Sambhavamma at Gudur, Andhra Pradesh. He has got married to Smt. Alladi Hima Bindu on May 02, 1995 and blessed with one son Chi. K.V. Abhishekh on July 13, 1996 and Chi. K.S.S. Madhu Priya on March 2, 1999.

He has acquired his B.Tech (Mechanical Engineering) degree from Sri Venkateswara University, Tirupati with first division in 1989 and M.E (Aeronautical Engineering) degree from Madras Institute of technology (M.I.T), Anna University, Chennai in first division in the year 1993. He got selected in campus interview under Integrated Guided Missile development Programme (IGMDP).

He started his career as Scientist 'B' in Structural Test Facility, Defence Research and Development Laboratory in the year 1993 and at present he is working as Scientist- F. He is responsible for dynamic testing of various missile sections. The dynamic testing consists of Modal testing and qualification testing. He has 12 publications out of which four are related to the present work.